VALIDATION

UNIFIED DISPERSION MODEL

DATE: December 2023

This report describes the validation of the UDM in its entirety by comparison with measurements from large-scale field experiments.

No.	Date	Reason for Issue	Prepared by	Verified by	Approved by
1	1999	PHAST 6.0	Holt and Witlox		
2	March 2000	PHAST 6.1	Holt and Witlox		
2	Oct 2005	SAFETI 6.5	Harper		
3	May 2011	Phast (Risk) 6.7	Witlox and Harper		
4	Aug 2014	Phast (Risk) 6.7 – added CO2 experiments	Witlox		
5	April 2015	Added UDM AWD results	Witlox&Fernandez	Fernandez&Harper	
6	Oct 2017	Phast 8.0	Fernandez&Witlox		
7	Dec 2020	Phast / Safeti 8.4	Hart & Harper		
8	May 2021	Apply new template	D. Vatier		
9	Oct 2021	Phast / Safeti 8.6	Hart & Harper		
10	June 2023	Add COSHER experiments	Harper & Hart		

Date: December 2023

Prepared by: Digital Solutions at DNV

ABSTRACT

This report describes the validation of the Unified Dispersion Model (UDM).

The UDM theory is described by an accompanying report. The UDM models the dispersion following a ground-level or elevated two-phase pressurised release. It effectively consists of the following linked modules: jet dispersion, non-equilibrium droplet evaporation and rainout and touchdown, pool spread and vaporisation, heavy gas dispersion, passive dispersion. The UDM allows for continuous, instantaneous and constant finite-duration releases. The UDM also allows for general time-varying releases. In addition to the non-equilibrium droplet thermodynamics model, UDM also allows for a two-phase HF thermodynamics model (including effects of polymerisation). Another feature of the UDM is possible plume lift-off, where a grounded cloud becomes buoyant and rises into the air. Rising clouds may be constrained to the mixing layer if it is reached.

This report includes a comprehensive description of the overall validation of the UDM model. This includes a description of each validation experiment, the details of the assumptions made for the UDM simulation plus a detailed discussion of the results obtained from a statistical and graphical comparison against the field data.

The UDM verification manual discusses the verification of the individual modules, which includes validation against wind-tunnel experiments. The current document is concerned with the validation of the overall model, which involves validation against the following field experiments:

- Continuous releases: Thorney Island (Freon and Nitrogen), Goldfish (HF), Prairie Grass (passive), Desert Tortoise (Ammonia), FLADIS (Ammonia), EEC (Propane) and Maplin Sands LPG experiments. Various other continuous releases, are included to assess vertical releases into a crosswind: Schatzmann (wind tunnel), Donat (wind tunnel), Vidali (wind tunnel), Li (wind tunnel) and a field experiment by Engie (LNG)
- Instantaneous releases: Thorney Island experiments (Freon and Nitrogen)
- Finite-duration releases: Kit Fox (CO2) and Jack Rabbit II (Chlorine) experiments.
- Buried pipeline ruptures (CO_2) COSHER experiments
- Continuous and time-varying pressurised CO2 experiments carried out at Spadeadam (BP and Shell data made available via CO2PIPETRANS JIP)
- PHMSA validation set: selection of experiments including
  - Dispersion from time-varying pools: Maplin Sands, Burro and Coyote (all LNG)
  - Continuous releases: Thorney Island (Freon and Nitrogen)
  - Wind-tunnel releases: CHRC-A (CO2), BA-Hamburg, BA-TNO (SF6)

The performance of the UDM in predicting peak centreline concentration and cloud widths is found to be overall very good.

Table of contents

Table of figures

List of Tables

1 INTRODUCTION

A full description of the theory underlying the UDM is described in the accompanying UDM theory manual. The UDM verification manual describes the verification of the individual modules, which were mainly carried out against *wind-tunnel* data. This report is concerned with the validation of the UDM in its entirety. To this end UDM predictions are compared with measurements from a selection of the available experimental *field* data. The basis and choice of these experiments stem from the model evaluation carried out by Hanna et al[10], the EU SMEDIS[1] programme (**S**cientific **M**odel **E**valuation of **D**ense gas d**is**persion models), and the UDM validation against the experiments in the US PHMSA LNG Model Validation database[2,3,4]. In addition more recent experiments have been added relating to both unpressurised and pressurised CO_2 releases, as well as for the PHMSA process for approving models for use with LNG in the US.

Chapters 2 and 3 provide full description of the validation sets and details of the methods used within the model to simulate the experimental conditions.

Chapter 4 presents and discusses results from the comparison of the UDM predictions with the measured experimental data.

All experimental simulations in this report can be supplied to licensed users as Phast .psux files.

2 DESCRIPTION OF THE VALIDATION EXPERIMENTS

The validation set consists of 13 sets of field scale experiments and 3 sets of wind tunnel experiments, covering a wide range of release scenarios. This includes continuous, instantaneous, finite-duration and time-varying releases, unpressurised and pressurised releases, and vapour and two-phase releases. A summary of each is provided in Table 1 whilst a more detailed, qualitative description of each experiment is presented below:

- Continuous releases (see Section 4.1; excluding CO_2 releases)
    - *Prairie Grass* – A small quantity of Sulphur dioxide was released at or near ground level over flat terrain. Experiments were carried out during both daylight and non-daylight hours giving rise to a wide range of atmospheric stabilities. Concentrations were measured from an array of sensors located on an arc at downwind distances of 50, 100, 200 400 and 800m.
    - *Desert Tortoise* – Liquefied ammonia was released under pressure in the downwind direction through a pipe which was situated approximately 1 m above the ground. At the exit of the pipe, the ammonia flashed to form a two-phase aerosol, a small quantity of which rained out downwind of the release. Concentration measurements were made from an array of sensors located on an arc at downwind distances of 100 and 800m.
    - *EEC* – In this experiment pressurised liquid propane was released approximately 0.5 m above the ground to form a two-phase aerosol. Concentrations were measured up to a maximum distance of 64m.
    - *FLADIS* – The experiment was designed to investigate the downwind dispersion of an ammonia aerosol. Liquefied ammonia was released under pressure through a nozzle situated at a height of 1.5m. These experiments differed from the Desert Tortoise experiments because the release rates were much lower, allowing for the investigation of far field passive effects. In addition, no liquid pool was observed as in the case of the Desert Tortoise experiments.[5]
    - *Goldfish* – In a similar manner to the Desert Tortoise experiments, pressurised hydrogen fluoride was released from an elevated pipe, forming a two-phase aerosol. No rainout of the HF was observed. Concentration measurements were made from an array of sensors located on an arc at downwind distances of 300, 1000 and 3000m.
    - *Maplin Sands LPG* – These experiments are similar in nature to the LNG dispersion case in the PHMSA set. LPG was spilled onto water and the continuous dispersion of the vapourising pool was monitored at various arc distances up to 650m downwind.
- Continuous releases (vertical/angled into a crosswind)
    - *Schatzmann* – 4 continuous elevated vertical releases of heavy gases (Wind tunnel)
    - *Donat* – 9 continuous elevated vertical, angled and horizontal releases of heavy gases (Wind tunnel)
    - *Vidali* – 1 continuous vertical CO2 release (Wind tunnel)
    - *Engie* – 3 continuous LNG vapour releases: 2 vertical, 1 horizontal
- *Thorney Island – Instantaneous (see Section 4.2)*
  In this experiment, approximately 2000m^3 of an unpressurised mixture of Freon and Nitrogen was released at ground level. Concentrations were measured up to 600m from the release point.
- *CO2PIPETRANS (BP and Shell; see Section 4.4)*
  These experiments involving pressurised CO_2 releases were carried out at Spadeadam by GL Noble Denton (previously Advantica, currently DNV) for BP in 2006 and for Shell in 2010, with the data made available via the DNV led CO2PIPETRANS JIP. The CO_2 was released from a nozzle (¼, ½, or 1") attached to a 5.5m 2" pipe attached to a horizontal cylindrical vessel. The modelled experiments include three set of experiments, i.e. cold steady-state and time-varying releases (liquid storage), and hot supercritical time-varying releases (dense vapour storage). For the cold steady-state tests nitrogen padding gas was used to maintain the pressure and to ensure that the CO_2 remained as liquid in the vessel. For the time-varying tests the CO_2 was released through the nozzle driven only by the pressure in the vessel with the vessel pressure decaying as the release progressed. See Witlox et al. (2014)[8] for further details and references.
- *Buried Pipeline and Crater (COSHER; see Section 4.5)*

The COSHER project was intended to understand releases from underground CO_2 transmission pipelines simulating loss of containment. As part of the project, two large scale experiments were completed by GL Noble Denton at Spadeadam to provide data under well- defined conditions studying the full-bore rupture of a CO_2 dense phase high pressure underground pipeline at large scale. Concentration data has been published from these tests, which we will refer to as COSHER 1 (Lowesmith, 2013)[6] and COSHER 2 (Ahmad, et al., 2015).[7]

- *Kit Fox (see Section 4.6)*
  In these experiments dense gas (CO_2) was released from a 1.5mx1.5m ground-level area source for continuous plumes and 20-second finite-duration releases, during both neutral and stable conditions. Experiments were carried out both for a uniform (URA; surface roughness estimated between 0.01 or 0.02 m; adopted value 0.01m) and also using an increased surface roughness (ERP; roughness estimated between 0.12 or 0.24 m closer to the source; adopted value 0.12m). Thus this set of experiments is an ideal set to investigate effects of finite-duration releases (along-wind diffusion) and effects of variable surface roughness. See Witlox et al. (2014)[8] and the Kit Fox validation report[9] for further details.

- *Jack Rabbit 2 (see Section 4.6)*

  In 2015 and 2016 nine large (up to ~ 10 tonnes) 2-phase chlorine releases were carried out at the US Army Dugway Proving Ground in Utah. Three were selected for validation against the UDM (1, 6 and 7). Test 1 incorporated an array of shipping containers (simulating an urban environment) and the other tests were carried out in flat terrain. Measurements of chlorine concentrations and estimates of widths were made out to a distance of 11 km downwind.

- *PHMSA Validation Set (see Section 4.7)*
  In the US, PHMSA has a process for accrediting dispersion models for use with LNG siting applications which involves comparison against a number of experiments. Many of these were already included in previous versions of this report, but we have now collated and updated them to reflect the current prescribed inputs and methods.

  - *LNG Pool Dispersion*

    - *Burro* – This experiment investigated the downwind dispersion that resulted from the spill of LNG onto a pool of water, 58 m in diameter and 1 m in depth. Concentrations were measured from an array of concentration sensors located on an arc at downwind distances of 57, 140, 400 and 800m.

    - *Coyote* – Like for the Burro experiments, the LNG liquid was released from an elevated height with a very low momentum. This results in almost 100% rainout onto a water basin.

    - *Maplin Sands* - The experiment investigated the downwind dispersion that resulted from a spill of LNG or LPG onto the surface of the sea.

  - *Continuous Release – Field Scale*

    - *Thorney Island – Continuous.* This experiment involved the continuous release of a mixture of Freon and Nitrogen. This has been modelled as a low-momentum continuous ground-level horizontal release.

  - *Continuous Release – Wind Tunnel*

    - *CHRC-A, BA-Hamburg, BA-TNO*. These wind-tunnel experiments involved isothermal releases of CO_2 (CHRC-A) and SF_6 (BA-Hamburg, BA-TNO), with all modelled as vapour area sources at ground level. Only the unobstructed experiments in each series have been modelled, each at field scale rather than at wind tunnel scale.

Validation Continuous Series	Runs	Material	Release	Experimental database
Prairie Grass (PG)	7-9,13,15,17,34, 41,50,58	SO_2	Continuous elevated passive dispersion (neutral buoyancy; modelled by UDM as passive Gaussian dispersion)	SMEDIS-8,17; MDA rest
Desert Tortoise (DT)	1,2,3,4	Ammonia	Continuous elevated two-phase jet release	SMEDIS 1,2;MDA 3,4
EEC	360,550,560	Propane	Continuous elevated two-phase jet release	SMEDIS
FLADIS	9, 16, 24	Ammonia	Continuous elevated two-phase jet release	SMEDIS
Goldfish (GF)	1,2,3	HF	Continuous elevated two-phase jet release	McFarlane et al.
Maplin Sands LPG	42, 43, 46, 46, 49, 50, 52, 54	LPG	Continuous LNG spill on to sea	MDA
Schatzmann et al.	4, 10, 11, 13	Various Heavy	Continuous elevated vertical releases of heavy gases (Wind tunnel)	-
Donal	1, 3, 4, 5, 10, 11, 19, 21, 44	Various Heavy	Continuous elevated vertical, angled and horizontal releases of heavy gases (Wind tunnel)	-
Vidali	1	CO2	Continuous elevated vertical release (Wind tunnel)	-
Engie	H6, V6, V18	LNG	Continuous elevated releases, horizontal and vertical	-
Thorney Island (TI)	6-9, 12, 13, 17-19	Freon/N2	Unpressurised instantaneous ground-level release	MDA
BP steady-state cold	1,2,3,5,6,11	CO2	continuous pressurised (cold liquid storage)	CO2PIPETRANS MDA
BP transient hot	8,8R,9	CO2	time-varying pressurised (supercritical vapour)	CO2PIPETRANS MDA
Shell steady-state cold	3,5,11	CO2	continuous pressurised (cold liquid storage)	CO2PIPETRANS MDA
Shell transient cold	1,2,4	CO2	time-varying pressurised (cold liquid storage)	CO2PIPETRANS MDA
Shell transient hot	14,16	CO2	time-varying pressurised (supercritical vapour)	CO2PIPETRANS MDA
COSHER	1, 2	CO_2	Buried long pipeline ruptures, dense phase	-
Kit Fox URA cont.	604,605,606,609,702,703,705,709,712,805,808,811	CO2	Continuous ground-level area source (uniform roughness)	MDA
Kit Fox ERP cont.	305,404,503,504,508	CO2	Ditto, but enhanced roughness	MDA
Kit Fox URA puff	601,602,603,607,608,704,706,708,710,711,714,801-804,806,807, 809,810,812	CO2	20 seconds ground-level areas source (uniform roughness)	MDA
Kit Fox ERP puff	301-304,306,307, 403,501,502,505,506,507	CO2	20 seconds ground-level areas source (enhanced roughness)	MDA
Jack Rabbit II	1, 6, 7	Chlorine	Short duration (20-40s) of liquid chlorine, vertical or angled downward.	-
Maplin Sands (MSN)	27, 34,35	LNG	Continuous methane spill onto sea	PHMSA
Burro (BU)	3,7,8,9	LNG	Continuous methane spill onto water basin	PHMSA
Coyote (CO)	3,5,6	LNG	Continuous methane spill onto water basin	PHMSA
Thorney Island (TI)	45,47	Freon/N2	Continuous low-momentum ground-level horizontal release	PHMSA
CHRC	CHRC-A	CO2	Continuous low-momentum ground level vapour source (Wind tunnel)	PHMSA
BA-Hamburg	DA0120, DAT233	SF6	Continuous low-momentum ground level vapour source (Wind tunnel)	PHMSA
BA-TNO	TUV01, FLS	SF6	Continuous low-momentum ground level vapour source (Wind tunnel)	PHMSA

Table 1. List of experiments for UDM validation

3 METHOD FOR UDM SIMULATIONS OF EXPERIMENTS

3.1 Definition of input data to validation runs

The input data for each validation run have been obtained from either Hanna et al (1991)[10] or data sheets provided for the SMEDIS[11] project, or from the PHMSA LNG database[2]. The Goldfish experiments are the exception to this rule, where the data were obtained from McFarlane et al[12]; see the UDM Hydrogen Fluoride verification chapter for a full discussion.

Unfortunately not all the input data required for the UDM are available from the above sources. The following general assumptions have been made when defining each validation run:

- Since no flash calculations are carried out within the UDM, the UDM model requires as input the post-flash data in the case of pressurised continuous or pressurised instantaneous releases. These data are the release velocity (continuous release) or expansion energy (instantaneous release), liquid fraction and initial mean droplet size.

  For cases DT1, DT2, EEC360, EEC550, EEC560, FLADIS9, FLADIS16 and FLADIS24 the release velocity and liquid fraction were supplied as part of the SMEDIS[11]project. The mean droplet sizes were not provided, and therefore a standalone droplet model was extracted from the Phast discharge model to calculate the mean droplet size. See the UDM thermodynamic theory manual for details.

  In the remaining cases the data were obtained by running the Phast discharge model using the specified source conditions; see Section 4.1.1 for a detailed comprehensive discussion.

- The release velocities, u_{cld}^R, for unpressurised releases (i.e. Prairie Grass), were obtained by dividing the release rate, m_c, by the source area, A, and the vapour density, ρ_c^v, of the material at atmospheric temperature, T_a, and pressure, P_a :

$$u_{cld}^R = \frac{m_c}{\left\{A\,\rho_c^V(T_a, P_a)\right\}} \qquad (1)$$

- The default value for the solar flux has been used.[1,2]

- For those experiments in which the UDM predicts rainout the surface type is an important parameter. The choice of surface has been based on the moisture data provided, however, if this is unavailable it is assumed that the surface is wet soil.

- Two averaging times are specified by Hanna[10] one "short" and the other "long". The data were calculated and compared at the longest of the available averaging time. This is except for the Burro and Coyote experiments, for which calculations are carried out for both short and long averaging times (as required by PHMSA).

- The core averaging time for each validation run was set equal to the experimental averaging time. This was carried out to avoid the discontinuities that may occur when applying an averaging time correction to the centreline concentration and cloud width after the transition to passive dispersion.

- UDM simulations for each validation experiment were carried out including the effects of both heat and (in case of dispersion above water) water transfer.

Further details of input data assumptions related to the individual experiments are presented in Chapter 4, while Appendix A lists the precise values of the input data used for the UDM simulation of each validation case is presented in Appendix A.

[1] Note that a relation exists between solar flux and the time of year and cloud cover. Since this relation is not implemented in the UDM model, it is chosen to adopt the default value (500 W/m ^{2}), which may well be inaccurate

[2] The solar flux is used exclusively within the pool model. It is shown by a sensitivity analysis that solar flux has little impact to the pool model predictions for spill on land.

3.2 Calculation of output data to validation runs

This report provides a graphical representation of the UDM predictions for each individual experiment. These figures also include comparison with the available experimental data. These were obtained from either Hanna et al[10] (including Goldfish) or SMEDIS data sheets[11]. The majority of experiments measured concentrations at one single height. However, a selection of the experiments, for example FLADIS and Desert Tortoise, measured concentrations at a number of different heights.

For each experiment the following figures are produced:

a) Centreline concentration, c(x, 0, z_{cld}), and concentration at a specified height H, C(x, 0, H), as a function of downwind distance, x(m).
b) Centre-line height z_{cld} (m) as a function of downwind distance x(m).
c) Cloud width and cloud depth, $H_{eff}(1+h_d)$, (m) as a function of downwind distance. See Appendix B for the full definition of cloud width. The definition for the cloud depth is laid out in the theory manual
d) Vapour and liquid temperature (K) as a function of downwind distance

For two-phase releases that form an evaporating pool the figures show the resulting dispersion for each pool segment.

3.3 Statistical measures of performance

Each experimental set (or series) was statistically evaluated to determine the accuracy and precision of the UDM predictions with the observed data. Formulas, as reported by Hanna et al.[10], were used to calculate the geometric mean bias, MG, and geometric variance, VG, for an experimental dataset.

Single experiment

A single experiment with N data points is considered. Let $x_0 = [x_{01}, x_{02}, \ldots. x_{0N}]$ be the array of observed data, and x_P be the array of predicted data = $[x_{P1}, x_{P2}, \ldots. X_{PN}]$. The geometric mean bias (MG) and variance (VG) are now defined as follows[3]

$$MG = \exp\left(\overline{\ln x_o} - \overline{\ln x_P}\right) = \exp\left(\overline{\ln \frac{x_0}{x_P}}\right) = \exp\left[\frac{1}{N}\sum_{i=1}^{N}\ln\left(\frac{x_{0i}}{x_{Pi}}\right)\right] \quad (2)$$

$$VG = \exp\left[\overline{\left(\ln x_0 - \ln x_P\right)^2}\right] = \exp\left[\overline{\ln\left(\frac{x_0}{x_P}\right)^2}\right] = \exp\left[\frac{1}{N}\sum_{i=1}^{N}\ln\left(\frac{x_{0i}}{x_{Pi}}\right)^2\right] \quad (3)$$

where *Σ* refers to summation of over the N data points, and $\overline{\chi}$ indicates a mean variable,

$$\overline{\chi} = \frac{1}{N}\sum_{i=1}^{N}\chi_i \quad (4)$$

Ideally, MG and VG would both equal 1.0. Geometric mean bias (MG) values of 0.5 and 2.0 can be thought of as a factor of 2 in over-predicting and under-predicting the mean, respectively"[13]. Likewise, a geometric variance (VG) of about 1.6 indicates scatter from observed data to predicted data by a factor of 2.

Dataset with multiple experiments

Secondly a dataset with M multiple experiments considered. For experiment j (j = 1,…., M), the arrays of observed and predicted data are given by

[3] In the MG formula for the concentration, both observed and predicted concentrations are set equal to a threshold concentration if their values are below this threshold (default = 0.001 mole %).

$$\mathrm{x}_{0\mathrm{j}} = [\mathrm{x}_{01\mathrm{j}}, \mathrm{x}_{02\mathrm{j}}, \ldots, \mathrm{x}_{0\mathrm{N}_\mathrm{j}\mathrm{j}}] \; , \quad \mathrm{x}_{\mathrm{Pj}} = [\mathrm{x}_{\mathrm{P1j}}, \mathrm{x}_{\mathrm{P2j}}, \ldots, \mathrm{x}_{\mathrm{PN}_\mathrm{j}\mathrm{j}}] \tag{5}$$

Where N_j is the number of data points from experiment j.

The values MG_{tot},VG_{tot} for the total dataset can be derived from the values MG_j , VG_j associated with the individual experiments as follows:

$$MG_{tot} = \exp\left[\frac{1}{N_{tot}} \sum_{j=1}^{M} \sum_{i=1}^{N_j} \ln\left(\frac{x_{0ij}}{x_{Pij}}\right)\right] = \prod_{j=1}^{M} \left\{\exp\left[\frac{1}{N_j} \sum_{i=1}^{N_j} \ln\left(\frac{x_{0ij}}{x_{Pij}}\right)\right]\right\}^{\frac{N_j}{N_{tot}}} = \prod_{j=1}^{M} \left\{MG_j\right\}^{\frac{N_j}{N_{tot}}} \tag{6}$$

$$VG_{tot} = \exp\left[\frac{1}{N_{tot}} \sum_{j=1}^{M} \sum_{i=1}^{N_j} \ln\left(\frac{x_{0ij}}{x_{Pij}}\right)^2\right] = \prod_{j=1}^{M} \left\{\exp\left[\frac{1}{N_j} \sum_{i=1}^{N_j} \ln\left(\frac{x_{0ij}}{x_{Pij}}\right)^2\right]\right\}^{\frac{N_j}{N_{tot}}} = \prod_{j=1}^{M} \left\{VG_j\right\}^{\frac{N_j}{N_{tot}}} \tag{7}$$

where *Π* refers to a product for all datasets, and the total number of data points N_{tot} is given by

$$N_{tot} = \sum_{j=1}^{M} N_j \tag{8}$$

Thus it follows that:

$$MG_{tot} = \left\{\prod_{j=1}^{M} \left(MG_j\right)^{N_j}\right\}^{1/N_{tot}}, \; VG_{tot} = \left\{\prod_{j=1}^{M} \left(VG_j\right)^{N_j}\right\}^{1/N_{tot}} \tag{9}$$

In case all experiments have the same number of data points, i.e. N_1=N_2=…=N_M, the above formulas further reduce to:

$$MG_{tot} = \left\{\prod_{j=1}^{M} \left(MG_j\right)\right\}^{1/M}, \; VG_{tot} = \left\{\prod_{j=1}^{M} \left(VG_j\right)\right\}^{1/M} \tag{10}$$

The above formula (10) has been used for the Kit Fox experiments (where 4 data points apply for each experiment), while the other more general formula (9) has been used for the other experiments. However for some cases one may consider to use nevertheless equation (10), e.g. to avoid that an experiment j with many experimental data points influences too much the total values MG_{tot} and VG_{tot}. This should be decided on the basis of the given dataset!

4 RESULTS AND DISCUSSION

4.1 Continuous releases (excluding CO_2)

4.1.1 Discharge data for two-phase jets

This section[4] details the results of discharge calculations associated with two-phase jets, i.e. the FLADIS ammonia, Desert Tortoise ammonia, EEC propane and Goldfish HF experiments. Input data for these calculations as well as additional input required for the dispersion calculations were obtained from SMEDIS for FLADIS, Desert Tortoise and EEC. For the Goldfish HF experiments, input data were obtained from Chapter 9 of the HGSYSTEM 1.0 Technical Reference Manual[14]. Note that these input data for Goldfish differ from those used in the MDA by Hanna et al.[10], while the SMEDIS Desert Tortoise data are in line with the values in the MDA. The data provided for the FLADIS experiments are in line with those presented by Nielsen and Ott[15].

The discharge calculations have been carried out using the leak scenario of the Phast discharge model DISC (version 7.1):

- The DISC model has two methods for modelling the expansion from stagnation conditions to orifice conditions, i.e.
  - the metastable liquid assumption: non-equilibrium at the orifice, liquid remains liquid at the orifice, orifice pressure = ambient pressure
  - flashing liquid assumption: equilibrium at the orifice, flashing may occur upstream of the orifice

- The DISC model has also the following three options for performing the expansion from the choke point in the orifice to the atmospheric pressure, namely:
  - Isentropic
  - Conservation of momentum
  - (default option) One of the two options above, with the option selected which results in minimum thermodynamic change between orifice conditions and final conditions. For all current sets of experiments, it was found that this default option corresponded with the isentropic option.

Table 2 summarises the DISC input data and results for the case of the default assumption of metastable liquid assumption in conjunction with conservation of momentum.

Flow rate predictions
Table 3 first compares observed flow rates (reported by SMEDIS for the FLADIS, EEC experiments and by Hanna for the DT, GF experiments) against DISC predictions for both cases of 'metastable liquid' and 'flashing':

- It is concluded that the Goldfish predictions are virtually identical for both cases with very close agreement with the data.
- Predictions for EEC and DT presuming 'flashing' are seen to provide considerably improved predictions compared to the 'metastable liquid' assumption. On the other hand, FLADIS results are best presuming 'metastable liquid', with significant under-prediction presuming 'flashing'. Overall the 'metastable liquid' is seen to provide conservative results, with an over-prediction of the observed flow rates.

Note there is an inherent inaccuracy in the measured flow rates with e.g. an accuracy of 18% quoted by Nielsen and Ott[15] for the case of the FLADIS experiments.

The results given in Table 3 are obtained by quick DISC simulations, and more accurate estimate of the input as well more accurate method of modelling may be able to be obtained by means of a more thorough analysis of the experimental data sets. However this was not part of scope of the current work.

Predictions of post-expansion data: liquid fraction, velocity and Sauter Mean Diameter (SMD)
Table 3 secondly compares predictions of post-expansion data using the range of model assumptions as described above, and compares these predictions against values of liquid fraction and velocity provided as part of the SMEDIS project:

- Post-flash liquid fractions provided by SMEDIS are in close agreement with the DISC predictions
- Velocity

[4] UPDATE. Part of the description of this section may be moved to the ATEX validation report[16], with a summary retained only in the current section only.

- DISC predictions of final post-expansion velocity presuming metastable liquid assumption are lower than presuming ‘flashing’ upstream of the orifice. DISC predictions of velocities presuming conservation of entropy result in significant larger velocities than presuming conservation of momentum.
- For the case of the FLADIS experiments, SMEDIS values for velocity are closest to the DISC predictions presuming metastable liquid and conservation of momentum. On the other hand, for the EEC and Desert Tortoise experiments, the SMEDIS values are closest to the DISC predictions presuming flashing and conservation of momentum. Using the isentropic approach, DISC predicts post flash velocities which are much higher than those provided as part of the SMEDIS project.

Selection of model assumptions

As indicated above regarding accuracy of flow-rate predictions and agreement of final post-expansion velocity with SMEDIS data, it could be considered to apply the ‘flashing’ assumption for the Desert Tortoise and EEC experiments. However it was found (see ATEX validation report[16]) that the metastable liquid assumption generates overall more accurate predictions (improved MG,VG values) using the metastable liquid assumption for all sets of experiments (FLADIS, Desert Tortoise and EEC).

With these observations in mind, it was concluded that any non-SMEDIS validation sets, which required post flash data, would obtain them using the Phast discharge model, adopting the conservation of momentum approach in conjunction with the metastable liquid assumption[5]. Thus this approach has been used to obtain values for all post-expansion data (liquid fraction, velocity, SMD).

Table 3 also gives droplet SMD values. The modified CCPS correlation (introduced as the default in Phast 6.7) was used. This should for these cases use the CCPS flashing correlation, but for the conservation of momentum method in conjunction with metastable liquid assumption in fact it uses the mechanical correlation[6] and thus SMD values may be less accurate. However in case rainout would not occur, the precise value of the SMD is not expected to significantly affect the dispersion calculations.

[5] UPDATE. At a later stage, it may be considered to no longer use the SMEDIS input data for the SMEDIS validation sets, and to use for these the same approach as for the non-SMEDIS validation datasets.

[6] Due to calculated partial expansion energy being < 0 (warning ATEX 1010)

Disc_2_Phase_Cons_Momentum.xls: Two-phase pressurised releases (FLADIS, EEC, Desert Tortoise) - Conservation of Momentum																
Input Description	**Units**	**FLADIS9**	**FLADIS16**	**FLADIS24**	**EEC170**	**EEC360**	**EEC550**	**EEC560**	**DT1**	**DT2**	**DT3**	**DT4**	**GF1**	**GF2**	**GF3**	**Comments** [Refs. SMEDIS emails, MDA data in Hanna (1991), Table 3.1 TNER.90.015 for GF, FLADIS report http://w w w .risoe.dk/rispubl/VEA/veapdf/ris-r-898.pdf - Table 2]
Material																
Stream name	-	Ammonia	Ammonia	Ammonia	Propane	Propane	Propane	Propane	Ammonia	Ammonia	Ammonia	Ammonia	Hydrogen F	Hydrogen F	Hydrogen Fluoride	
Storage state																
Specification flag (0 = P&T&LF, 1 = P&T, 2 = Tbub, 3 = Pbub, 4 = Tdew, 5 = Pdew, 6 = P&LF, 7 = T&LF)	-	6	1	6	1	1	1	1	1	1	1	1	1	1	1	6 (saturated liquid), 1 (pressurised non-saturated liquid)
Gauge pressure	Pa	5.91E+05	6.96E+05	4.69E+05	8.40E+05	6.70E+05	9.10E+05	9.23E+05	9.22E+05	1.02E+06	1.05E+06	1.09E+06	7.66E+05	7.93E+05	8.07E+05	SMEDIS for FLADIS/EEC; Hanna (1991) for DT; TNER.90.015 for GF - lower values in Hanna
Temperature	K	286.85	290.25	282.6	284.05	286.15	286.45	286.65	294.7	293.3	295.3	297.3	313.15	310.95	312.55	SMEDIS for FLADIS/EEC; Hanna (1991) for DT; TNER.90.015 for GF
Liquid fraction (MOLE basis)	mol/mol	1														
Vessel data																
Orifice diameter	m	0.0063	0.004	0.0063	0.0155	0.004	0.0155	0.0155	0.081	0.0945	0.0945	0.0945	0.0419	0.0242	0.0242	not affects final post-expansion data; SMEDIS for FLADIS,EEC; Hanna (1991) for DT,GF
Atmospheric expansion data																
Atmospheric pressure	Pa	102000	102000	101300	100000	100000	102500	100000	90888	90990	90586	90280	101325	101325	101325	SMEDIS for FLADIS/EEC; Hanna (1991) for DT; TNER.90.015 for GF (Hanna more accurate!)
Atmospheric temperature	K	288.7	290	291	288.15	289	282.9	285	302	304	307.05	306.9	310.4	309.38	310	SMEDIS for FLADIS/EEC; Hanna (1991) for DT; TNER.90.015 for GF
Atmospheric humidity	-	0.86	0.62	0.536	0.55	0.7	0.99	1	0.132	0.175	0.148	0.213	0.0562	0.126	0.35	SMEDIS for FLADIS/EEC; Hanna (1991) for DT; TNER.90.015 for GF
PARAMETERS (values to be changed by expert users only)																
Flashing allowed to orifice?	-	FALSE														Metastable liquid assumption (frozen liquid) **or (nondefault) flashing**
Use Bernoulli model for metastable liquid releases?		FALSE														use default compressible model
Orifice L/D ratio	-	1														
ATEX expansion method (0 = min thrm change, 1 = isentropic, 2 = cons moment)	-	2														**Nondefault: conservation of momentum**
Droplet correlation (0=original CCPS, 1= JIPII, 2=TNO, 3=Tilton, 4= Melhem, 5=JIPIII, 6=modified CCPS, 7=modified CCPS excl. 2PH pipe)	-	6														Modfied CPPS droplet size calculation (default)
													27.13	10.16	10.07	Observed flow rate for GF from Table 3.1 in TNER.90.015 (used for UDM calcs.)
Description	Observ	0.4	0.27	0.46	2.9	0.11	3	3	79.7	111.5	130.7	96.7	27.67	10.46	10.27	Observed flow rate: from Hanna for DT/GF, from SMEDIS for FLADIS,EEC
	Predict	1.426133	0.920825	1.111064	1.19118	1.863356	1.195527	1.203554	1.464976	1.505258	1.294841	1.780888	1.111402	1.001237	1.025875	for FLADIS metastable better results; for EEC, DT flashing better; GF almost same
ERROR STATUS		***WARN***	***WARN***	***WARN***	***WARN***	***WARN***	***WARN***	***WARN***	***WARN***	***WARN***	***WARN***	***WARN***	***OK***	***OK***	***OK***	
Release state																
Pressure	Pa	693000	798000	570000	940000	769500	1012500	1022625	1012500	1115775	1137038	1178550	867342	894699.8	907872	
Temperature	K	286.7446	290.25	281.0403	284.05	286.15	286.45	286.65	294.7	293.3	295.3	297.3	313.15	310.95	312.55	
Liquid fraction (MASS basis)	kg/kg	1	1	1	1	1	1	1	1	1	1	1	1	1	1	
Orifice state																
Pressure	Pa	102000	102000	101300	100000	100000	102500	100000	90888	90990	90586	90280	101325	101325	101325	
Temperature	kg/kg	286.5729	290.0382	280.9139	283.3719	285.5879	285.6882	285.8753	294.4025	292.9758	294.9598	296.9364	312.8714	310.6659	312.2579	
Liquid fraction (MASS basis)	-	1.00E+00	1	1	1	1	1	1	1	1	1	1	1	1	1	
Velocity	m/s	49.27421	53.70876	43.57772	59.3913	53.25518	62.07802	62.52898	62.16053	65.41988	66.28532	67.78113	41.13356	41.73085	42.17135	
Vena contracta diameter	m	4.88E-03	3.10E-03	4.88E-03	1.20E-02	3.10E-03	1.20E-02	1.20E-02	6.27E-02	7.32E-02	7.32E-02	7.32E-02	3.25E-02	1.87E-02	1.87E-02	
Final (post-expansion) state																
Temperature	K	239.8804	239.8804	239.7426	230.7823	230.7823	231.3409	230.7823	237.5967	237.6186	237.5315	237.4653	292.7764	292.7764	292.7764	
Liquid fraction (MASS basis)	kg/kg	0.840029	8.28E-01	0.85978	0.702604	0.688616	0.690474	0.686789	0.804972	0.810237	0.802746	0.795301	0.857297	0.873391	0.861785	
Velocity	m/s	49.27421	53.70876	43.57772	59.3913	53.25518	62.07802	62.52898	62.16053	65.41988	66.28532	67.78113	41.13356	41.73085	42.17135	
ATEX outputs																
Droplet diameter	m	1.44E-04	1.22E-04	1.87E-04	4.54E-05	5.67E-05	3.97E-05	4.06E-05	1.08E-04	9.78E-05	9.67E-05	9.29E-05	3.60E-04	3.54E-04	3.54E-04	
Flashing or mechanical (1 = mechanical, 2 = flash, 3 = transition)	-	1	1	1	1	1	1	1	1	1	1	1	2	2	2	
ATEX expansion method (1 = isentropic, 2 = cons momentum)	-	2	2	2	2	2	2	2	2	2	2	2	2	2	2	
Expanded diameter	m	5.18E-02	3.40E-02	4.90E-02	9.68E-02	2.55E-02	9.73E-02	0.098936	0.768146	0.885142	0.90201	0.917972	0.220967	0.120745	0.125752	
Partial expansion energy	J/kg	-9.55E+02	-1069.59	-747.668	-521.6	-1014.24	-555.684	-556.245	-1139.79	-838.102	-993.043	-1125.03	629.7134	685.458	681.7128	
Other data																
Discharge coefficient	-	0.6	0.6	0.6	0.6	0.6	0.6	0.6	0.6	0.6	0.6	0.6	0.6	0.6	0.6	
Mass release rate	kg/s	5.70E-01	0.248623	0.511089	3.454422	0.204969	3.586581	3.610661	116.7585	167.8362	169.2357	172.2119	30.75249	10.47294	10.53573	
Release duration	s	3600	3600	3600	3600	3600	3600	3600	3600	3600	3600	3600	3600	3600	3600	

Table 2. DISC input spreadsheet for large-scale flashing experiments (FLADIS, EEC, DT, GF) – metastable liquid assumption

	FLAD 9	*FLAD 16*	*FLAD 24*	**EEC170**[xvii][vii]	*EEC360*	*EEC550*	*EEC560*	*DT1*	*DT2*	*DT3*	*DT4*	*GF1*	*GF2*	*GF3*
FLOW RATE														
Observed, kg/s	0.4	0.27	0.46	2.9	0.11	3	3	79.7	111.5	130.7	96.7	27.67	10.46	10.27
Predicted (metastable)	0.57	0.25	0.51	3.45	0.20	3.59	3.61	116.8	167.8	169.2	172.2	30.75	10.47	10.54
Predicted (flashing)	0.15	0.08	0.13	2.78	0.11	2.89	2.92	63.0	116.1	110.9	108.2	30.69	10.46	10.52
Pred./Obs. (metastable)	**1.43**	**0.92**	**1.11**	1.19	1.86	1.20	1.20	1.46	1.51	1.29	1.78	1.11	1.00	1.03
Pred./Obs. (flashing)	0.38	0.28	0.29	**0.96**	**0.99**	**0.96**	**0.97**	**0.79**	**1.04**	**0.85**	**1.12**	1.11	1.00	1.02
SMEDIS														
Liquid Fraction	0.84	0.83	0.83	0.72	0.71	0.70	0.70	0.82	0.82	-	-	-	-	-
Velocity (m/s)	65.17	67.85	55.87	85.21	84.2	68.5	89.03	90.3	72.7	-	-	-	-	-
DISC (conservation of momentum; metast.)														
Liquid Fraction	**0.84**	**0.83**	**0.86**	0.70	0.69	0.69	0.69	0.80	0.81	0.80	0.80	0.86	0.87	0.86
Velocity (m/s)	**49.3**	**53.7**	**43.6**	59.4	53.3	62.1	62.5	62.2	65.4	66.3	67.8	41.1	41.7	42.2
SMD (µm)	**144**	**122**	**187**	45	57	40	41	108	98	97	93	360	354	354
DISC (conservation of momentum; flashing)														
Liquid Fraction	0.84	0.83	0.86	**0.70**	**0.69**	**0.69**	**0.69**	**0.81**	**0.81**	**0.80**	**0.80**	0.86	0.87	0.86
Velocity (m/s)	122.7	119.4	113.1	**65.6**	**82.2**	**68.3**	**68.7**	**82.2**	**71.1**	**75.0**	**79.2**	41.3	41.8	42.3
SMD (µm)	23	25	28	**325**	**268**	**319**	**318**	**275**	**316**	**304**	**293**	348	344	343
Phast (Isentropic; metastable)														
Liquid Fraction	0.85	0.84	0.87	0.73	0.72	0.72	0.72	0.82	0.83	0.82	0.82	0.86	0.88	0.87
Velocity (m/s)	201.8	216.9	178.1	172.0	176.5	178.0	180.4	246.0	241.0	249.5	258.1	70.7	66.0	69.9
SMD (µm)	113	102	131	141	137	136	134	84	87	82	77	265	275	267

Table 3. Large-scale flashing experiments: flow rate predictions, SMEDIS versus Phast 7.1 post-expansion predictions

[vii] Previously SMD was presumed 40 micrometer, but now it has been calculated as 45 micro meter. Given the small difference, the original value of 40 micro meter has been obtained.

4.1.2 Dispersion

The results of the statistical comparison of the UDM predictions with the centre-line concentration measurements for the continuous experiments are presented in Table 4. The following observations may be made:

- For the neutrally buoyant, Prairie Grass experiments, the UDM performance is satisfactory. The UDM significantly over-predicts the measured centre-line concentration in the case of run 7.
- The UDM predictions of the measured centre-line concentrations in the Desert Tortoise experiments are very good.
- The performance of the UDM against the EEC experiments is reasonable.
- The UDM performance is good for the centre line concentration predictions in the FLADIS experiments, with a slight over-prediction observed in general.
- The UDM under-predicts the centre-line concentrations for the Goldfish experiments. A closer investigation indicates that agreement between predicted and experimental results is good prior to the transition to passive dispersion. Downwind of the transition the under-prediction increases due to the larger passive spread rate[viii]. Furthermore, the under-prediction of the centre-line concentrations and over-prediction of the cloud width may be related to the absence of a gravity collapse criterion in the UDM.
- The UDM under-predicts the centre-line concentrations for the Maplin Sands LPG experiments. It is noted that while the Phast defaults are used here, the results are sensitive to the particular choice of parameters[ix]

The statistical comparison of the UDM cloud width predictions with the experimental data are also presented in Table 4. The following conclusions may be drawn:

- The performance of the UDM against the neutrally buoyant Prairie Grass experiments is good.
- The performance of the UDM against the aerosol releases of Desert Tortoise, EEC and FLADIS, in which both heavy and jet entrainment dominates, is reasonable.

[viii] All the validation cases were rerun with the Richardson Number transition criterion temporarily set to a lower value of 2.5. The Goldfish series of experiments were the only cases that were seriously affected, giving better comparison against experimental data. However, it was noted that the distance to passive transition increased dramatically, possibly leading to a large under-prediction of averaging time effects. With this observation in mind the Richardson number transition criterion was left at the current value of 15.

[ix] In particular the choice of number of pool observers. The default of 10 is used here but increasing this number improves agreement with observed concentrations.

Experiment / Group ID	Arcwise conc MG	Arcwise conc VG	Arcwise width MG	Arcwise width VG	Pointwise conc MG	Pointwise conc VG
Desert Tortoise[x]						
DT01	1.08	1.38	1.17	1.05	0.66	5.79
DT02	1.15	1.10	0.98	1.00	1.01	21.66
DT03	0.83	1.05	1.09	1.06	0.00	0.00
DT04	0.96	1.23	1.00	1.01	0.00	0.00
All	1.00	1.18			0.84	11.91
EEC						
EEC170	0.00	0.00	0.00	0.00	2.96	10.22
EEC560	1.30	1.07	1.83	1.48	5.33	3233.16
TUNEC360	1.82	1.48	1.48	1.20	2.28	150.94
TUNEC550	1.16	1.04	1.47	1.19	3.65	385.08
All	1.37	1.16	1.60	1.29	3.38	165.98
FLADIS						
FLADIS09	0.73	1.64	1.77	1.46	2.48	24.17
FLADIS16	0.62	1.76	1.26	1.08	1.72	12.22
FLADIS24	1.04	1.69	1.21	1.14	2.69	25.34
All	0.78	1.69	1.39	1.17	2.29	20.03
Goldfish						
GF01	0.73	1.27	0.69	1.20	0.00	0.00
GF02	0.77	1.36	0.76	1.08	0.00	0.00
GF03	1.11	1.10	0.86	1.10	0.00	0.00
All	0.87	1.22	0.77	1.13	-	-
Prairie Grass[x]						
PG07	0.27	8.28	0.62	1.26	0.00	0.00
PG08	0.88	1.26	1.0	1.01	1.19	15.96
PG09	0.70	1.24	1.45	1.15	0.00	0.00
PG13	1.17	1.32	0.00	0.00	0.00	0.00
PG15	2.20	2.15	0.57	1.39	0.00	0.00
PG17	1.84	1.57	0.64	1.33	0.45	15.44
PG34	0.64	1.22	0.00	0.00	0.00	0.00
PG41	1.41	1.30	0.00	0.00	0.00	0.00
PG50	0.76	1.23	1.29	1.07	0.00	0.00
PG58	1.48	1.27	0.00	0.00	0.00	0.00
All	0.95	1.69			0.89	15.80
Maplin Sands LPG						
MSP42	2.34	2.68	0.00	0.00	0.00	0.00
MSP43	2.10	1.77	0.00	0.00	0.00	0.00
MSP46	2.12	1.89	0.00	0.00	0.00	0.00
MSP47	1.23	1.13	0.00	0.00	0.00	0.00
MSP49	2.64	2.60	0.00	0.00	0.00	0.00
MSP50	1.67	1.37	0.00	0.00	0.00	0.00
MSP52	1.08	1.33	0.00	0.00	0.00	0.00
MSP54	2.62	2.65	0.00	0.00	0.00	0.00
All	1.87	1.83	-	-	-	-

Table 4: MG and VG values for centre-line concentrations and widths (continuous)

[x] No summary width given – mixture of Hann and SMEDIS methods

4.2 Continuous releases (angled & vertical)

In this section we are specifically concerned with continuous releases (typically vertical or angled) into a crosswind. There are a number of experimental studies to validate against here, although given the nature of the geometry these are usually wind tunnel studies of heavy gas releases, with the Engie experiments being the only field-scale cases considered. We have introduced this validation set from Phast 8.6 to coincide with the "Morton extended" model being introduced as default. This model addresses observations that for previous releases of Phast there has been a systematic tendency to underestimate near-field dispersion distances for vertical releases.

In most of these experiments, arrays of sensor locations are arranged vertically at fixed downwind locations on the centre line, and the concentration distribution along the vertical array reported. An example is shown in Figure 1. At each downwind observation location we can use the maximum concentration and the height at which this concentration was observed for comparison with calculations[xi].

The validation set comprises 17 individual experiments:

- Schatzmann et al[17]. : 4 wind-tunnel experiments, all vertical.
- Donat[18]: 9 wind-tunnel experiments, 6 vertical, 1 angled, 2 horizontal.
- Vidali et al.[19]: 1 vertical wind-tunnel experiment.
- Quillatre[20] (Engie): 3 field experiments, 2 vertical, 1 horizontal

All wind-tunnel cases have been simulated at field-scale rather than wind-tunnel scale, and the appropriate input data are presented in Table 5

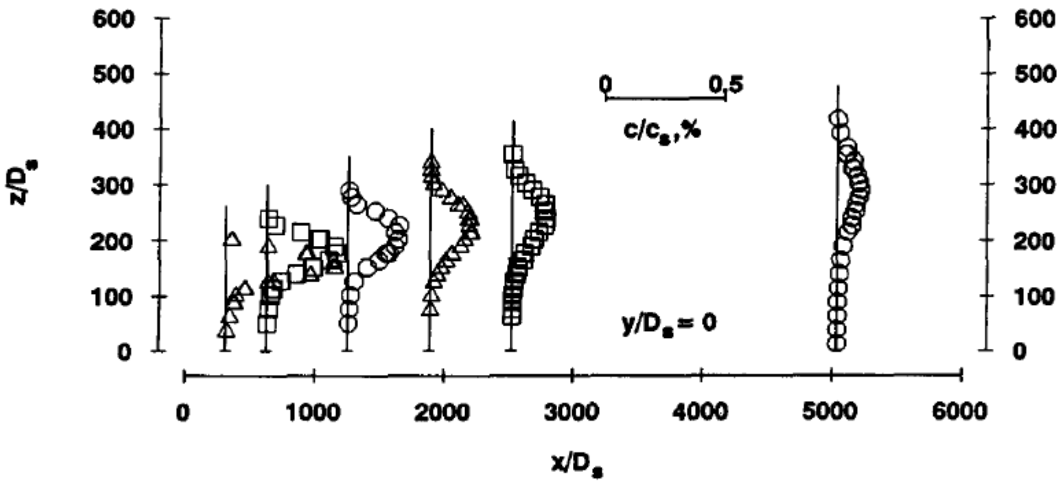

Figure 1: Concentration reporting in crosswind experiments (from Schatzmann et al)

[xi] This way we can separate out trajectory and entrainment comparisons. If we were to use concentrations at specific (sensor) points, a poor estimate of height would inevitably lead to a low concentration prediction.

	S4	*S10*	*S11*	*S13*	*D1*	*D3*	*D4*	*D5*	*D10*	*D11*	*D19*	*D21*	*D44*	*V1*	*ENH6*	*ENV6*	*ENV18*
Release angle	90	90	90	90	90	90	90	90	45	90	0	90	0	90	0	90	90
Release rate, kg/s	23.9	57.9	57.9	212.3	21.7	31.9	31.9	116.9	45.4	29.3	34.1	31.8	52.5	43.6	0.57	0.43	1.02
Density [at release] (kg/m3)	2.0	2.77	2.77	5.88	1.88	2.77	2.77	5.88	2.77	2.77	2.77	2.77	2.77	1.83	1.38	1.38	1.38
Release temperature (°C)	19.5	19.5	19.5	19.5	19.85	19.85	19.85	19.85	19.85	19.85	19.85	19.85	19.85	20	-122.2	122.2	122.2
Ambient temperature (°C)	19.5	19.5	19.5	19.5	19.85	19.85	19.85	19.85	19.85	19.85	19.85	19.85	19.85	20	20	20	20
Vent diameter (m)	0.159	1.27	1.27	1.27	0.58	1.00	1.00	1.00	0.80	0.80	0.30	0.30	0.58	1.2	0.152	0.152	0.457
Vent elevation (m)	5.0	8.5	8.5	8.5	6.96	6.70	6.70	6.70	12.00	12.00	9.00	9.00	8.70	7.2	5.65	4.65	4.45
Wind speed at ref height (m/s)	20.70	6.66	13.39	11.49	8.91	12.32	12.92	10.62	15.68	10.14	12.04	11.23	18.34	8.81	1.38	2.17	4.73
Reference height (m)	10	10	10	10	10	10	10	10	10	10	10	10	10	10	5.7	5.7	4.15
Stability class	D	D	D	D	D	D	D	D	D	D	D	D	D	D	D	D	D
Surface roughness (m)	0.037	0.037	0.037	0.037	0.008	0.008	0.190	0.008	0.070	0.070	0.070	0.070	0.008	0.011	0.010	0.010	0.010

Table 5. Phast input data for the crosswind calculations (Schatzmann, Donat, Vidali and Engie)

Calculated MG and VG for the predicted centreline concentration at the downwind observation points are presented in Table 6 and plotted in Figure 2 where the different experiments are plotted as separate series. These use the new 'Morton extended' model.

We see particularly from Figure 2 that the data points are scattered evenly around MG=1, demonstrating that the new default model does not present any observable bias to overpredict or underpredict these experiments. Most cases sit in a narrow band around MG=1 and well within the 'factor of 2' range.

The extent of the of improvement in comparison with Phast 8.4 is shown in Figure 3, where the Phast 8.4 points can be seen to underpredict across all experiments. The extension of this model to include high velocity vertical releases is expected in future work.

Experiment / Group ID	Arcwise conc MG	VG
Continuous crosswind cases		
SC10S	1.16	1.12
SC11S	0.75	1.18
SC13S	1.37	1.26
SC4S	1.60	1.34
D10s	0.89	1.03
D11s	0.98	1.00
D19s	1.38	1.14
D1s	1.08	1.03
D21s	1.27	1.08
D3s	0.68	1.20
D44s	1.37	1.14
D4s	0.80	1.07
D5s	0.97	1.06
V1	1.21	1.08
ENGH6	1.24	1.28
ENGV18	0.56	1.44
ENGV6	1.39	1.12
Schatzmann	1.16	1.23
Donat	1.02	1.08
Vidali	1.21	1.08
Engie	1.05	1.27
All	1.07	1.06

Table 6. MG and VG values for the maximum plume centreline concentration

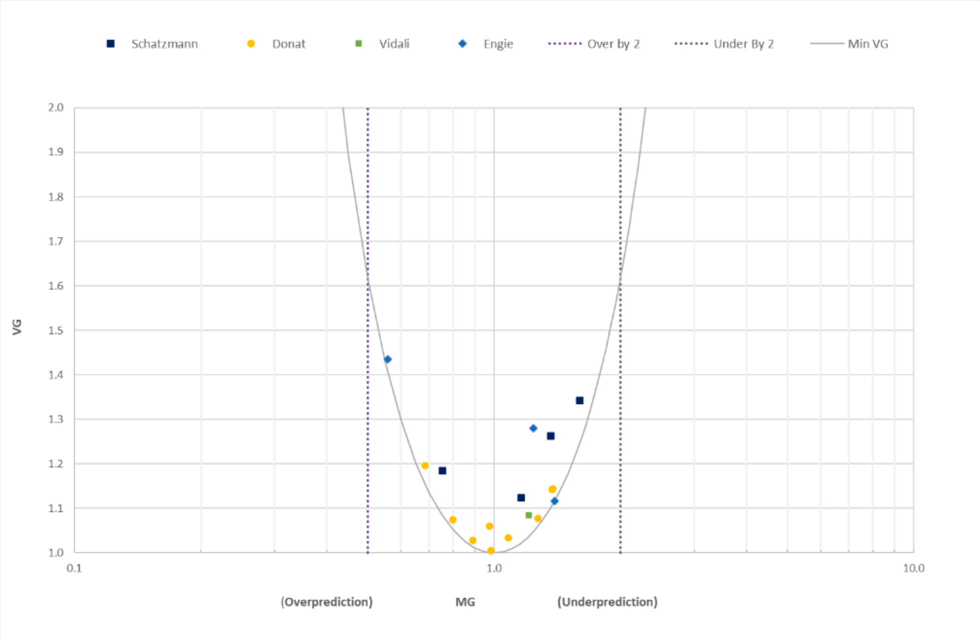

Figure 2: MG and VG plots for the plume centreline concentration

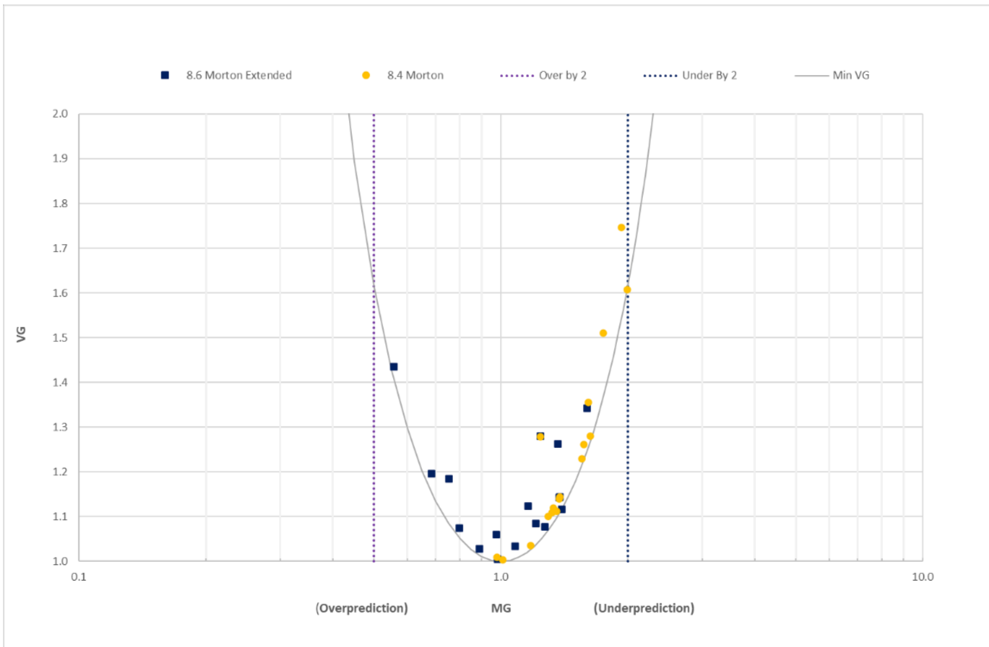

Figure 3: MG and VG plots for the plume centreline concentration (8.6 vs 8.4)

4.3 Instantaneous dispersion

Table 4 includes the results of the statistical comparison of the UDM predictions of the centreline concentration with the measured experimental data. As can be seen the performance is somewhat variable with an overall trend towards over-predicting the experimental data. Predictions for runs 7, 9 and 12, which are at relatively low wind speeds, are less accurate.

Experiment / Group ID	Arcwise conc MG	VG
Thorney Island (inst)		
TI06	1.07	1.10
TI07	1.37	1.30
TI08	0.88	1.18
TI09	1.53	1.33
TI12	1.41	1.41
TI13	0.85	1.10
TI17	0.53	1.78
TI18	0.53	1.61
TI19	0.64	1.29
All	0.87	1.35

Table 7. MG and VG values for centre-line concentrations (instantaneous),

4.4 Pressurised CO2 releases (BP and Shell experiments)

Figure 4 depicts the Phast modelling of discharge and dispersion for an elevated two-phase pressurised release. The discharge modelling includes the expansion from orifice (pipe exit) conditions to atmospheric pressure during which liquid to solid/vapour expansion occurs. In case of initial supercritical temperature (above 31ºC), vapour to vapour, or vapour to two-phase solid-vapour expansion occurs. The applied Phast discharge models are DISC (steady-state releases) and TVDI (time-varying releases) and they predict the post-expansion conditions subsequently used as the source term (starting condition) for the UDM dispersion model. The discharge and dispersion modelling allows for the presence of solid CO_2 downstream of the orifice/pipe exit.

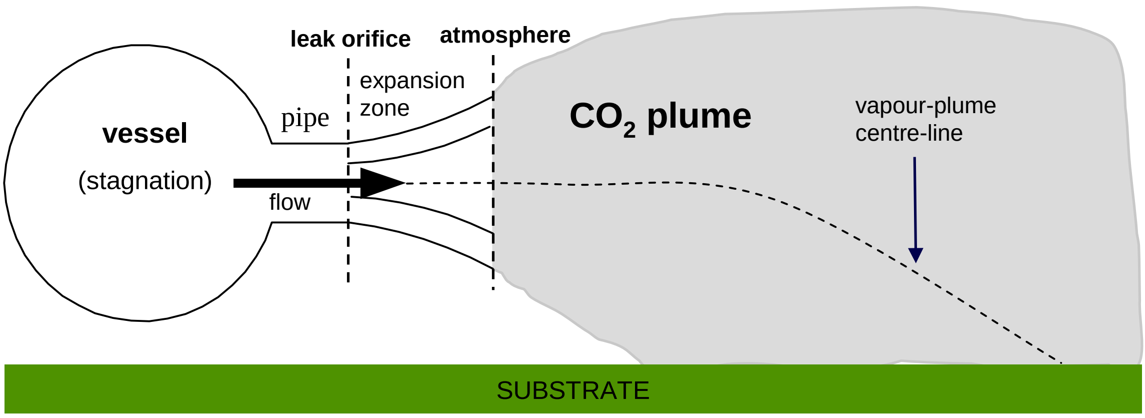

Figure 4. Discharge modelling (DISC/TVDI) and dispersion modelling (UDM)

4.4.1 Phast discharge model predictions

For the Shell experiments, the flow rate and density were measured accurately using a coriolis flow meter. In addition for both the Shell and BP experiments, the vessel weight was measured using load cells. Thus for the BP supercritical vapour releases, the flow rate was derived from the measured vessel weight using load cells. For the BP cold steady-state liquid releases, the flow rate was estimated by Advantica (Evans and Graham, 2007)[21] from the load cells by assuming that the total flow rate (kg/s; derived from vessel mass as measured by the load cells) equals dM/dt = ρCO2VCO2 – ρN2VN2. Here ρCO2 is the CO2 density (kg/m3), VCO2 the CO2 volume rate (m3/s), ρN2 the nitrogen density (kg/m3), and VN2 the nitrogen volume flow rate (m3/s). Pressure and temperature were measured at a range of locations upstream of the vessel, inside the vessel, and downstream of the vessel along the pipe and the release valve.

The Phast discharge models either assume the release to be directly from an orifice from a vessel ('Leak' scenario), or from a short pipe attached to a vessel (with orifice diameter = pipe diameter, i.e. full-bore rupture). Except for the 1" orifice tests (BP test 5 and Shell tests 2,5), the observed pressure at the discharge end was seen to be very close to the observed pressure at the vessel inlet and vessel outlet. Thus the Phast 'Leak' scenario was applied, while neglecting the pressure loss from the stagnation conditions to the nozzle conditions. Also the 1" orifice tests can be modelled using the 'Leak' scenario, provided that measured nozzle pressure/temperature are specified as model input instead of storage pressure/temperature (at vessel outlet).

The Phast discharge model DISC was used to simulate the steady-state liquid releases, while the Phast discharge model TVDI was used to model the time-varying releases. Default Phast parameters were applied with two exceptions. First the metastable assumption (non-equilibrium with liquid 'frozen') was not applied, but flashing was allowed at the orifice (equilibrium at the orifice) to account for the pipework upstream of the orifice. Secondly, conservation of momentum was applied for the expansion from orifice to post-expansion conditions, since this assumption was previously found to provide source terms giving the most accurate concentration predictions by the subsequent UDM dispersion model [e.g. against the SMEDIS experiments; 4.1.1 for details].

4.4.1.1 Time-varying releases

Table 8 shows that the measured initial CO2 density derived from the coriolis flow meter for the time-varying Shell tests is very close to values predicted by the Span-Wagner (SW) equation of state in line with recommendations of a report by EON (2011). Also accurate predictions are obtained of the liquid density in Phast using the (non-default)

Peng-Robinson (PR) equation of state (EOS). The default method in Phast presumes the liquid density equal to the saturated liquid density at the given temperature, i.e. independent of the pressure. This was shown to result in accurate predictions of the liquid density after depressurisation to saturated conditions, but to lead to a significant under-prediction of the initial liquid density (i.e. total initial vessel mass).
Table 8 also demonstrates that improved predictions are obtained of the initial vapour density for the hot tests 14 and 16 using the PR equation of state.

Input	Test1	Test2	Test4	Test14	Test16	Comments
storage phase	liquid	liquid	Liquid	vapour	vapour	
storage pressure (bara)	149.3	148.1	149.2	152.6	151.6	= gauge + ambient pressure
storage temperature (^oC)	26.7	24.6	20.1	71	36.7	
Predicted and measured density						
Phast default density (kg/m3)	686	719	773	445	704	Phast (default method)
Phast PR density	854	868	901	476	779	Phast (modified method)
Span-Wagner density (kg/m^3)	866	878	903	507	803	derived via interpolation of data in EON report
measured density (kg/m^3)	890	919	907	493	826	measured by Coriolis flow meter

Table 8. Predicted versus observed initial CO_2 density for time-varying Shell tests

Figure 5 includes TVDI-predicted (default Phast density) and observed values for flow rate (kg/s) versus time (s) for the time-varying releases. The thick solid lines represent the experimental data. The other lines represent TVDI predictions, while allowing flashing at the orifice.

For the liquid releases, Figure 5a includes TVDI predictions using both the default EOS and (using a new more robust development version of TVDI) the PR EOS. The default EOS predicts both the initial flow rate and the flow rate after depressurisation to saturated conditions quite accurately. However less accurate results are obtained during the regime of depressurisation to saturated, with a too rapid decrease of flow rate caused by the usage of the too low saturated liquid CO2 density. The PR EOS using a more accurate CO2 density provides more accurate predictions of the flow rate for all regimes.

For the hot vapour releases,
Figure 5b includes predictions of the current TVDI model (version 6.7) using both the default EOS and the PR EOS. For the BP tests, the observed values for the flow rates are averaged over a period over 8 seconds to reduce oscillations caused by inaccuracies of the load-cell measurements. This was not necessary for the coriolis flow meter measurements. The following can be concluded from
Figure 5b:

- For the very hot BP tests 8, 8R (storage temperature about 150oC), the vapour remains vapour within the vessel upon depressurisation (condensation not relevant), and it is seen that very close agreement is obtained between TVDI predictions and observed data using both the default and PR EOS, since they both provide very accurate predictions of CO2 vapour density.
- For the BP test 9 and the Shell test 14 (temperature about 70oC), PR EOS is seen to produce most accurate results. Furthermore the default-EOS TVDI runs are seen to terminate prematurely, which was due to convergence problems apparently caused by the release temperature being lower and closer to the critical temperature. An under-prediction of the flow rate is seen at larger times.
- For Shell test 16 the above effects are seen to be even more pronounced, since the initial storage temperature is only a few degrees above the critical temperature. At larger times the vessel fluid may become liquid, but the transition from vapour to liquid is not modelled by TVDI resulting in under-prediction.

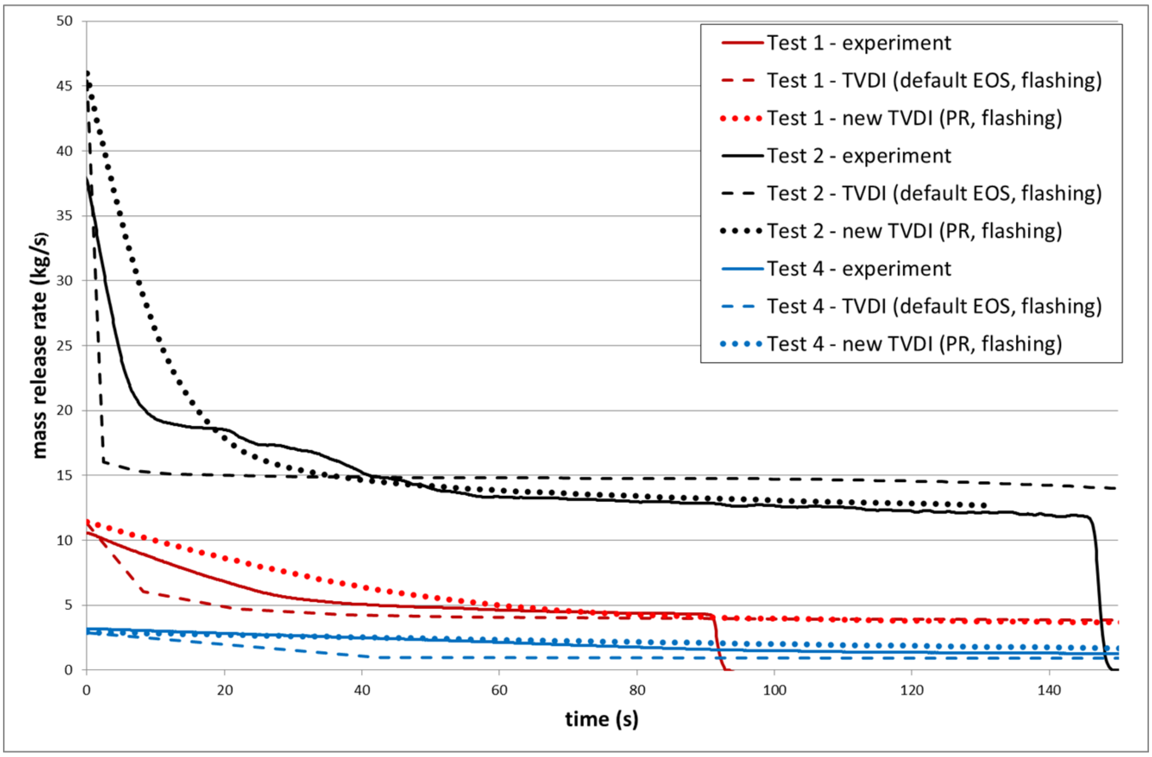

(a) cold liquid releases (Shell tests 1, 2, 4)

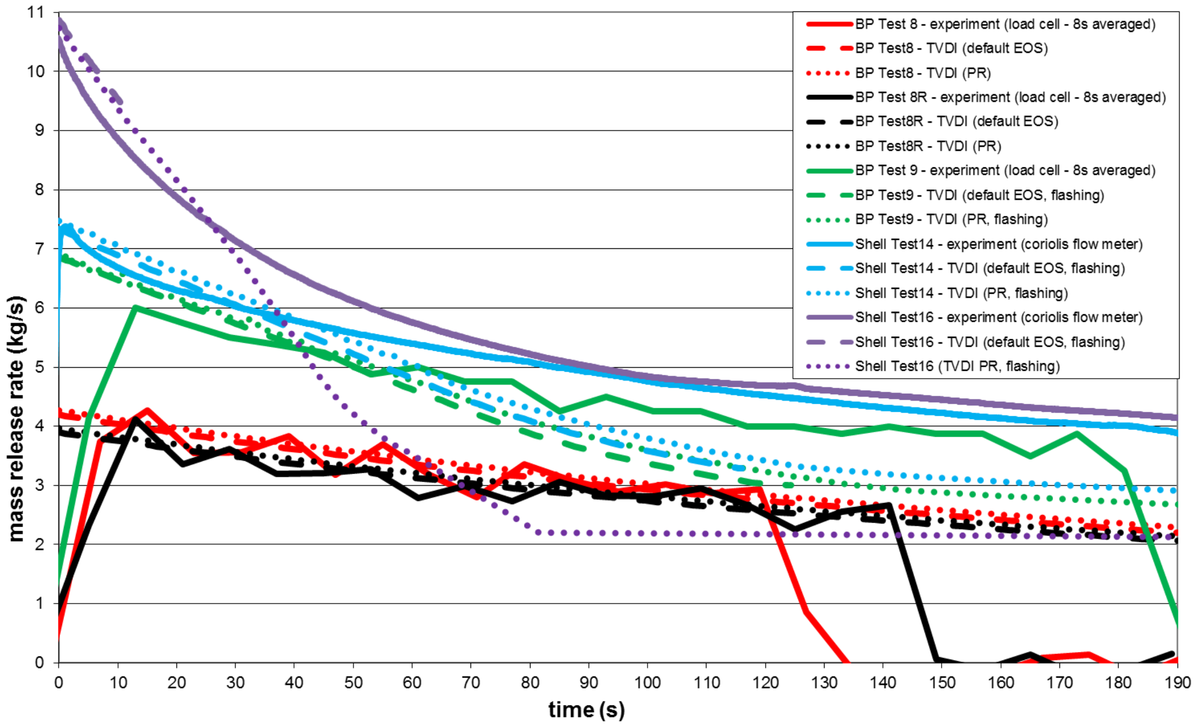

(b) hot vapour releases (BP tests 8, 8R, 9 and Shell tests 14, 16)

Figure 5. TVDI validation of flow rate for time-varying CO2 releases (BP&Shell tests)

4.4.1.2 Initial rate for steady-state and time-varying releases

BP tests

Table **29** summarises the overall results of the discharge rates for all BP tests. For the steady-state tests only the DISC initial release rate is given, while for the time-varying releases also the TVDI-predicted averaged release rate over the first 20 seconds is indicated. It is noted that the difference between the averaged and initial rate is relatively small. From the table it is seen that the time-varying Phast predictions align well with the observed discharge rate for the hot tests 8, 8R and 9. The predicted flow rate for the cold releases, with the exception of test 5 (1" release), is also very close to that of the experiments.

	Test1	Test 2	Test3	Test 5	Test6	Test 11	Test 8	Test 8R	Test 9
Discharge rate									
DISC initial discharge rate (kg/s)	8.84	10.98	9.988	50.75	3.21	7.03	4.19	3.90	6.86
DISC/TVDI discharge rate (kg/s) (averaged over first 20 seconds for tests 8,8R,9)	8.84	10.98	9.988	50.75	3.21	7.03	4.01	3.73	6.25
Observed discharge rate (kg/s) (averaged over first 20 seconds for tests 8,8R,9)	8.2	11.41	9.972	41.17	3.50	7.12	4.07	3.80	6.05
Deviation predicted from observed	7.8%	-3.9%	0.16%	+23%	-8.2%	-1.1%	-1.5%	-1.8%	+3.4%
Final (post-expansion) state (UDM input)									
Discharge rate (kg/s) (from experiments)	8.2	11.41	9.988	41.17	3.50	7.12	4.07	3.80	6.05
Temperature (K) (DISC output)	194.6	194.1	194.26	194.4	193.8	194.1	198.2	204.8	194.1
Solid fraction (-) (DISC output)	0.397	0.403	0.384	0.399	0.397	0.330	0	0	0.154
Velocity (m/s) (DISC output)	156.7	189.8	179.2	191.7	191.3	154.2	466.5	472.8	289.0

Table 9. Predicted versus observed flow rates; UDM source-term data (BP CO_2 tests)

For test 5 (1'' release) the flow rate is over-predicted with 23% (50.74 kg/s predicted versus 41.17 kg/s experimental) using the 'Leak' scenario, while using the pipe ('Line Rupture') scenario it is under-predicted with 34.5% (26.95 kg/s predicted versus 41.17 kg/s). The over-prediction for the orifice scenario is believed to be caused by the fact that pressure loss is ignored along the pipework (hose/spool/nozzle). Test 5 has the largest orifice diameter (1") and therefore will be most susceptible to upstream pressure loss and reduced flow rate. Indeed if a more accurate pressure would be applied of 128.6 barg (corresponding to averaged observed pressure close to the orifice) a release rate of 45.34 kg/s is predicted using the 'Leak' scenario corresponding to a much smaller over-prediction of 10.1%.

As indicated above the flow rate changes little for the time-varying tests 8, 8R, 9 within the first 20 seconds, and it is believed that within 20 seconds the maximum concentrations will be achieved within the first 80 meter (given relatively large initial jet momentum and relatively large values of wind speed). Therefore in the next section the dispersion calculations are modelled as steady-state using the averaged flow rate over the first 20 seconds for tests 8, 8R and 9, while for the other tests the values observed over the duration is adopted; see Evans and Graham[21] on further details of the evaluation of the observed flow rate. All other UDM input data (temperature, solid fraction, velocity) are chosen as predicted above by the discharge model DISC.

Shell tests

Table **10** summarises the overall DISC predictions of the initial discharge rates for all Shell tests. In this table a range of model assumptions is applied:

- Time-varying releases are calculated either based on measured initial storage (vessel outlet) pressure/temperature or measured initial nozzle pressure/temperature; as expected, particularly for the largest 1" orifice size (test 2), usage of nozzle data significantly improves the predictions given the significant pressure decay between storage and nozzle conditions; for the smallest ¼" orifice size identical results are obtained because of negligible pressure decay.
- Phast liquid density either based on default (saturated density) or more accurate Peng Robinson density, with more accurate results obtained using the Peng-Robinson equation of state
- Flashing (non-default Phast) or non-flashing (default Phast; metastable liquid assumption). Using Peng-Robinson density, this is seen to affect results very little. Using the saturated density, the default non-flashing option provides conservative results while the non-default flashing assumption produces significantly more accurate results.

prescribed pressure/temperature	mean nozzle			initial nozzle					initial storage (vessel discharge end)				
release type	**STEADY-STATE LIQUID**			**TRANSIENT LIQUID**			**TRANSIENT HOT**		**TRANSIENT LIQUID**			**TRANSIENT HOT**	
Shell CO_2 test number	**Test 3**	**Test5**	**Test11**	**Test1**	**Test2**	**Test4**	Test14	Test16	**Test1**	**Test2**	**Test4**	Test14	Test16
Predicted flow rate (kg/s)													
- default density, flashing	11.93	43.38	8.89	11.23	40.90	2.85	7.82	10.92	11.29	45.36	2.85	7.33	10.87
- default density , no flash.	13.58	50.88	10.21	13.61	49.48	3.39	7.46	Error	13.95	55.30	3.39	7.22	Error
- PR density, flashing	12.37	44.36	9.10	11.38	41.26	2.92	7.67	10.88	11.40	45.94	2.92	7.45	10.74
- PR density, no flashing	12.16	43.92	9.29	11.12	41.15	2.85	7.71	Error	11.06	44.71	2.85	7.45	Error
Observed flow rate	**12.4**	**44.7**	**8.9**	**10.55**	**38**	**3.17**	**7.37**	**10.5**	**10.55**	**38**	**3.17**	**7.37**	**10.5**
Ratio predicted/observed													
- default density, flashing	96.2%	97.1%	99.9%	106.4%	107.6%	90.0%	106.1%	104.0%	107.0%	119.4%	90.0%	99.5%	103.6%
- default density , no flash.	109.5%	113.8%	114.7%	129.0%	130.2%	106.9%	101.2%	Error	132.2%	145.5%	106.9%	97.9%	Error
- PR density, flashing	99.8%	99.2%	102.2%	107.9%	108.6%	92.0%	104.1%	103.6%	108.0%	120.9%	92.0%	101.1%	102.3%
- PR density, no flashing	98.0%	98.3%	104.4%	105.4%	108.3%	89.8%	104.7%	Error	104.8%	117.7%	89.8%	101.1%	Error

Table 10. Predicted versus observed flow rates – vary Phast assumptions (Shell tests)

prescribed pressure/temperature	mean nozzle			initial nozzle			initial storage	
release type	STEADY-STATE LIQUID			TRANSIENT LIQUID			TRANSIENT HOT	
Shell CO_2 test number	**Test 3**	**Test5**	**Test11**	**Test1**	**Test2**	**Test4**	Test14	Test16
Discharge rate								
DISC initial discharge rate – PR,fl. (kg/s)	12.37	44.36	9.10	11.38	41.26	2.92	7.45	10.74
Observed rate (kg/s) (initial rate for transient tests)	12.4	44.7	8.9	10.55	38	3.17	7.37	10.5
Deviation predicted from observed	-0.24%	-0.77%	2.25%	7.86%	8.59%	-8.03%	1.08%	2.26%
Final (Post Expanded) State (UDM input)								
Discharge rate (kg/s) (from experiments)	12.4	44.7	8.9	10.55	38	3.17	7.37	10.5
Temperature (K) (DISC output)	194.82	193.37	194.55	194.69	194.67	194.30	194.67	194.57
Solid fraction (-) (DISC output)	0.40	0.37	0.42	0.34	0.35	0.36	0.15	0.29
Velocity (m/s) (DISC output)	176.25	170.94	132.23	187.93	170.80	187.48	292.91	208.16

Table 11. Predicted versus observed flow rates and UDM source-term data (Shell tests)

Tab**le 11** includes results and UDM source terms based on nozzle data, the Peng-Robinson Equation of state and the flashing assumption. Note that unlike the BP experiments, the UDM dispersion data are chosen to depend on the initial rate rather than on the averaged rate during the first 20 seconds. This choice was made, since as discussed later the concentration sensors only measured accurately the initial concentration, and not the concentration at subsequent times.

4.4.2 UDM dispersion predictions

The CO2 concentration was largely measured via O2 cells for both BP and Shell experiments; see Figure 6 [taken from Allason and Armstrong (2011)[22]] for the location of the O2 concentration sensors. Thus a total of 43 sensors was applied at downstream distances of 5m (sensor OC01), 10m (OC02), 15m (OC03), 20m (OC04-OC08), 40m (OC9-OC21), 60m (OC22-OC28) and 80m (OC29-OC43), with sensors position at a range of different heights (0.3, 1 or 3 m) and cross-stream distances (between -20 and +20 degrees from the release direction) with two additional Servomex CO2 analysers.

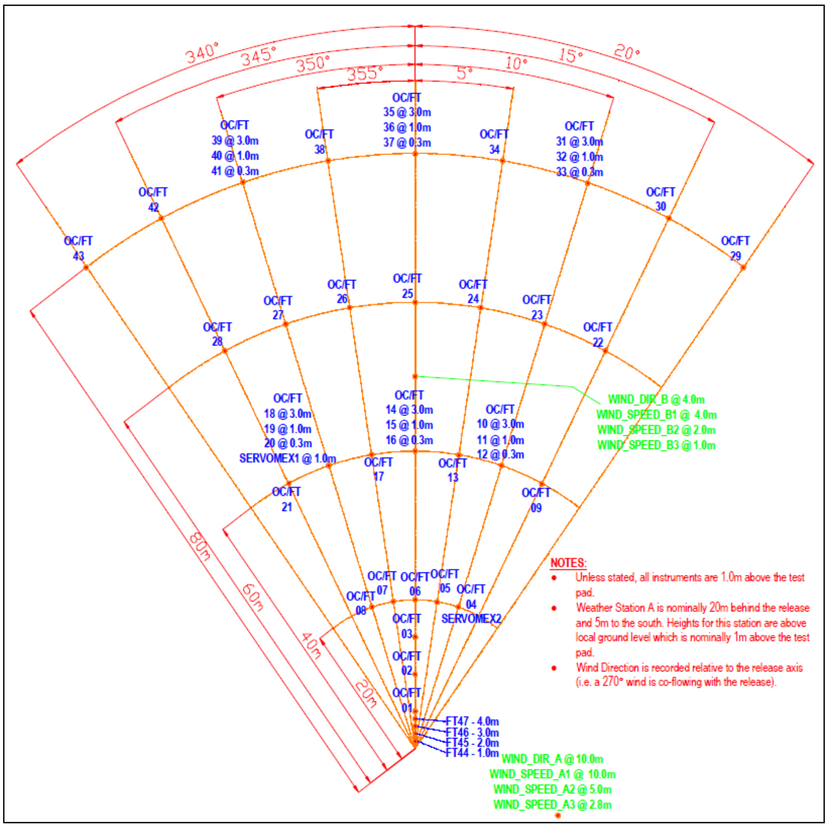

Figure 6. Field detector array for concentration measurements (Shell CO2 tests)
Figure corresponds to Shell tests, but concentration sensor location is also applicable to BP tests.

Phast assumes that the release direction is the same as the wind direction, while for some of the experiments (see Table 29 and Table 30) there is a significant deviation from the wind direction. This may lead to less accuracy of the predictions in the far-field but will not significantly affect the prediction for the momentum-driven dispersion in the near-field.

<u>BP tests</u>
Figure 7 plots for test 11 the maximum values over time of the measured concentration along with the Phast predicted concentrations as a function of downstream distance. The measured data include the maximum concentration of the raw data over all times, 11-second, 20-second and 59-second averaged concentrations. For the measured data at a given downstream distance the maximum value of all sensors at that distance is taken, Sensor 14 (located at 40m downstream, 3 meter height) has been excluded since it appeared to give erroneous too high readings (higher than sensors at 1 meter height and sensors further upstream). Furthermore no further analysis has been carried out (e.g. via spline fitting of the measured values to obtain a better fit of the crosswind concentration profile and a better estimate of the maximum concentration) to further refine this maximum value. The Phast predictions were found not to be affected by time-averaging effects due to plume meander (transition to passive dispersion occurring downwind of 80m).

In the near field (< 20 m) the 59-seconds averaged concentration predicted by Phast is close to the measured concentrations. This is also in line with UDM validation against previous experiments, where very close agreement was obtained in the near-field, jet-momentum dominated regime. Further downstream (at 20 meter and 40 meter) it is seen that the spread in the measured concentrations becomes larger with a larger effect of averaging. This is because of (a) larger relative inaccuracy of the sensors, and (b) the CO2 plume centre-line more likely to be further away from the sensor (also because of plume meander). Thus for this case, as is clearly illustrated by Figure 9 , the maximum value would lead to too large (rather random) value of the maximum concentration (it would increase with the release duration), while on the other hand the 59-second averaged concentration may lead to too small values.

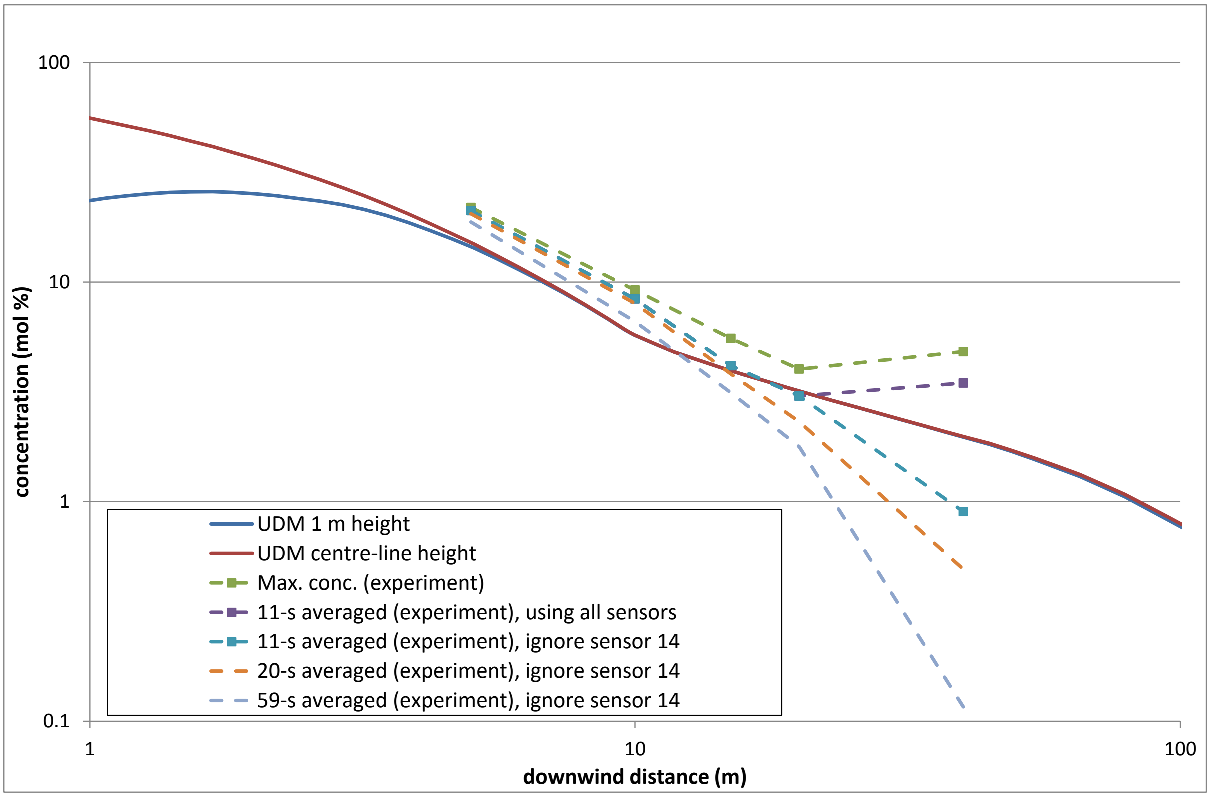

Figure 7. BP Test 11 – UDM validation for maximum contraction versus distance[xii]

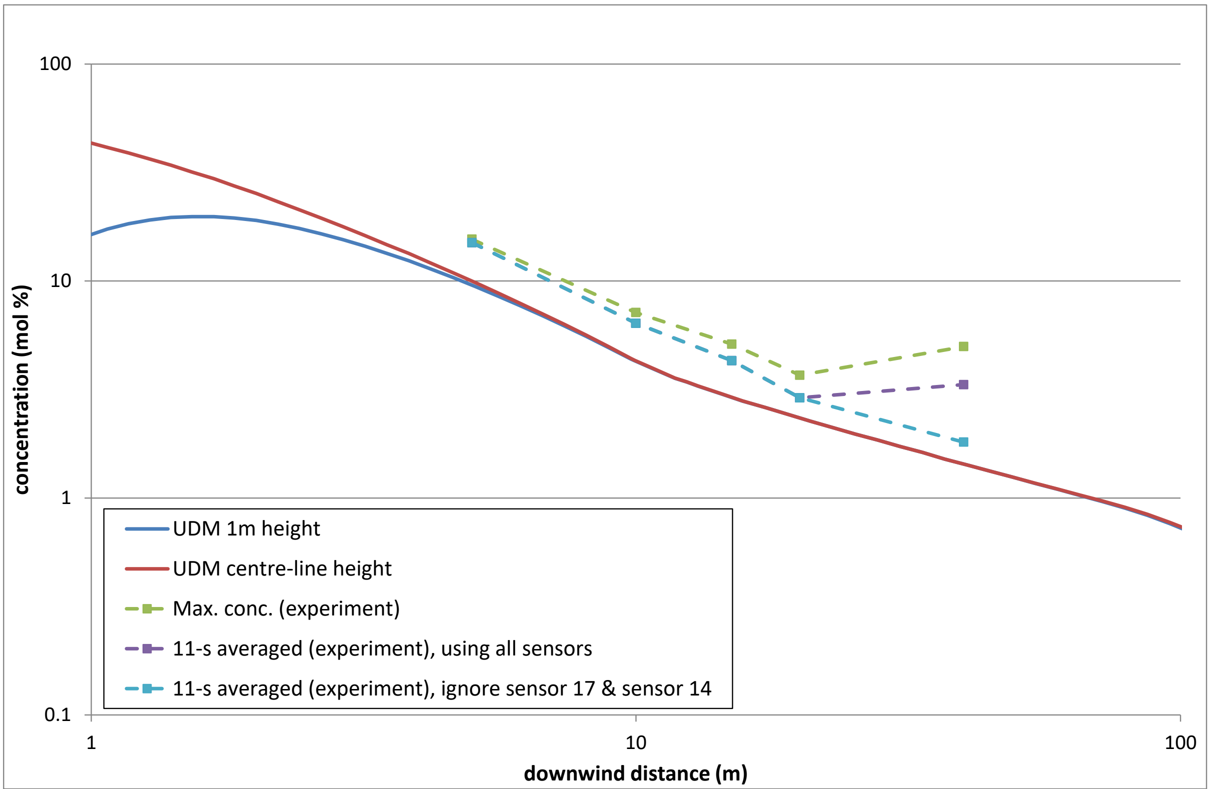

Figure 8. BP Test 9 – UDM validation for maximum concentration versus distance

[xii] Very close agreement confirmed between 7.1 and UDM AWD results; therefore no update of Figure 7, Figure 8, Figure 9, Figure 10 and Figure 11.

Figure **8** includes results of UDM validation for maximum concentration versus downstream distance for the time-varying test 9 (vapour release). It is again seen that good agreement with the processed averaged experimental data is obtained. For this test, sensors 17 and 14 were considered to give possible incorrect readings for similar reasons to sensor 14 in test 11.

Shell tests

For the Shell tests, a limited number of 3rd party commercial CO2 detectors including instruments from Draeger as well as two Servomax gas analysers were used in addition to the O2 sensors in order to verify the accuracy of the O2 sensors. From the results of this it was deduced that the O2 sensors did reasonably predict the initial (maximum) value of the concentration, but did subsequently show an erroneous decay with time which could have been caused by significant cooling of the sensors. This erroneous behaviour of the O2 sensors was confirmed by the experimentalists.

Figure 9, Figure 10 and Figure 11 plot for tests 11 (steady-state cold release), 16 (transient hot release) and 1 (transient liquid release) the maximum values over time of the measured concentration along with the Phast predicted concentrations as a function of downstream distance. The measured data include maximum values and (for steady-state test 11 only) averaged values (over release duration) for the O2 sensors, Servomax sensors, and (if present) Draeger sensors.

Overall it is seen that the maximum O2 values agree well with the UDM predictions, where negligible difference was observed between UDM predictions at 1 meter release height and centre-line (C/L) height. Because of erroneous decay with time, the averaged O2 values result in too low observed values for Test 11. The maximum concentration derived from the Draeger sensors is reasonably aligned with that derived from O2 sensors, but it is particularly less accurate in the far-field because of an insufficient number of sensors (and thus the Draeger sensors may miss the centre-line of the plume).

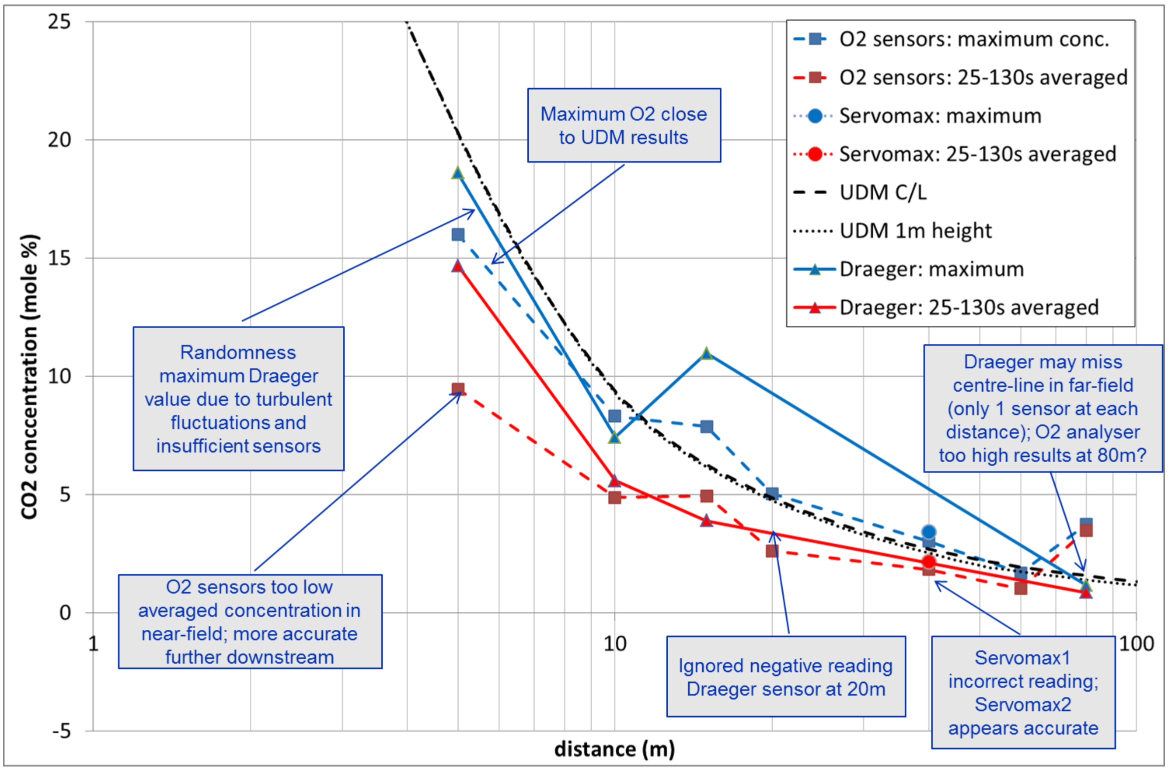

Figure 9. Shell Test 11 – UDM validation for maximum contraction versus distance

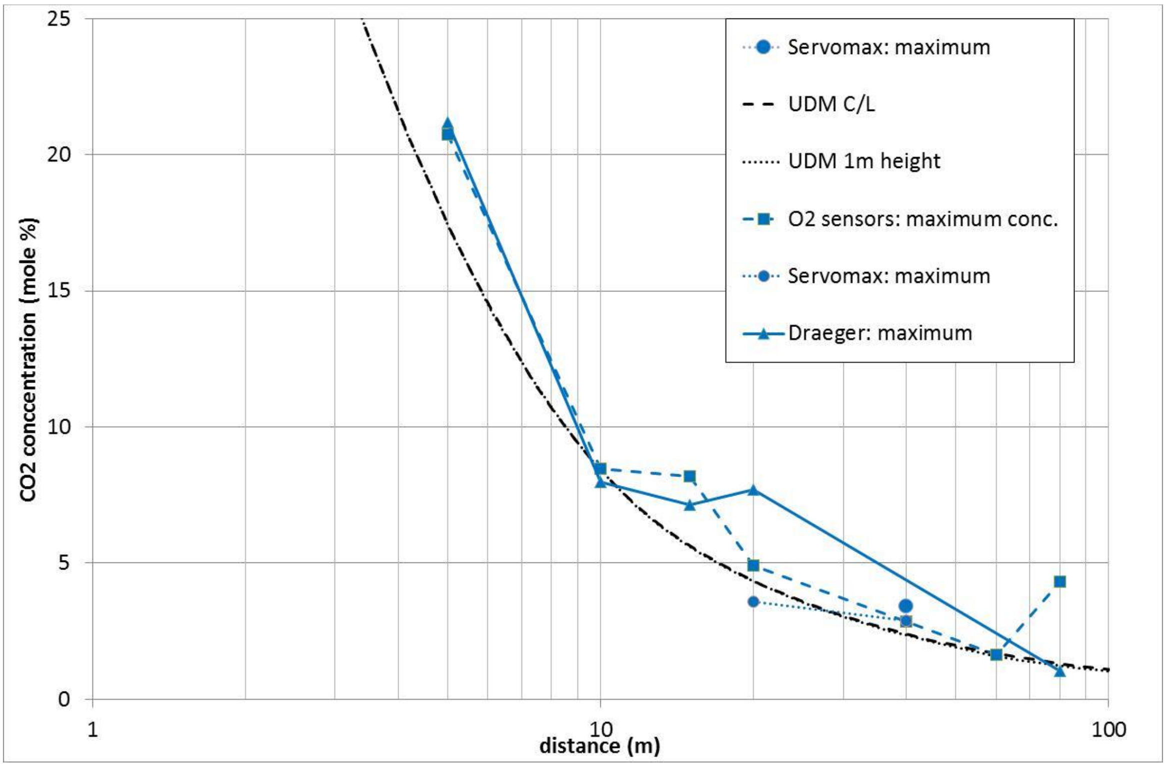

Figure 10. Shell Test 16 – UDM validation for maximum concentration versus distance

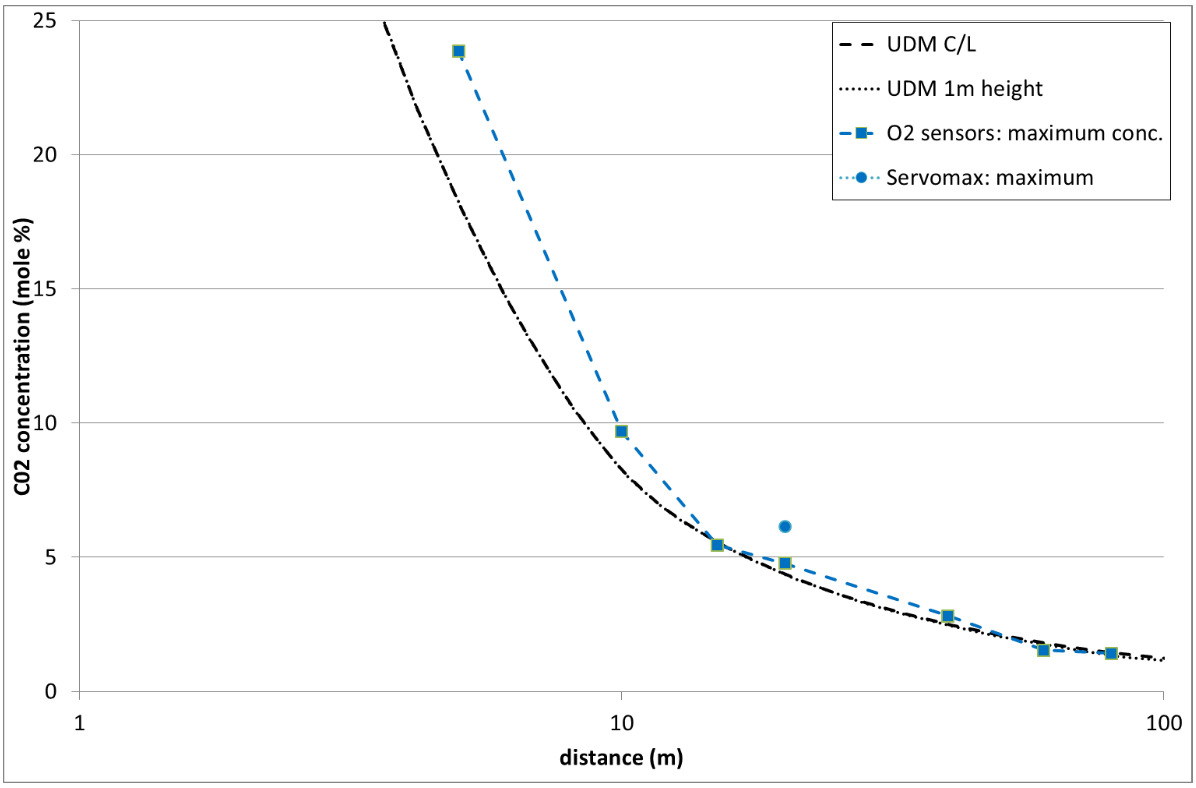

Figure 11. Shell Test 1 – UDM validation for maximum concentration versus distance

DNV

4.4.3 Comparison statistics between predicted and observed concentrations

Table 12 and Figure 12 include the predictions of MG and VG for the BP and Shell experiments. It is noted that all MG values are well within the range of [0.5, 2], and all variances less than 1.6 which is normally considered to be excellent agreement with the experimental data. In Table 12 and Figure 12 the observed maximum concentration at a downstream distance is taken as the maximum value of all sensors at that downstream distance.

Experiment / Group ID	Arcwise conc MG	Arcwise conc VG	Comments
BP CO2			
BP1	0.88	1.19	steady-state cold
BP2	1.45	1.15	steady-state cold
BP3	1.60	1.30	steady-state cold
BP5	1.58	1.24	steady-state cold
BP6	1.66	1.33	steady-state cold
BP11	1.00	1.20	steady-state cold
BP8	1.26	1.07	transient hot
BP8R	1.25	1.12	transient hot
BP9	1.41	1.13	transient hot
BPSSC	1.35	1.24	All steady-state cold
BBTH	1.31	1.11	All transient hot
All	1.34	1.19	All cases
Shell CO2			
SH3	1.37	1.11	steady-state cold
SH5	1.03	1.03	steady-state cold
SH11	1.16	1.17	steady-state cold
SH1	1.07	1.02	transient cold
SH2	1.05	1.03	transient cold
SH4	1.07	1.02	transient cold
SH14	1.20	1.08	transient hot
SH16	1.35	1.28	transient hot
SHSSC	1.18	1.10	All steady-state cold
SHTC	1.07	1.02	All transient cold
SHTH	1.27	1.17	All transient hot
All	1.14	1.08	All cases

Table 12. UDM values of MG and VG for BP and Shell CO_2 experiments

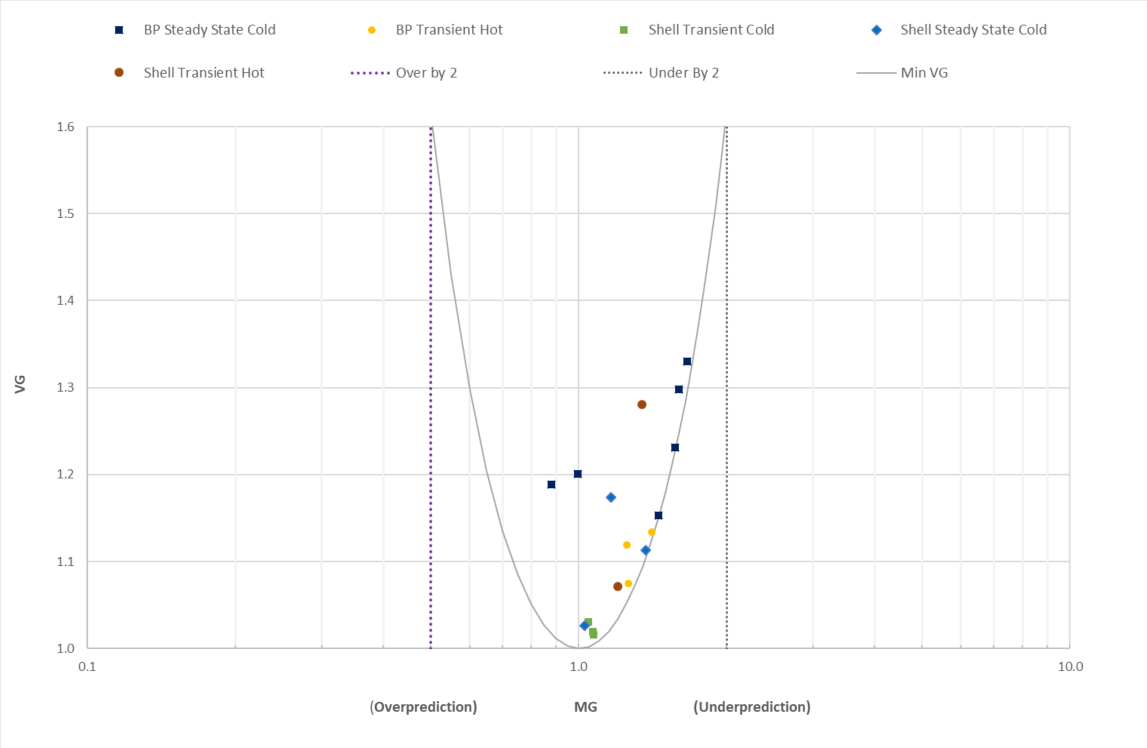

Figure 12. UDM values of MG and VG for BP and Shell CO2 experiments

For the BP experiments, the maximum value over all times of the 11-second averaged concentrations has been applied and sensors of apparent false readings have been ignored. Therefore conservative estimates are obtained of the averaged observed concentrations for the steady-state cold releases (1, 2, 3, 5, 6, 11), which may (partly) explain the under-prediction of the concentrations for the experiments 2, 3, 5, 6. For tests 1, 3, 6 there was a significant difference between the wind direction (averaged over the entire release duration) and the release direction. However the above results show that the plume centre-line did not significantly miss the sensors. Further downstream this may have been caused because we adopt 11-second averaged concentrations (maximum overall all times) rather than concentrations averaged over the entire release duration. Furthermore it must be noted that for tests 3 and 6 a 2" 1.44 m extension tube was attached downstream to the ½" (test 3) and ¼" (test 6) nozzle, which is not expected to affect the discharge flow rate but is likely to have affected the dispersion. This may explain the largest under-prediction of the concentrations (largest MG values) for tests 3 and test 6.

For the Shell experiments, maximum concentrations for the O2 sensors were used, and none of the O2 sensors was ignored even though they may provide a less accurate reading. This may have caused the overall under-prediction for the Shell experiments. Furthermore for the steady-state releases a higher accuracy is obtained than for the BP experiments, because of (a) input of more accurate measured flow rate and (b) use of conservative 11-second average estimate (maximum over all times during release duration) for the BP experiments.

4.5 Buried pipeline / Crater Releases (COSHER)

4.5.1 Facility and measurement grid

Both of the COSHER experiments used the same facility at the GL test site at Spadeadam. It comprised a 117.1 m long, 1321 mm (52") diameter steel pipeline connected to a 226.6 m long pipeline loop formed from 200 mm (8") diameter steel pipe. A 4 m rupture spool was located at the halfway point of the loop. The arrangement is shown in Figure 13 (Ahmad, et al., 2015).

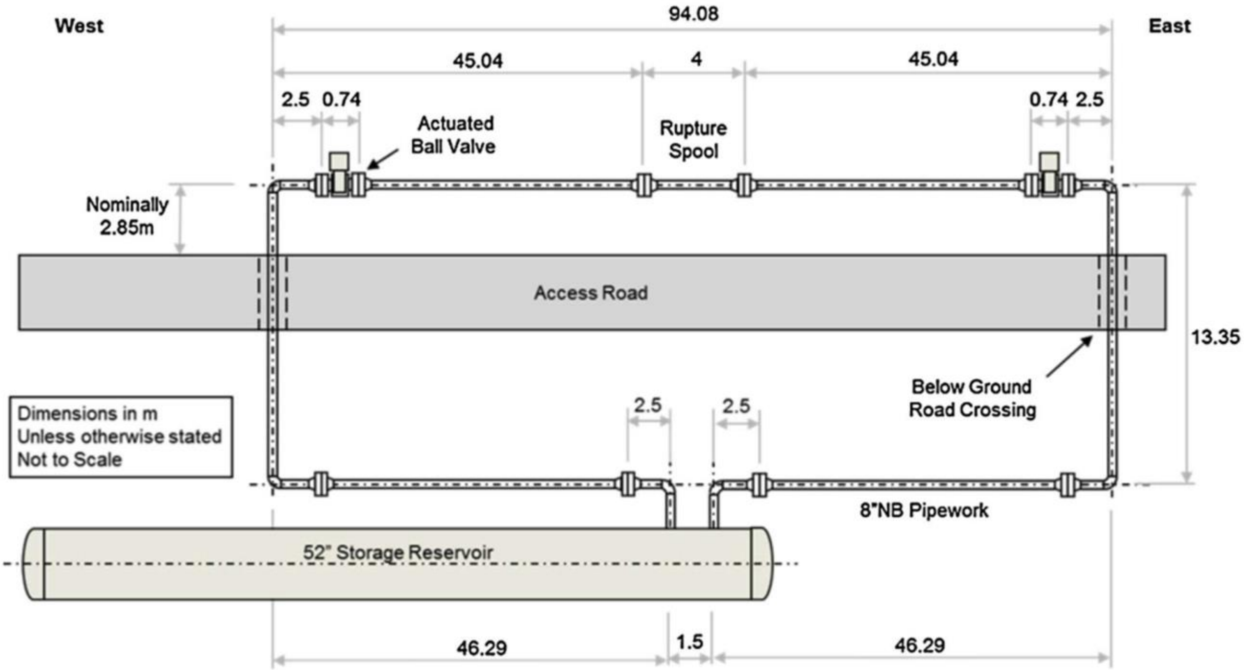

Figure 13: The experimental facility

Details of the test rig are given in Table Table 13.

Summary of dimensional and constructional information of the rig.

	Reservoir	Loop
Steel	API-5LX80	A333 grade 6
Outside diameter	1320.8	219.1
Wall thickness	25.8	12.7
Internal diameter	1269.2	193.7
Surface roughness	–	Range: 7.8–3.7 μm Ra. Average: 5.5 μm Ra
Length	117.1 m (between dome ends)	226.6
Dome end volume (each)	0.3 m^3	–
Reservoir slope	0.494°	0
Volume	148.752 m^3	6.677 m^3
Total volume	155.429 m^3	

Table 13. The COSHER test rig

The sensor locations are given for Test 1 by Lowesmith, though are likely the same for Test 2. However for each test wind direction is different, and locations must be corrected. The locations relative to a fixed grid north are shown in Figure 14.

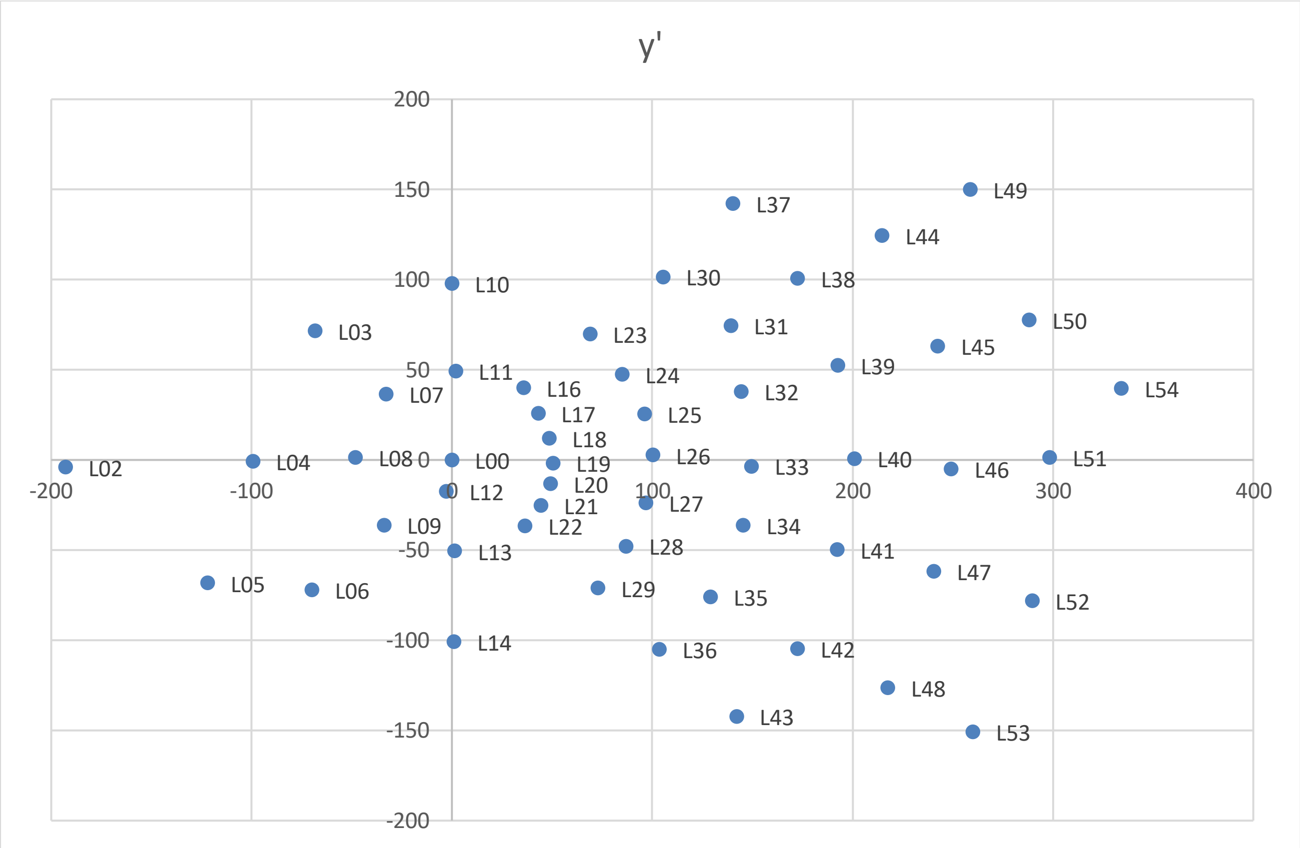

Figure 14. Instrumentation locations

Input	Test 2 (Ahmad)	Test 1 (Lowesmith)
Initial pressure (barg)	**150.8**	**151.7**
Initial temperature (degC)	**13.1**	**7.5**
Inventory (tonnes)	**146.8**	**151.4**
Ambient pressure (mbar)	**997.0**	**980.1**
Ambient temperature (degC)	**17.4**	**6.3**
Relative humidity (frac)	**0.715**	**0.796**
Windspeed (m/s)	**1.9**	**4.7xiii**
Wind reference height (m)	**?**	**5**
Wind direction relative to grid north (deg)	**261**	**255**

Table 14. The COSHER test conditions

Ahmad and Lowesmith observe that the release was (pseudo-) steady state between 50-180s (Test 2), and 50-250s (Test 1). Using the long-pipeline model as described above (i.e. in the absence of a 52" storage reservoir) produces a strongly time-varying release, and so we have represented it used a single segment averaged over a time (10 s for Test 2, 20s for Test 1) such that the rate closely matches the experimentally observed one. The resulting source term is shown in Table 15.

[xiii] Using location L02 as suggested in text

Result	Phast prediction COSHER 2	COSHER 1	Notes
Release rate (kg/s)	754	618[xiv]	Matched by varying averaging time
Release duration (s)	153	200	Inventory released in 1 hr
	Post-expansion		
Temperature (degC)	-78.6	-78.6	Solid/vapour equilibrium
Solid mass fraction	0.38	0.40	
Velocity (m/s)	205.1	198.0	
	Post-crater (Defined area model)		
Solid mass fraction	0.38	0.40	
Velocity (m/s)	19.28	15.31	
Mass flow of air (kg/s)	203.2	166.6	

Table 15. Baseline Phast source term from matching release rates

4.5.2 Crater modelling

Buried pipelines invoke the crater model. This predicts the size and shape of crater formed immediately after the rupture, as well as a reduction in velocity and a mass of air entrained by mixing within the crater. These modifications are given at the bottom of Table 15. It is not clear what crater size correlations predict – averaged or maximum dimensions. Here the observed maximum dimensions are given, as these are clearer to interpret from the published information (essentially plan views).

	Width (m)	Length (m)	Depth (m)
COSHER 2			
Observed	**4.2**	**5.2**	**1.2**
Predicted	**4.36**	**5.62**	**1.08**
Ramirez-Camacho	**3.52**	**6.56**	**1.75**
COSHER 1			
Observed	**5.1**	**4.5**	**0.8**
Predicted	**4.36**	**5.65**	**1.08**
Ramirez-Camacho	**3.52**	**6.56**	**1.75**

Table 16. Maximum observed and predicted crater dimensions

Also given are the predictions of the correlations for natural gas pipelines by Ramirez-Camacho et al. (2019) derived from multivariate regression of historical accident data.

4.5.3 Concentration measurements

The UDM is run using the post-crater source term. We left all parameters at default values. Validation data came from Figures 11 and 12 in the Ahmad paper and Figures 32-35 in Lowesmith. We captured at the sampler locations the maximum concentration for each time series and compared it with Phast predicted maximum concentrations. In addition we used a subset of these as the arcwise maximum concentrations – i.e. for a given arc (50m, 100m etc) the maximum experimental concentration.
The sampler locations from the paper were adjusted to account for a wind direction offset of 9° and 15^o from the sampling grid. The local sensor heights of 1m was used universally, although Ahmad suggests some sensor locations may have been at a height of 1.8m. .

For the reduced set of arcwise maximum comparison, the Y co-ordinate of all points for the simulation was set to zero

[xiv] Not measured directly – estimated from inventories

4.5.4 Dispersion Results

The maximum concentrations (observed and predicted; arcwise and pointwise) for the two COSHER tests are shown in Figure 15 and Figure 16.

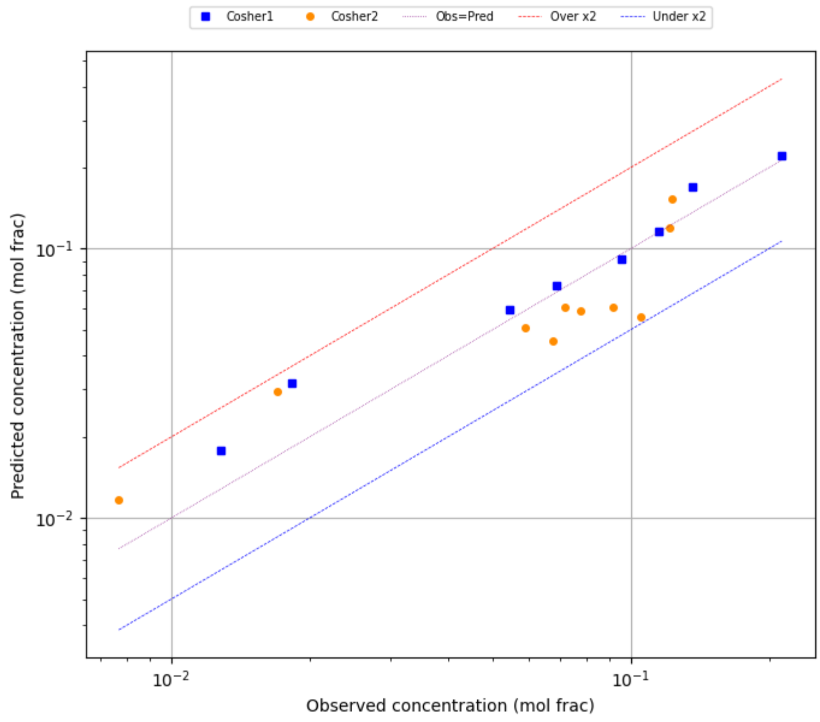

Figure 15. Maximum arcwise concentration for COSHER experiments

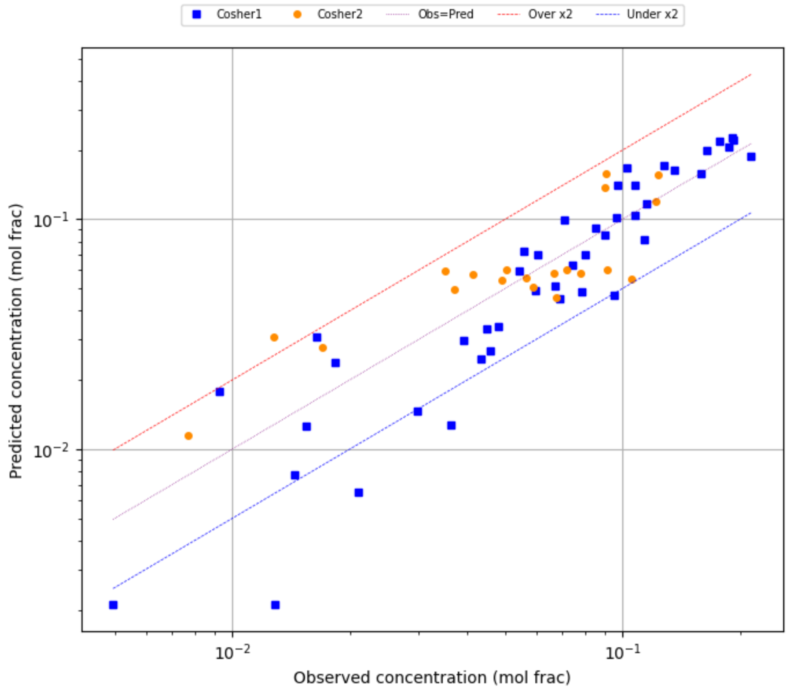

Figure 16. Maximum pointwise concentration for COSHER experiments

Table **17** gives the summary MG and VG values for arcwise and pointwise concentrations

Experiment / Group ID	Arcwise conc MG	Arcwise conc VG	Pointwise conc MG	Pointwise conc VG
COSHER				
COSHER1	0.86	1.06	1.16	1.29
COSHER2	1.09	1.15	0.90	1.17
All	0.98	1.11	1.07	1.25

Table 17. Arwise and pointwise MG/VG values for COSHER CO_2 simulations

The results indicate good agreement between Phast and the experimental concentrations. Cosher 1 does show some under-prediction at low pointwise concentrations, but this is mainly limited to concentrations below the 1% level and therefore of less interest for CO_2 toxicity.

Results are much improved over previous (v8.71 and earlier) Phast versions, which greatly under-predicted ground level concentrations – especially upwind and crosswind of the release point.

Both cases are using the new defined-area source term model, and the gas blanket dispersion model. These are the default options in v8.9 for CO_2. Those interested are referred to the Crater Model and UDM Theory technical documents for further details.

4.6 Finite-duration dispersion

4.6.1 Kit Fox experiments

UDM input data have been obtained from the MDA database given by Hanna and Chang (1999)[23]; see Appendix A.4. The ground-level area source is modelled as a circular source of vapour-phase CO_2 with diameter 1.69 m with corresponding source area A equal to that of the actual 1.5m x 1.5m square source; see Figure 17.

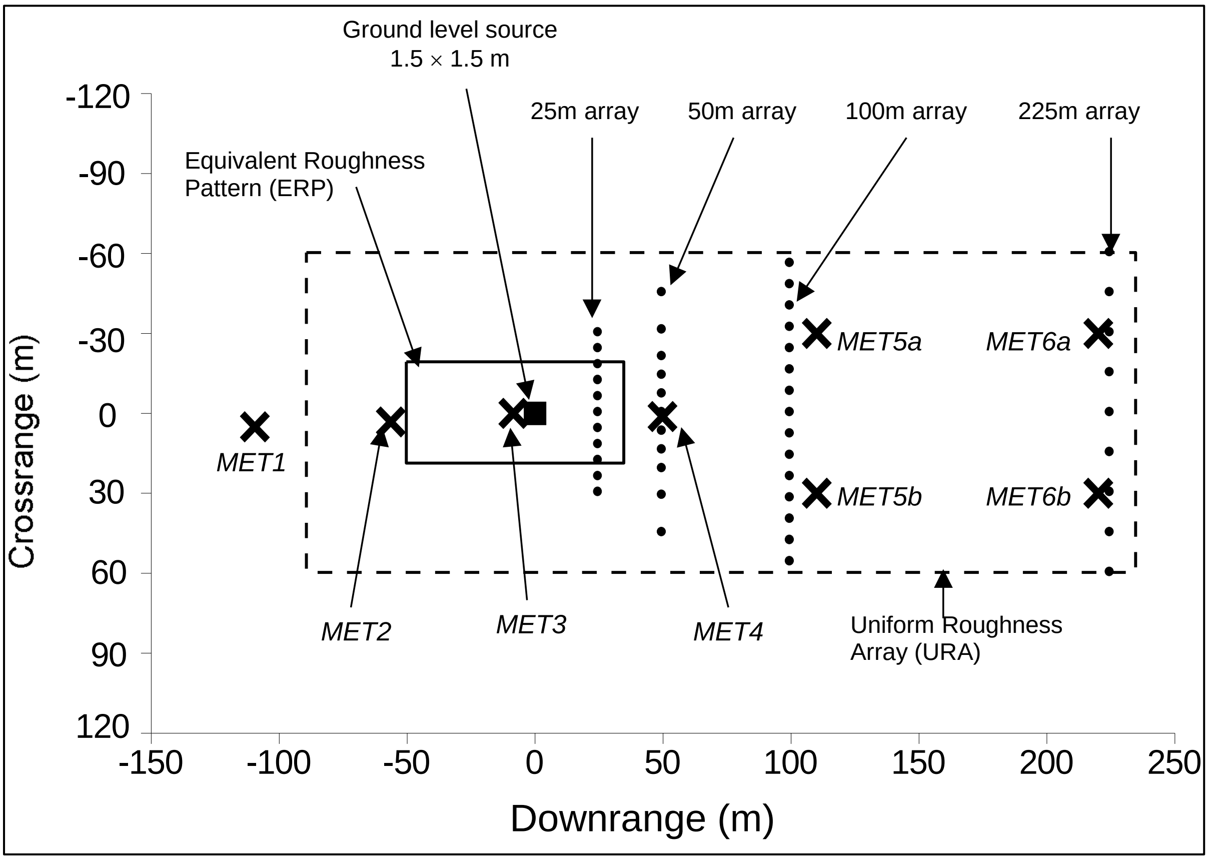

Figure 17. Plot plan of the Kit Fox site

In this section results are reported of experiments with a uniform surface roughness only (URA; roughness estimated between 0.01 and 0.02 m; adopted value 0.01m); see Table 18.

Kit Fox Series (URA)	duration (s)	flow rate (kg/s)	release velocity (m/s)	Experiments grouped by stability class		
				D	E	F
continuous	≥ 120	1.5-2.1	0.4-0.6	604, 805	702,808,605,703,705	606,811,709, 609,712
puff	20	1.1-1.8	0.3-0.5	801,601,803,802, 804,602,603,806	807,809,706,810,812	704,708,710,607,711, 608,714

Table 18. List of URA Kit Fox experiments for UDM validation

The release is modelled from an area source where observers are released from the upstream edge. The ground-level cloud is modelled physically more correctly above the source and in the near-field. No additional time-averaging applied to the calculated concentrations at each arc.

Table 19 presents the predictions of MG and VG for the KitFox URA experiments. The individual results are split into continuous and puff experiments. Combined results by stability are also provided. A graphical presentation of the overall MG and VG validation results for the arc-wise concentrations from Table 19 is shown in Figure 18. The overall results can be summarised as follows:

- URA continuous: excellent prediction for both concentration and cloud widths
- URA puff: there is over-prediction for, all results. This is most pronounced for the D weather state, reducing for E and is much improved for F (only a slight over-prediction).

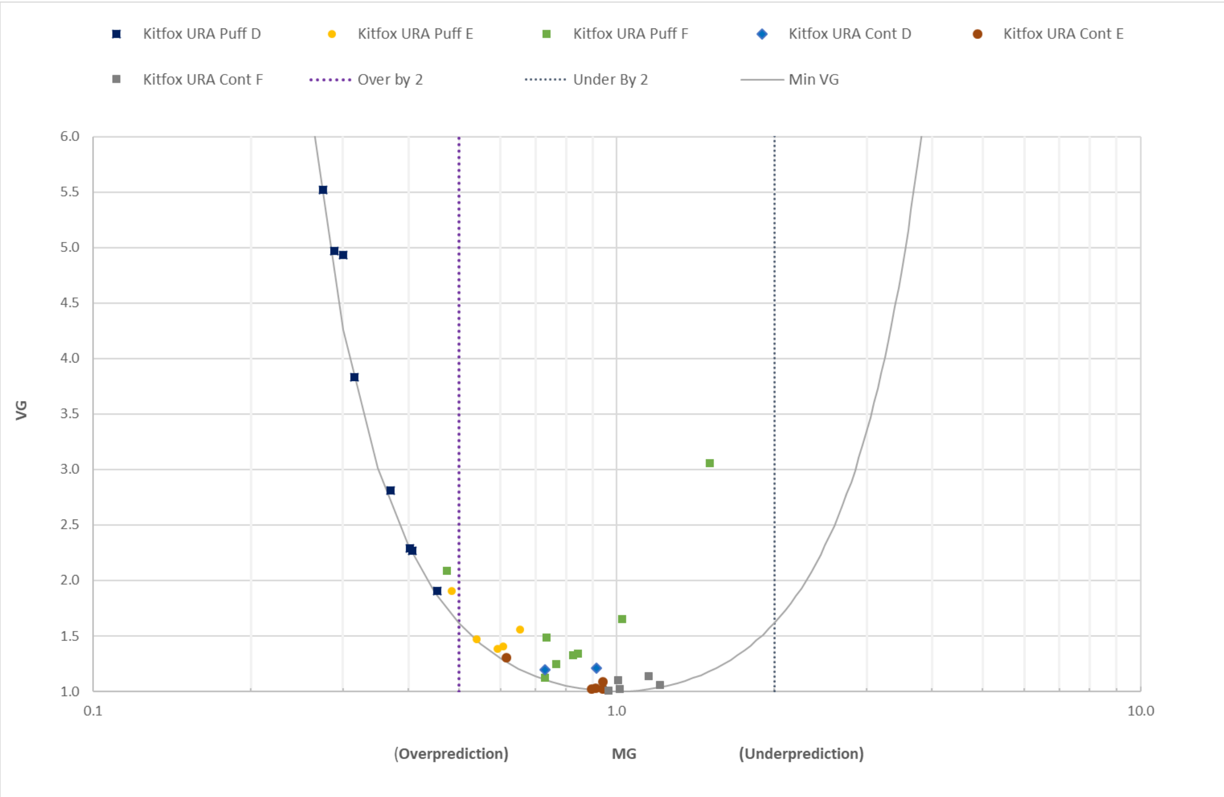

Figure 18. UDM validation statistics for Kit Fox URA experiment

Experiment / Group ID	Arcwise conc MG	Arcwise conc VG	Width MG	Width VG	Comments
KitFox URA (Continuous)					
KF0604	0.91	1.21	0.88	1.03	Kitfox URA Cont D
KF0805	0.73	1.20	0.99	1.01	Kitfox URA Cont D
KF0605	0.94	1.09	0.81	1.06	Kitfox URA Cont E
KF0702	0.90	1.02	1.18	1.06	Kitfox URA Cont E
KF0703	0.91	1.03	1.30	1.09	Kitfox URA Cont E
KF0705	0.95	1.02	1.19	1.04	Kitfox URA Cont E
KF0808	0.61	1.30	1.08	1.02	Kitfox URA Cont E
KF0606	1.15	1.14	0.98	1.02	Kitfox URA Cont F
KF0609	1.01	1.02	1.12	1.01	Kitfox URA Cont F
KF0709	0.96	1.01	0.90	1.03	Kitfox URA Cont F
KF0712	1.21	1.06	1.34	1.15	Kitfox URA Cont F
KF0811	1.00	1.10	0.81	1.07	Kitfox URA Cont F
Continuous D	0.81	1.20	0.93	1.02	Continuous, Weather D
Continuous E	0.85	1.09	1.09	1.05	Continuous, Weather E
Continuous F	1.06	1.06	0.99	1.05	Continuous, Weather F
All	0.93	1.10	1.03	1.05	Continuous, All
KitFox URA (Puff)					
KF0601	0.30	4.94	0.84	1.09	Kitfox URA Puff D
KF0602	0.29	4.97	1.05	1.03	Kitfox URA Puff D
KF0603	0.45	1.90	0.79	1.06	Kitfox URA Puff D
KF0801	0.28	5.46	1.13	1.07	Kitfox URA Puff D
KF0802	0.31	3.86	0.88	1.04	Kitfox URA Puff D
KF0803	0.37	2.82	0.94	1.06	Kitfox URA Puff D
KF0804	0.40	2.29	0.91	1.03	Kitfox URA Puff D
KF0806	0.41	2.27	0.58	1.35	Kitfox URA Puff D
KF0706	0.59	1.38	0.65	1.22	Kitfox URA Puff E
KF0807	0.54	1.48	0.62	1.29	Kitfox URA Puff E
KF0809	0.61	1.40	0.73	1.12	Kitfox URA Puff E
KF0810	0.48	1.90	0.75	1.11	Kitfox URA Puff E
KF0812	0.65	1.56	0.60	1.34	Kitfox URA Puff E
KF0607	1.02	1.65	0.65	1.22	Kitfox URA Puff F
KF0608	0.73	1.48	0.65	1.22	Kitfox URA Puff F
KF0704	0.73	1.12	0.71	1.16	Kitfox URA Puff F
KF0708	0.77	1.25	0.72	1.12	Kitfox URA Puff F
KF0710	0.83	1.33	0.67	1.19	Kitfox URA Puff F
KF0711	0.84	1.34	0.67	1.19	Kitfox URA Puff F
KF0713	1.51	3.06	1.23	1.11	Kitfox URA Puff F
KF0714	0.48	2.08	1.05	1.00	Kitfox URA Puff F
Puff D	0.35	3.31	0.87	1.09	Puff, Weather D
Puff E	0.57	1.53	0.67	1.21	Puff, Weather E
Puff F	0.82	1.58	0.75	1.17	Puff, Weather F
All	0.54	2.08	0.77	1.15	Puff, All

Table 19: UDM values of MG and VG for KitFox URA experiments

4.6.2 Jack Rabbit II experiments

In 2015 and 2016 nine large (up to ~ 10 tonnes) 2-phase chlorine releases were carried out at the US Army Dugway Proving Ground in Utah. These are known as the Jack Rabbit 2 (JR2) tests. Measurements of chlorine concentrations were made out to a distance of 11 km downwind. The 2015 tests were centred in an array of shipping containers (simulating an urban environment) and the 2016 tests were carried out in flat terrain.

A number of models (including Phast) were invited to take part in the Modelling Working Group (MWG), which would simulate the tests using a standardised set of inputs and outputs. Three trials were selected: 1, 6 and 7. Trial 1 from 2015 used the array of shipping containers, while Trials 6 and 7 from 2016 did not. The results of the cross model comparison was published by Mazzola et al[24]:

Information was provided to try to standardise the input in the models participating in the MWG . The general information on the trials is provided in Table 24, and more detailed information about the release is shown in Table 21. These represent quite complex releases involving a flashing liquid, with Trials 1 and 6 impinging downwards from 1m while trial 7 impinges downwards at a 45° angle from 1.48m. Table 24 attempts to quantify how much of the initial release became vapour, and how much rained out into a pool and was subsequently evaporated. There is clearly much uncertainty around this.

Given the uncertainty around the source term, the Phast modelling of these releases has been made as simple as possible. As the release and pool evaporation are of short duration the results are actually not overly sensitive to however the source is modelled. We have taken the total vapour generation rate from the 'Modified for rainout' and 'Evaporated rainout' sections of Table 21 as a constant vapour flow rate, and modified the duration so that the total mass of vapour released is equal to that as calculated from Table 21. The Phast parameters used are presented in Table 22

	Trial 1	Trial 6	Trial 7
Release Parameters			
Location, all at Dugway Proving Grounds; Zone 12 UTM coordinates	Northing 4445633.9 m Easting 288109.2 m Elevation 1295.5 m	Northing 4445633.9 m Easting 288109.2 m Elevation 1295.5 m	Northing 4445633.9 m Easting 288109.2 m Elevation 1295.5 m
Date and Time (hh:mm:ss UTC)	24 August 2015 13:35:45	31 August 2016 14:23:35	2 September 2016 13:56:00
Tank Inventory (kg of Cl2)	4500	8400	9100
Pressure measured at top of tank (psia)[1]	104.4	86.8	86.9
Liquid temperature (ºC)[1]	15.7	16.0	15.9
Release jet orientation (deg from tank top centre)	180	180	135
Release height (m)	1.0	1.0	1.48
Hole diameter	6.0 in = 0.152 m	6.0 in = 0.152 m	6.0 in = 0.152 m
Weather/Environment			
Weather conditions			
Atmospheric pressure (mbar)	873.7	871.1	868.5
Initial wind speed[2] (m/s) at z = 2 m	1.45	2.42	3.98
Initial wind direction[2] at z = 2 m	147.4	146.9	149.6
Initial temperature (ºC) at z = 2 m	17.5	22.3	18.7
Surface roughness (mm)	0.5	0.5	0.5
Friction velocity[3], u* (m/s)	0.108	0.093	0.210
Sensible heat flux[3], Hs, (K-m/s)	-0.012	-0.0034	-0.0160
Inverse Monin-Obukhov length (m^{-1})	0.124	0.056	0.0229
Pasquill Class	E/F	E	D/E

Table 20: General information provided to modellers for Jack Rabbit II

	Trial 1	Trial 6	Trial 7
Primary release			
Discharge rate (kg/s)	224.	260.	259
Discharge period (s)	20.3	32.2	33.3
Temperature (°C)	-37.3	-37.4	-37.4
Vapor fraction (ignoring KE effects)	0.171	0.172	0.172
Density (kg/m^3)	18.32	18.15	18.12
Velocity (m/s)	50.8	44.2	44.2
Area (m^2)	0.241	0.324	0.323
Primary release modified for rainout			
Discharge rate (kg/s)	145	168	162
Discharge period (s)	20.4	32.4	33.6
Temperature (°C)	-37.3	-37.4	-37.4
Vapor fraction (ignoring KE effects)	0.264	0.266	0.274
Density (kg/m^3)	11.89	11.79	11.41
Velocity (m/s)	50.8	44.2	44.2
Area (m^2)	0.240	0.323	0.322
Evaporated rainout			
Discharge rate (kg/s)	43.2	34.0	34.0
Discharge period (s)	36.8	86.4	93.4
Temperature (°C)	-37.3	-37.4	-37.4
Vapor fraction	1	1	1
Density (kg/m^3)	3.160	3.152	3.144
Area (m^2)	491	491	491

Table 21: Detailed release data for Jack Rabbit II

	Trial 1	Trial 6	Trial 7
Primary release			
Discharge rate (kg/s)	188	202	196
Discharge period (s)	24.16	41.4	44
Temperature (°C)	-37.3	-37.4	-37.4
Vapor fraction (ignoring KE effects)	1	1	1
Density (kg/m^3)	18.32	18.15	18.12
Velocity (m/s)	50.8	44.2	44.2

Table 22: Simplified release data used in Phast model

Phast 8.23 was identified in the Mazzola paper as predicting much wider clouds to 20ppm (and 200ppm for Trial 7) than the other models, and also under-predicting concentrations in the far-field. In Phast 8.6 we have introduced the gravity spreading collapse model (GSC) to address these issues (see UDM Theory document for details), and it is therefore useful to update the results.

Calculated MG and VG for the predicted centreline concentrations and widths to 20 ppm are presented in Table 23, and the concentrations are also plotted in Figure 19. The equivalent calculations without the new gravity spreading collapse model are presented in Figure 19 for comparison. We see a significant improvement in the concentration prediction with GSC activated, with a clear move away from under-prediction. It follows that Phast 8.6 results are significantly improved over Phast 8.23.

The MG/VG analysis can mask the detail of the changes in the calculation, and what we are seeing is similar concentrations in the near to mid-field, but GSC overall maintaining a higher concentration in the far field. An example of this is presented in the concentration vs distance plot in Figure 20, where the impact of GSC specifically on far field concentrations is more evident.

Experiment	Arcwise conc		Max Width to 20 ppm	
/ Group ID	MG	VG	MG	VG
Jack Rabbit II chlorine cases				
Trial 1	1.01	1.51	0.27	5.75
Trial 6	0.67	2.36	0.31	4.03
Trial 7	1.41	1.74	0.38	2.54
All	0.98	1.87	0.32	3.89

Table 23: MG and VG values for the plume centreline concentration and width to 20 ppm

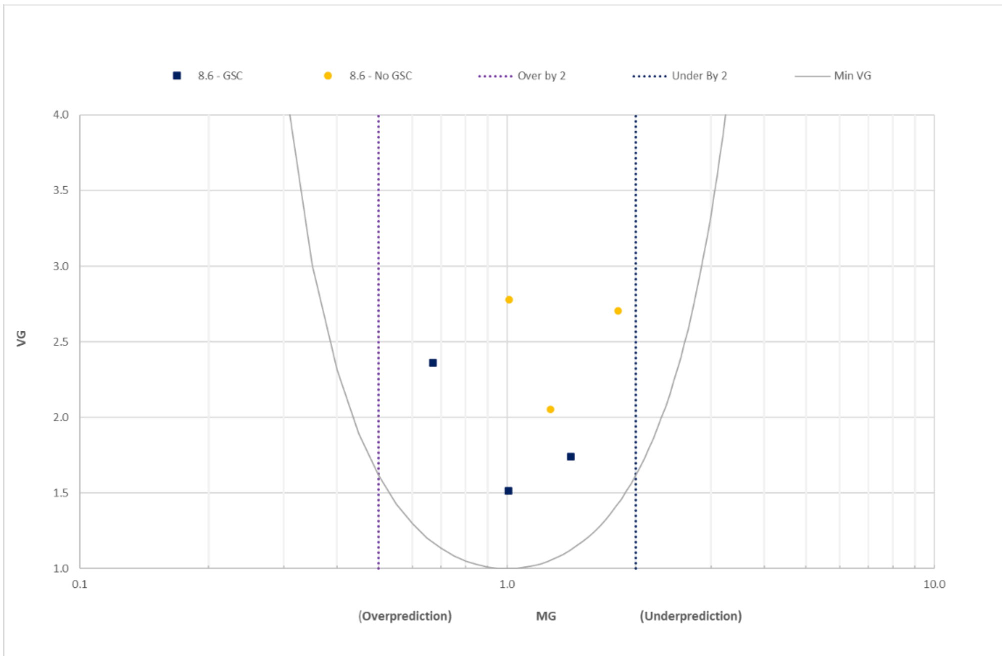

Figure 19: MG and VG values plot the plume centreline concentration (without GSC included for comparison)

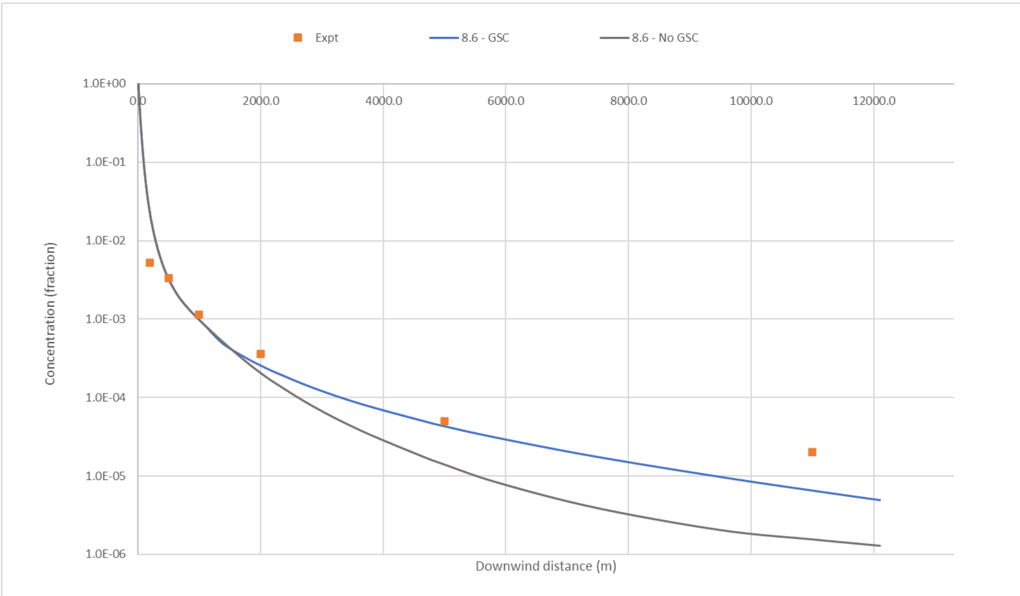

Figure 20: Concentration vs Distance for Trail 1, with and without GSC

4.7 PHMSA Validation

Phast 8.4 has undergone an external assessment process by the US Department of Transport Pipeline and Hazardous Materials Safety Administration (PHMSA) requiring the comparison of results with a set of field-scale and wind-tunnel tests. This process was previously granted for Phast 6.7 in 2011, with approval sought in 2021 for Phast 8.4. The field-scale experiments have a strong focus on time-varying releases from LNG pool sources, with three of the experiments (Maplin Sands, Burro and Coyote) involving dispersion from an evaporating pool. The validation has been based on the guide to the LNG Model Validation Database by Stewart et al. (Stewart, Coldrick, Gant, & Ivings, 2016)[25] and the technical report by Ivings et al. (Ivings, et al., 2016)[26]. The input data and concentration measurements are chosen as prescribed by version 12 of the modelling dataset Excel spreadsheet supplied by PHMSA.

Results in this section are specifically for Phast 8.6, which includes features not present in 8.4.

4.7.1 Selection of experiments

The Phast model UDM cannot account for obstacles, slopes or fences. Hence model results are only provided for experiments without obstructions, i.e.

- Large-scale LNG experiments: Maplin Sands (27,34,35), Burro (3,7,8,9), Coyote (3,5,6)
- Large-scale Thorney Island Freon/Nitrogen experiments (TI45, TI47)
- Wind-tunnel ground-level area sources: CHRC-A CO2 (16), BA Hamburg SF6 (DA0120, DAT223) and BA-TNO SF6 (TUV01, FLS).

Table 24 lists the experiments against which the UDM model has been validated and lists how each model has been modelled by the UDM. The UDM (without source calculations) is invoked in Phast as a ‘user-defined source’. This allows us to use exactly the inputs specified in the V12 database. The scenario selection is carried out in the ‘Discharge’ tab of the ‘User-defined source’. The ‘Leak’ scenario is selected for all field experiments (low momentum horizontal release), while the ‘Pool source’ scenario is selected for all wind-tunnel experiments (ground-level vapour pool source).

Experiment	Trial Number	Field (F) or Wind tunnel (WT)	Material	Modelled by UDM as
Maplin Sands	27 34 35	F	LNG	Low momentum elevated horizontal release
Burro	3 7 8 9	F	LNG	Low momentum elevated horizontal release
Coyote	3 5 6	F	LNG	Low momentum elevated horizontal release
Thorney Island	45 47	F	Freon & N_2	Low momentum ground-level horizontal release
CHRC	A	WT	CO2	Ground-level vapour pool source
BA-Hamburg	DA0120 DAT223	WT	SF_6	Ground-level vapour pool source
BA-TNO	TUV01 FLS	WT	SF_6	Ground-level vapour pool source

Table 24: List of experiments for PHMSA UDM validation

4.7.2 Analysis & Discussion

The geometric mean (MG) and geometric variance (VG) are probably the most common statistical measures used to assess model performance with experiment and are used in this section to form the basis of the results analysis.

MG and VG values for the experiments assessed are provided in Table 25 and Table 26 for point-wise and arc-wise analysis respectively. The PHMSA "Method 2" rolling average approach is used for time averaging where required as this is best aligned the UDM. Concentrations from Phast have been imported into the V12 database and the MG and VG calculated within the database are provided in the tables.

For reference and context, the MG and VG values submitted for the previously submitted Phast 8.4 are also provided, assessed against the sate data-set using the same methodology

MG VG plots for individual experiments and by the experiment groups for both point wise and arc wise calculations are presented in Figure 21-Figure 24.

Case	v8.9		v8.4	
	MG	VG	MG	VG
Maplin Sands 27 (short)	8.61	>1000	12.52	>1000
Maplin Sands 34 (short)	1.57	1.3	3.30	4.69
Maplin Sands 35 (short)	16.91	>1000	33.82	>1000
Coyote 3 (short)	1.08	2.32	1.20	2.70
Coyote 5 (short)	0.89	1.73	0.98	1.83
Coyote 6 (short)	0.49	4.02	0.55	4.26
Coyote 3 (long)	0.70	3.27	0.75	3.32
Coyote 5 (long)	0.35	6.12	0.41	5.20
Coyote 6 (long)	0.30	9.39	0.29	9.45
Burro 3 (short)	1.54	1.75	1.60	1.85
Burro 7 (short)	0.64	3.29	0.67	3.12
Burro 8 (short)	1.57	1.89	1.36	1.53
Burro 9 (short)	0.93	1.37	0.97	1.38
Burro 3 (long)	0.95	1.62	0.99	1.62
Burro 7 (long)	0.44	7.40	0.46	7.03
Burro 8 (long)	1.16	1.58	1.04	1.53
Burro 9 (long)	0.66	2.00	0.71	1.98
Thorney Island 45 (long)	1.37	2.24	2.14	3.22
Thorney Island 47 (long)	1.25	4.88	1.73	6.29
CHRC A (S)	1.71	2.20	1.72	2.18
BA Hamburg DA01020 (S)	3.33	4.48	3.29	4.31
BA Hamburg DAT223 (S)	1.90	1.65	1.90	1.66
BA TNO TUV01 (S)	1.67	1.58	1.67	1.58
BA TNO FLS (S)	2.41	2.78	2.34	2.69

Table 25: Point-wise MG and VG results

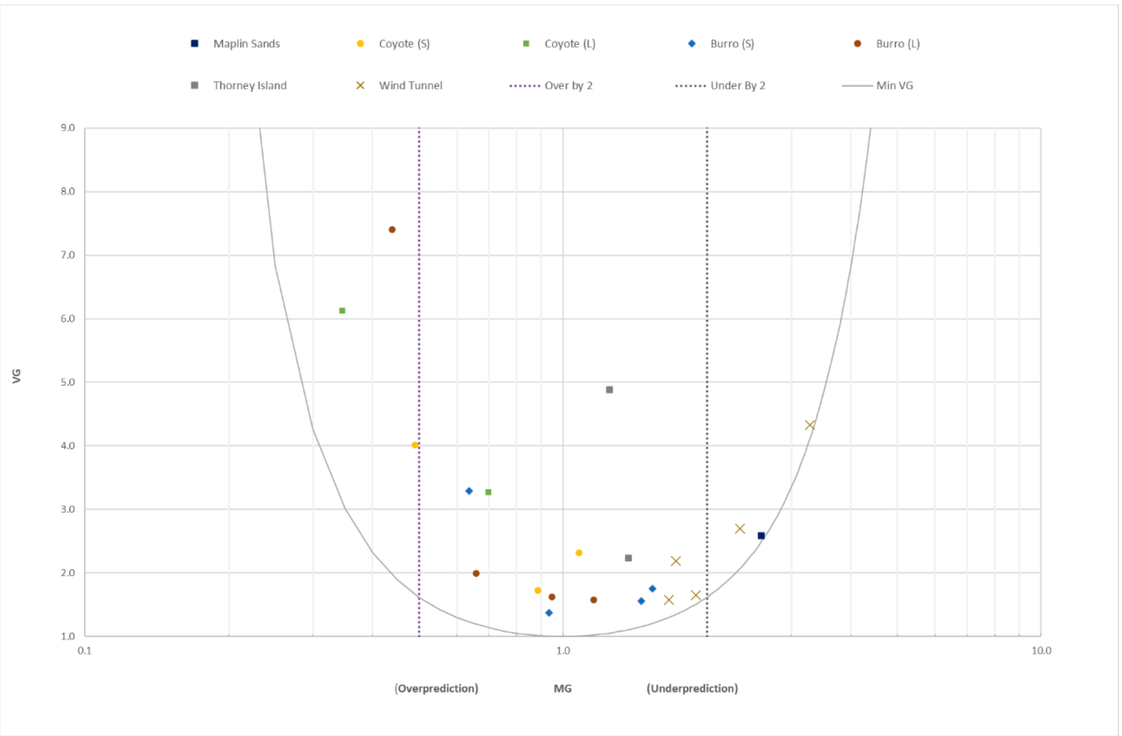

Figure 21: Pointwise MG VG Plot for PHMSA individual experiments (Phast 8.6)

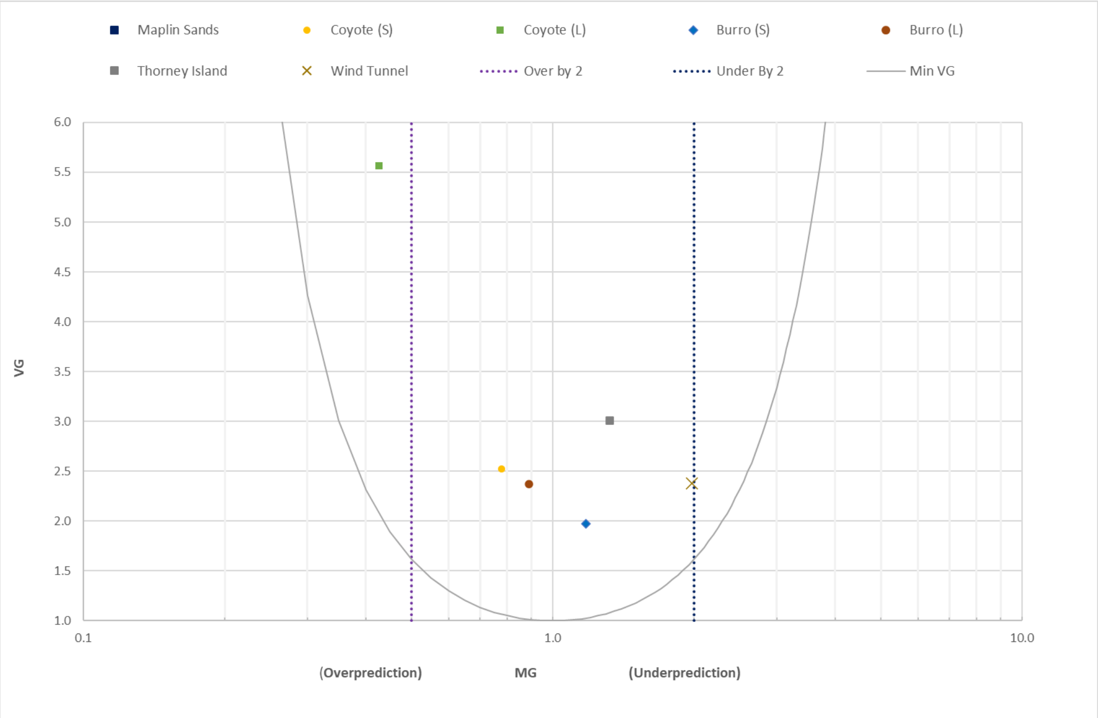

Figure 22: Pointwise MG VG Plot for PHMSA grouped experiments (Phast 8.6)

Case	v8.6		V8.4	
	MG	VG	MG	VG
Maplin Sands 27 (short)	6.76	115.38	8.33	373.80
Maplin Sands 34 (short)	2.80	3.16	3.66	6.58
Maplin Sands 35 (short)	20.66	>1000	41.80	>1000
Coyote 3 (short)	1.07	3.69	1.22	4.98
Coyote 5 (short)	0.93	1.88	0.81	1.27
Coyote 6 (short)	0.79	1.63	0.95	2.08
Coyote 3 (long)	0.83	4.76	0.90	5.21
Coyote 5 (long)	0.38	4.64	0.34	3.89
Coyote 6 (long)	0.67	1.30	0.61	1.39
Burro 3 (short)	1.24	1.35	1.28	1.38
Burro 7 (short)	0.80	1.23	0.83	1.23
Burro 8 (short)	2.83	3.24	2.48	2.51
Burro 9 (short)	0.98	1.29	1.01	1.29
Burro 3 (long)	0.80	1.47	0.84	1.44
Burro 7 (long)	0.67	1.41	0.70	1.36
Burro 8 (long)	2.57	2.83	2.22	2.41
Burro 9 (long)	0.72	1.50	0.77	1.50
Thorney Island 45 (long)	0.91	1.48	1.95	1.81
Thorney Island 47 (long)	0.60	2.70	1.05	1.35
CHRC A (S)	2.51	2.42	2.51	2.41
BA Hamburg DA01020 (S)	3.29	4.32	3.29	4.31
BA Hamburg DAT223 (S)	2.08	1.81	2.09	1.82
BA TNO TUV01 (S)			-	-
BA TNO FLS (S)	3.33	4.41	3.32	4.37

Table 26: Arc-wise MG and VG results

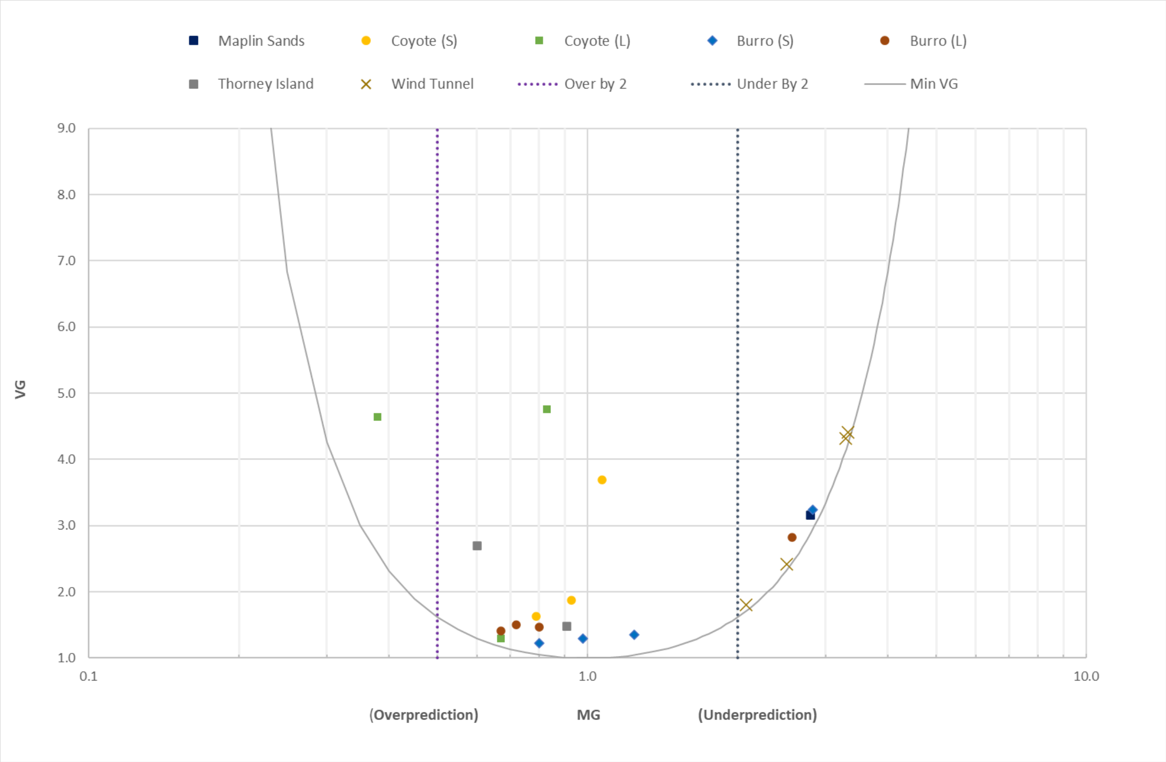

Figure 23: Arcwise MG VG Plot for PHMSA individual experiments (Phast 8.6)

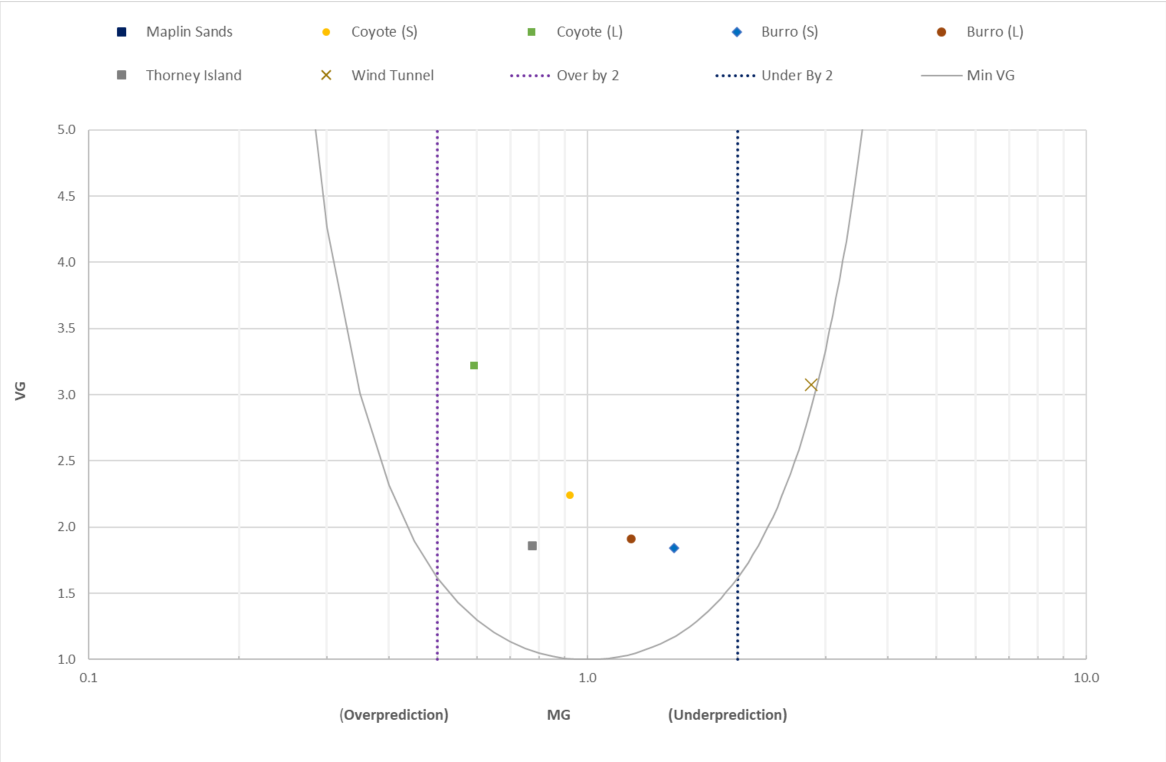

Figure 24: Arcwise MG VG Plot for PHMSA grouped experiments (Phast 8.6)

4.7.3 Summary

Overall the pattern of Phast 8.6 results is very similar to those submitted for Phast 8.4 as Table 25 and Table 26 show. In the main, there are minor fluctuations to the MG and VG values reported between these releases for most experiments, with the major changes being for Maplin sands and for Thorney Island, where both show large improvements overall.

Maplin Sands, despite the improvement remains significantly under-predicted. The possible causes for this are well known. The spatial (x,y) resolution of the sensors relative to the plumes in the Maplin Sands experiments was not good. Two of the three experiments took place in high wind conditions leading to very narrow plumes which missed most sensors completely. Using the given wind direction, the sensors are 'off-centreline' to an extent that they lie at (or beyond) the edge of the cloud predicted by the UDM. In fact, using the UDM centreline concentration vastly improves alignment with experiment.

The improvement in Thorney Island can be attributed to the inclusion of the Gravity Spreading Collapse model. This restricts the spreading rate when the appropriate conditions are met and subsequently keeps centreline concentrations higher. Only a few of the PHMSA simulations meet the criteria for gravity collapse, the Thorney Island both in that group and the increased concentrations post-collapse are reflected in their MG/VG results which show much reduced under-prediction.

4.8 Conclusions and summary overall UDM statistics for all experiments

For each experimental data set, the summary MG and VG values for point wise and arc wise concentrations (and widths where available) are presented in Table 27, and centreline concentrations are plotted in Figure 25. See Sections 4.1.2 (flashing jets excluding CO_2), 4.2 (instantaneous releases), 4.4 (CO_2 jets) 4.6 (Kit Fox) and 4.5 (PHMSA) for a discussion of the results.

Assumptions for UDM AWD runs
The UDM AWD results for PHMSA correspond to the PHMSA specified inputs, with few other required or non-default inputs set as described in Appendix A.5.

The UDM AWD results for the Kit Fox URA experiments are based on the pool-source assumption including additional time averaging, i.e. the results correspond to those shown in Figure 18.

Conclusions

1. Data sets not involving time-varying source terms

    a. The performance of the UDM against the Prairie Grass, Desert Tortoise, BP, Shell, EEC and Kitfox continuous experiments is good or excellent.
    b. The performance of the UDM against the aerosol releases of Desert Tortoise, EEC and FLADIS, in which both heavy and jet entrainment dominates, is reasonable.
    c. The performance against the CO2 pressurised releases, including the COSHER buried pipelines, is excellent
    d. The performance against the Kit Fox continuous experiments is excellent.
    e. Results in Phast 8.6 have not significantly changed from Phast 8.4, except for Goldfish which has improved due to the Gravity Spreading Collapse model

2. Instantaneous and short duration (URA puff) experiments

    a. Thorney Island results are good, and consistent with earlier versions.
    b. The new UDM AWD method produces overall lower MG values (more conservative concentration predictions) than the FDC method.
    c. Results are best for Stability F (with a slight over-prediction), and worst for Stability D (a significant under-prediction).

3. Buried pipeline experiments (COSHER)

    a. Performance is excellent using the new modelling introduced in Phast / Safeti 8.9, although the COSHER 1 experiment is under-predicted at low concentration levels
    b. With only 2 experiments, there is a worrying lack of suitable validation data

4. Experiments involving dispersion from pool:

    a. All pool-based dispersion (Burro, Maplin Sands, Coyote) has been redone since 8.4 using different data and methodology as prescribed by PHMSA. The results for 8.6 remain in line with those for 8.4.
    b. The results for Burro and Coyote (short) remain good, with only minor variations in statistics since 8.4 Maplin Sands and Thorney island have improved significantly, although for Maplin Sands there remains a large under-prediction (using fixed and widely spaced crosswind sensor locations for narrow plumes can lead to gross under-estimation of concentrations).

5. Wind-tunnel experiments
    a. CHRC, BA-TNO and BA-Hamburg simulations all under-estimate concentrations, However predictions are significantly better than those obtained for Phast 6.7 (Witlox et al, 2011)[2]
    b. All wind-tunnel experiments were simulated at field scale rather than wind-tunnel scale using input provided by PHMSA. It is possible that scaling of these releases has affected results[xv]

[xv] Wind-tunnel scale was recommended for the simulations, but this is not currently possible in the UDM due to limitations

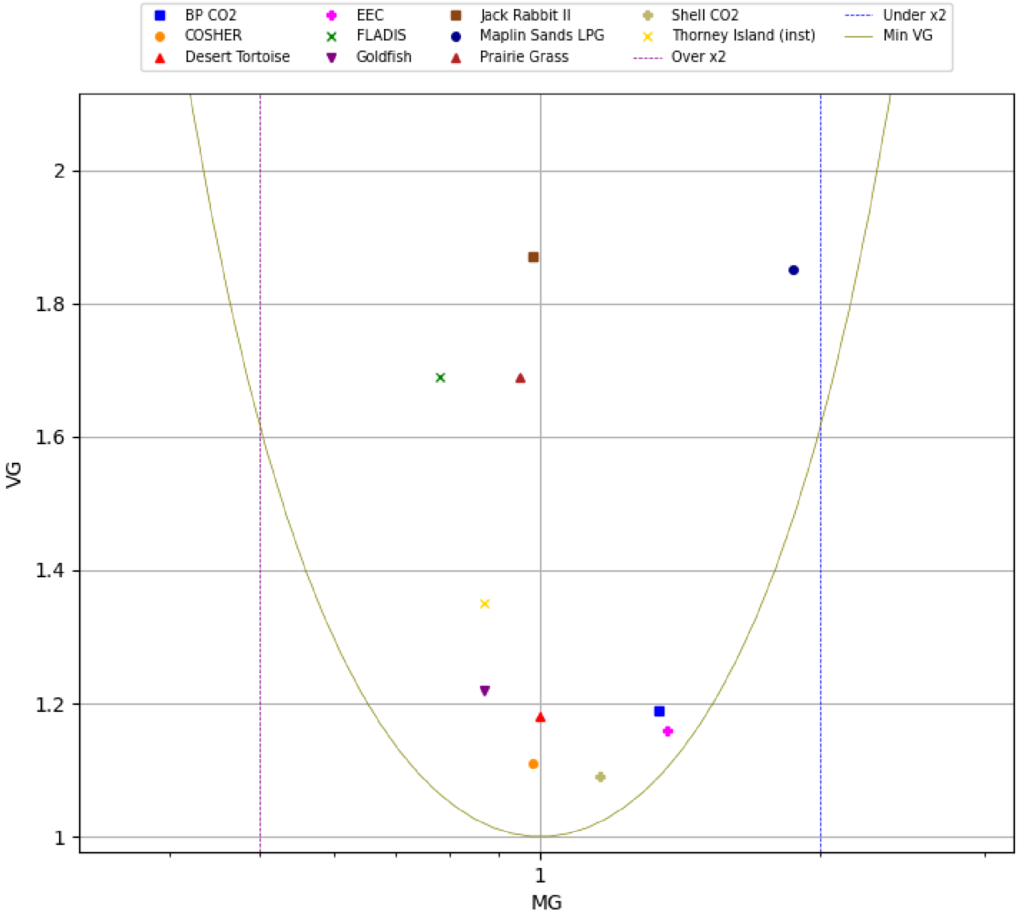

Figure 25. Summary MG and VG values for arcwise maximum concentration

Series	Arcwise max conc		Half-width		Pointwise max conc	
	MG	VG	MG	VG	MG	VG
BP CO2	1.34	1.19				
Burro (long)					0.89	2.37
Burro (short)					1.18	1.97
COSHER	0.98	1.11			1.07	1.25
Coyote (long)					0.43	5.57
Coyote (short)					0.78	2.52
Desert Tortoise	1.00	1.18	1.07	1.02	0.84	11.91
EEC	1.37	1.16	1.60	1.29	3.38	165.98
FLADIS	0.78	1.69	1.39	1.17	2.29	20.03

Goldfish	0.87	1.22	0.77	1.13		
Jack Rabbit II	0.98	1.87	0.32	3.89		
Maplin Sands LNG					6.52	456.54
Maplin Sands LPG	1.87	1.85				
Prairie Grass	0.95	1.69	0.90	1.21	0.89	15.81
Shell CO2	1.16	1.09				
Thorney Island (cont)					1.32	3.01
Thorney Island (inst)	0.87	1.35				

Table 27: Summary MG and VG values from Phast 8.6 for concentration for all experimental data sets[xvi]

Widths used are Hanna (Prairie Grass except 8 and 17, Goldfish, Desert Tortoise 3 and 4, URA puff, URA continuous), SMEDIS (EEC, FLADIS, Desert Tortoise 1 and 2) and max width to concentration (JR2). In line with the most recent PHMSA MEP, only pointwise concentrations are compared for the PHMSA set of experiments.

[xvi] Crosswind experiments not included as point-wise and arc-wise calculations of MG/VG are not used to assess them

APPENDICES

Appendix A. Notes on Input data for validation runs

A.1 Continuous (excluding CO_2)

Series	**Prairie Grass**
Substance	Sulphur Dioxide
Release type	Continuous
Duration, s	600
Release height, m	0.45
Jet type	Horizontal
Dispersing surface	Land
Surface roughness length, m	0.006
Ref. height for wind speed, m	2
Ref. height for air temp, m	2
Atmospheric pressure, Pa	101325
Relative humidity fraction	0.7
Solar flux, W/m^2	500
Averaging time, s	600

PG7	**PG8**	**PG9**	**PG13**	**PG15**	**PG17**	
0.0899	0.0911	0.092	0.0611	0.0955	0.0565	Release rate, kg/s
17.1	17.3	17.2	11.1	17.5	10.5	Release velocity, m/s
305.15	305.15	301.15	293.15	295.15	300.15	Release temperature, K
B	C	C	F	A	D	Stability class
4.2	4.9	6.9	1.3	3.4	3.3	Wind speed at reference height, m/s
305.15	305.15	301.15	293.15	295.15	300.15	Ambient temp., K
305.15	305.15	301.15	293.15	295.15	300.15	Dispersing surface temp., K

PG34	**PG41**	**PG50**	**PG58**	
0.0974	0.0399	0.1028	0.0405	Release rate, kg/s
18.4	7.3	19.5	7.5	Release velocity, m/s
304.15	294.15	304.15	299.15	Release temperature, K
D	E	C	F	Stability class
9	4	6.6	1.9	Wind speed at reference height, m/s
304.15	294.15	304.15	299.15	Ambient temp., K
304.15	294.15	304.15	299.15	Dispersing surface temp., K

1) The data for PG8 and PG17 were provided from SMEDIS[11]
2) The dispersing surface temperature was set to the temperature at the reference height.

Series	**Desert Tortoise**
Substance	Ammonia
Release type	Continuous
Release height, m	0.79
Jet type	Horizontal
Dispersing surface	Land
surface roughness length, m	0.003
Solar flux, W/m^2	500
Bund Surface	Dry Soil

DT1	**DT2**	**DT3**	**DT4**	
80	112	130.7	96.7	Release rate, kg/s
126	255	166	381	Duration, s
0	0	0	0	Bund diameter, m
D	D	D	E	Stability class
7.42	5.8	7.6	4.64	Wind speed at reference height, m/s
302	304	307.05	306.9	Ambient temp., K
0.132	0.175	0.148	0.213	Relative humidity fraction
90888	90990	90586	90280	Atmospheric pressure, Pa
304.8	304	304.8	304	Dispersing surface temp., K
0.82	0.82	0.803	0.795	Discharge liquid mass fraction
0.051	0.079	0.122	0.119	Drop diameter, mm
90.3	72.7	59	60	Release velocity, m/s
2	2	3.36	3.36	Ref. Ht. for wind speed, m
2.46	2.46	16.19	16.19	Ref. Ht. for air temp, m
80	160	120	300	Averaging Time (s)

1) Data for DT1 and DT2 are taken from SMEDIS[11] who provided post flash data. DT3 and DT4 post-flash velocity and liquid fraction are calculated using DISC / ATEX and the conservation of momentum method.
2) All the cases predict rainout. The pool segment giving the largest vaporisation rate during the release was selected for version comparison
3) Bund temperature and surface temperature taken from Hanna's[10] report who specifies a soil temperature.

Series	**EEC**
Substance	Propane
Release type	Continuous
Release height, m	0.5
Jet type	Horizontal
Dispersing surface	Land
Surface roughness length, m	0.006
Solar flux, W/m^2	500

EEC170	**EEC 360**	**EEC 550**	**EEC 560**	
2.9	0.11	3	3	Release rate, kg/s
160	50	150	360	Duration, s
D	D	D	C	Stabiltiy class
3.9	3.4	2.67	2.43	Wind speed at reference height, m/s
288.15	289	282.9	285	Ambient temp., K
0.55	0.7	0.99	1	Relative humidity fraction
100000	100000	102500	100000	Atmospheric pressure, Pa
288.15	289	282.9	285	Dispersing surface temp., K
0.72	0.71	0.7	0.7	Discharge liquid mass fraction
85.21	84.2	68.5	89.03	Release velocity, m/s
3.3	3.3	6	6	Reference height for wind speed, m
3.3	3.3	6	6	Reference height. for air temp, m
0.04	0.057	0.04	0.041	Drop diameter, mm
60	50	150	100	Averaging time (s)

1) These data were provided as part of the SMEDIS[11] project.
2) Droplet size was calculated using Phast[xvii]
3) The reference height for temperature was set to the reference height for wind speed.
4) The surface temperature was set to the ambient temperature at the reference height.
5) To bring the predictions in line with the SMEDIS results, the cut-off evaporation rate parameter was changed to 0.1 kg/s.

[xvii] Except for EEC170, where no pre-release conditions were available. Value assumed to be 40 μm, in line with other experiments; see Section 4.1.1. EEC170 also has no arc-wise maximum concentration data.

Series	**FLADIS**
Substance	Ammonia
Release type	Continuous
Release height, m	1.5
Jet type	Horizontal
Dispersing surface	Land
Surface roughness length, m	0.04
Solar flux, W/m^2	500

FLADIS 9	**FLADIS 16**	**FLADIS 24**	
0.4	0.27	0.46	Release rate, kg/s
900	1140	600	Duration, s
D	E	C	Stabiltiy class
5.6	4.4	5.03	Wind speed at reference height, m/s
288.7	290	291	Ambient temp., K
0.86	0.62	0.536	Relative humidity fraction
102000	102000	101300	Atmospheric pressure, Pa
288.7	290	291	Dispersing surface temp., K
0.84	0.83	0.83	Discharge liquid mass fraction
65.17	67.85	55.87	Release velocity, m/s
10	10	10	Reference height for wind speed, m
10	10	10	Reference height. for air temp, m
0.0823	0.0772	0.114	Drop diameter, mm
600	600	400	Averaging time (s)

1) These data were provided as part of the SMEDIS project
2) For FLADIS16 the stability class was given as being D/E. This option is not available within the UDM, hence stability class E was taken as a conservative option.
3) The reference height for temperature was set equal to the reference height for windspeed.
4) The surface temperature was set to the temperature at the reference height.

Input	Units	Value
Series		**Goldfish**
Substance		Hydrogen Fluoride
Release type		Horizontal, continuous, over land
Release height	m	1.263
Surface roughness	mm	0.2
Wind speed ref. height	m	2
Air temp. ref height	m	2
Stability		D
Averaging time	s	60
Air pressure	Pa	101325

Input	Units	Goldfish 1	Goldfish 2	Goldfish 3
Release rate	Kg/s	27.13	10.26	10.07
Duration	S	125	360	360
Release velocity	m/s	41.1	41.7	42.2
Release liq. Frac.	Kg/kg	0.86	0.88	0.87
Wind speed	m/s	5.6	4.2	5.4
Air temperature[xviii]	K	310.15	309.15	309.65
Relative humidity	frac	0.0562	0.126	0.35
Droplet diameter	mm	0.117	0.111	0.113

1) Goldfish input data were obtained from McFarlane et al [12]
2) The surface temperature was set to the temperature at the reference height.

[xviii] Surface temperature assumed same value

Description	Units	Limits Lower	Limits Upper	TI45	TI47	Notes (Ground-level horizontal Freon-12/Nitrogen release)
RELEASE DATA						
duration/segments						
Flag: instantaneous (1), continuous (2)		1	2	2		
Number of release segments (time-varying release only)		1	11	1		
Duration of release segments (for non-instantaneous only)		0	3600	455	465	
material/mass/thermodynamics						
Released material name (from material database)				FR12_N2		mixture: 68% N2, 32% Freon-12 [CASID75-71-8; added via admin mode; set as inert]
Initial released mass	kg (inst) or kg/s (st)	1.00E-01	1.00E+09	10.67	10.22	
Initial mass of air mixed in	kg (inst) or kg/s (st)	0	1000000000	0		
Initial state descriptor [<0 liquid mass fraction (2-phase), >0 temperature (vapour)]	(fraction) or K	-1	900	286.25	287.45	
Droplet size	m	0	1	0		
release location/speed						
Release height	m	0		0		Complex release geometry modelled as horizontal ground-level release
Release angle [0 = horizontal, pi/2 = vertical upwards; cont.only]	radians	-1.57	1.571	0		
Expansion energy (instantaneous only)	(J/kg)	0		0		
Release velocity (continuous only)	m/s	0	500	1.382885377	1.324563	velocity (m/s) = ratio of spill rate(m3/s) and source area (diam.2m) [Phast density 2.456kg/m3]
Impingement flag (0 -horizontal, 1 - angled, 2 - vertical, 3 - along ground, 4 - impinged)		0	4	1		
AMBIENT DATA						
Pasquill stability class (1-A,2-A/B,3-B,4-B/C,5-C,6-C/D,7-D,8-E,9-F,10-G)		1	10	9	9	Using F for TI45 while database gives E-F (E-F cannot be selected in Phast)
Wind speed at reference height	m/s	0.1	50	2.3	1.5	
Reference height for windspeed	m	0.1	100	10		
Temperature at reference height	K	200	350	286.25	287.45	
Pressure at reference height	N/m2	50000	120000	101325		Assumed value - not measured
Reference height for temperature and pressure	m	0.1	100	2		
Atmospheric humidity (fraction)	-	0	1	1	0.974	
SUBSTRATE DATA						
Surface roughness length	m	0.0001	3	0.01		
Dispersing surface type (1-land,2-water)		1	2	1		
Temperature of dispersing surface	K	200	500	285.95	287.65	
POOL DATA						
Pool surface type (1-dry soil,2-wet soil, 3 - concrete, 4 - insulated concrete, 5 - deep		1	9	2		
Temperature of pool surface	K	0		285.95	287.65	
Bund diameter (<= 0: no bund)	m	0		0		
AVERAGING TIME						
Averaging time	s	1	3600	30		'Long' averaging time only
TERMINATION CRITERION						
Min. concentration of interest	mole %	0	100	0		
Max. distance of interest	m	0	1.00E+08	472		

Table 28. UDM input data for Thorney Island experiments (continuous)

1) The release height is given as 0m, with diameter 2m, but the geometry of the release was complicated: a vertical pipe with a 2m diameter plate 0.5m above the surface to ensure low vertical momentum. It is not obvious how this should be modelled in Phast. We have chosen a very low momentum horizontal jet, with horizontal velocity u equal to the calculated source exit velocity assuming a pipe of diameter D_{source} = 2 m: $u = Q / (A\rho_v)$. Here Q is the release rate (kg/s), A is the source area (= 0.25 π D_{source}^2) and ρ_v the vapour density of the Freon-12 / N_2 mixture. Receptor height has likewise been assumed to be ground level.
2) For TI45, the actual stability class is E-F, whereas in Phast one must choose either E or F. We have chosen F, but using F does not make very much difference with E especially down to the 1% or so concentration level.

Series	**Maplin Sands**		
Substance	LPG (propane)		
Release type	Continuous	Dispersing surface	Water
Initial air mixed	0	Surface roughness length, m	3.00E-04
Discharge liquid mass fraction	0	Ref. Ht. for wind speed, m	10
Disharge temperature, K	231.1	Ref. Ht. for air temp, m	10.1
Droplet diameter, m	1.00E-02	Pasquill-Gifford class	D
Release height, m	0	Pressure, Pa	101325
Jet type	Horizontal	Solar flux, W/m^2	485
Bund diameter, m	300		
Bund surface	5		

MSP42	MSP43	MSP46	MSP47	MSP49	MSP50	MSP52	MSP54	
20.87	19.2	23.37	32.57	16.71	35.89	44.25	19.2	Spill/evap rate, kg/s
180	330	360	210	90	160	140	180	Duration, s
0	0	0	0	0	0.5	0	0	Expansion velocity, m/s, or e
14.9	14.3	15.7	18.6	13.3	19.5	21.7	14.3	Pool diameter, m
3.7	5.5	8.1	5.6	6.2	7.9	7.9	3.8	Wind speed, m/s
291.49	290.12	291.86	290.57	286.7	283.66	285.05	281.63	Upper ambient temp., K
0.751	0.75	0.71	0.78	0.88	0.79	0.63	0.85	Relative humidity fraction
291.7	292.1	290.5	290.3	286.2	283.1	285.1	282.6	Soil temperature, K
0.9	0.9	0.9	0.9	0.9	0.9	0.9	0.5	Receptor height, m

1) These experiments were not included in the PHMSA dataset.
2) We have used the MDA quoted release height of zero (unlike for the 7.1 simulation for the LNG experiments; ground-level spill)
3) Relative humidity for MSP42 and MSP43 were not included in the MDA
4) The cases are modelled as continuous spills at minimum release velocity (0.1 m/s) and with the maximum droplet diameter (0.01m)

A.2 Instantaneous

Series	**Thorney Island - Instantaneous**
Substance	Freon-12 + Nitrogen
Release type	Instantaneous
Release height, m	0
Dispersing surface	Land
Ref. height for wind speed, m	10
Ref. height for air temp, m	2
Averaging time, s	10
Solar flux, W/m2	500
Expansion energy, J/kg	0

TI6	**TI7**	**TI8**	**TI9**	**TI12**	
1624	2388	2004	1900	4353	Release mass, kg
1523	1861	1954	1966	1383	Initial mass of air (kg)
291.83	290.46	290.68	291.45	283.29	Release temperature, K
0.018	0.018	0.012	0.008	0.018	Surface roughness length, m
D	E	D	F	E	Stability class
2.8	3.4	2.4	1.7	2.5	Wind speed, m/s
291.83	290.46	290.68	291.45	283.29	Ambient temperature, K
0.748	0.807	0.876	0.873	0.662	Relative humidity fraction
101325	102136	102237	101933	101325	Atmospheric pressure, N/m2
291.83	290.46	290.68	291.45	283.29	Surface temperature, K
0.21	0.24	0.21	0.2	0.44	Mole fraction of Freon-12

TI13	**TI17**	**TI18**	**TI19**	
3148	8711	2368	3797	Release mass, kg
1652	0	1513	1680	Initial mass of air (kg)
286.88	289.21	289.66	286.51	Release temperature, K
0.01	0.018	0.005	0.01	Surface roughness length, m
D	D	D	D	Stability class
7.3	5	7.4	6.4	Wind speed, m/s
286.88	289.21	289.66	286.51	Ambient temperature, K
0.741	0.94	0.813	0.948	Relative humidity fraction
101933	100818	100717	100616	Atmospheric pressure, N/m2
286.88	289.21	289.66	286.51	Surface temperature, K
0.32	1	0.28	0.36	Mole fraction of Freon-12

1) The experimental concentration data was multiplied throughout by the mole fraction of Freon in the release so that a direct comparison could be made with the UDM results.
2) The assumption of 0 J/kg for the expansion energy is a reasonable assumption as this is an unpressurised release.
3) The dispersing surface temperature was set to the temperature at the reference height.
4) Mole fraction of Freon-12 was calculated from the molecular weight for each experiment given in the MDA, but not used. Consistent with previous versions of this report (but unlike the Thorney Island continuous experiments) the material used is pure Freon-12 (CAS 75071-8).

A.3 Pressurised CO_2 releases (BP and Shell experiments)

Key Phast discharge and dispersion input data

Table 29 summarises the key BP experimental data required as input to the Phast discharge models DISC (steady-state or initial rate) and TVDI (time-varying releases) and the UDM dispersion model. In this table the values of the storage pressure and the storage temperature are taken at the discharge end of the vessel (upstream of the pipework), with mean values during the release applied for the steady-state liquid releases and with initial values applied for the transient vapour releases. The ambient data were measured upwind of the release and mean values are adopted for these data during the release. This is with the exception of the wind-speed measurement taken 40m downwind of the release at 1.65m above the pad. Since this measurement was disturbed by the CO_2 jet, the value listed in
Table 29 corresponds to the mean value prior to the release.

Input	Test1	Test2	Test3	Test5	Test6	Test11	Test8	Test8R	Test9	Input for models
Discharge data										
steady-state/transient	steady	steady	steady	steady	steady	steady	trans.	trans.	trans.	-
storage phase	liquid	liquid	liquid	liquid	liquid	liquid	vapour	vapour	vapour	DISC,TVDI
storage pressure (barg)	103.4	155.5	133.5	157.68	156.7	82.03	157.76	148.7	154.16	DISC,TVDI
storage temperature (^oC)	5	7.84	11.02	9.12	9.48	17.44	147.12	149.37	69.17	DISC,TVDI
vessel volume (m^3)	-	-	-	-	-	-	6.3	6.3	6.3	TVDI
orifice diameter (mm)	11.94	11.94	11.94	25.62	6.46	11.94	11.94	11.94	11.94	DISC,TVDI
orifice length (mm)	46.78	46.78	46.78	72.41	47.79	46.78	46.78	46.78	46.78	-
release duration (s)	60	59	60	40	120	58	120	132	179	-
Ambient data										
ambient temperature (^oC)	14.2	7.5	10.6	5.8	6.1	11.6	11.19	11.1	8.2	DISC,TVDI,UDM
ambient pressure (mbara)	999.4	958.2	972.5	985.4	938.4	960.2	957.99	957.1	958.9	DISC,TVDI,UDM
relative humidity (%)	74.4	96	95.8	96.7	1	94	100	100	99.9	DISC,TVDI,UDM
wind direction (degrees)	322.4	265.6	288.8	278.6	299	270.8	269.3	270	270.7	UDM uses 270^o
wind speed (m/s)	4	3.44	3.37	5.13	2.20	5.99	4.71	0.76	4.04	UDM

Table 29. Experimental conditions for BP CO_2 tests

Input	Test3	Test5	Test11	Test1	Test2	Test4	Test14	Test16	Input for models
Discharge data									
steady-state/transient	steady	steady	steady	trans.	trans.	trans.	trans.	trans.	-
storage phase	liquid	liquid	liquid	liquid	liquid	liquid	vapour	vapour	DISC,TVDI
storage pressure (barg)	147.3	148.8	81.9	148.3	147.1	148.2	151.6	150.6	DISC,TVDI (either storage or
nozzle pressure (barg)	144.8	126.4	80.3	143	118	148.2	147.7	146.0	nozzle pressure is input)
storage temperature (^oC)	9.8	17.8	-0.2	26.7	24.6	20.1	71	36.7	DISC,TVDI (either storage or
nozzle temperature (^oC)	8.2	13.7	-1.4	23	18	20.1	65.0	31.7	nozzle temperature is input)
vessel volume (m^3)	-	-	-	6.3	6.3	6.3	6.3	6.3	TVDI
orifice diameter (mm)	12.7	25.4	12.7	12.7	25.4	6.3	12.7	12.7	DISC,TVDI
orifice length (mm)	47.78	46.84	47.78	47.78	46.84	47.79	47.78	47.78	-
release duration (s)	120	40	120	90	145	>700	315	370	-
Ambient data									
ambient temperature (^oC)	11.2	9	3.6	14.7	10.3	13.8	0	-2.9	DISC,TVDI,UDM
ambient pressure (mbara)	1017	905	995	1006	1005	975.5	1005	997	DISC,TVDI,UDM
relative humidity (%)	66	91	78	83	77	77	88	88	DISC,TVDI,UDM
wind direction (degrees)	267	213	261	263	250	215	303	292	UDM uses 270^o
wind speed (m/s)	4.05	1.30	2.76	3.93	5.43	1.98	1.34	1.48	UDM

Table 30. Experimental conditions for Shell CO_2 tests

Likewise Table 30 summarises the key Shell experimental data required as input to the Phast models. In this table the values of the storage pressure and the storage temperature are taken at the discharge end of the vessel (upstream of the pipework) and the nozzle pressure/temperature are taken along the nozzle, with mean values during the release applied for the steady-state releases and with initial values applied for the transient releases. The wind speed data were taken from tower A [20m west (behind) and 5 meter south of release point] at 10 meter height (averaged prior to release) given anomalies observed at other measurement locations.

Furthermore, based on an analysis of the experimentally observed vertical wind-speed profiles a surface roughness of 0.1m and a stability class of D was assumed for all (BP and Shell) tests. Finally with respect to the wind direction it is noted that the release direction corresponds to 270^o.

MDA format

Data for the BP and Shell CO_2 experiments have been included in the format of the MDA database by Witlox[27,28] and these data are given by Table 31 and Table 32.

The following further additional notes are given for Table 31 (BP tests):

Tests 1-3, 6, 11 were truly steady-state releases where the pressure was kept constant using a padding gas and therefore a reliable estimate of flow rate was obtained.

For the steady-state liquid tests the mean values of pressure and temperature at the vessel outlet (discharge end of the vessel) during the release are specified, while for the time-varying hot tests initial values are specified. Thus the specified exit gauge pressure may be too high for test 5, since for this test the pressure was not kept constant and frictional effects upstream of the orifice were important.

Tests 8, 8R, 9 were time-dependent releases, where the flow rate was accurately measured. The pressures listed in the table are initial pressures, while the reported flow rates in the table are averaged flow rates over the first twenty seconds.

The un-averaged peak concentrations have been based on ALL sensors, and any possible faulty sensors have not been excluded. The averaged maximum concentrations are based on 11-second averaged concentrations excluding faulty sensors. These observed estimates may be somewhat conservative since the maximum value over all times of the11-second averaged has been applied. Furthermore no further analysis has been carried out (e.g. via spline fitting of the measured values to obtain a better fit of the crosswind concentration profile and a better estimate of the maximum concentration) to further refine this maximum value.

The following further additional notes are given for Table 32 (Shell tests):

Tests 3,5,11 were truly steady-state releases where the pressure was kept constant using a padding gas. Tests 1, 2, 4 were time-varying releases from a vessel initially fully filled with pressurized liquid. Tests 14 and 16 were time-varying releases from a vessel initially filled with pressurized vapour (at supercritical temperature).

For the 1" tests 5 and 2 there was a significant pressure drop along the pipework between the vessel outlet and the nozzle. Therefore for the steady-state liquid tests mean nozzle values during the release are specified, while for the time-varying liquid tests initial nozzle values are specified. For the ½" vapour tests 14 and16 the initial vessel outlet values are specified.

Servomex and Draeger sensors were only positioned at limited locations and therefore these have not been used. O_2 sensors showed an erroneous drop with time in the near-field, and therefore averaged values for the O_2 sensors have not been used. Thus the maximum value of the peak values for the O_2 sensors located at a given downstream distance have been used to determine the measured peak concentration at a given downstream distance. No further analysis has been carried out (e.g. via spline fitting of the measured values to obtain a better fit of the crosswind concentration profile and a better estimate of the maximum concentration) to further refine this maximum value.

MDA INPUT VARIABLE										MEANING INPUT VARIABLE	REFERENCE / ADDITIONAL NOTE
BP DF1 C02 pressurised field releases, SpadeAdam										Name of field experiments	
Carbon Dioxide										Chemical released	
CO2									:	3-char. abbreviation of chemical	
9									:	number of trials included in MDA	
?									:	time zone designation	??? To apply GMT time
CO2BP1	C02BP2	CO2BP3	CO2BP5	CO2BP6	CO2BP11	CO2BP8	CO2BPR	CO2BP9	:	trial ID	tests: steady liquid (1,2,3,5,6,11), transient vapour (8,8R,9)
1	21	28	16	7	20	17	22	16	:	day	Advantica report - Appendix A,B,C,E,F,L,H,I,J
11	11	11	12	12	11	11	11	11	:	month	Advantica report - Appendix A,B,C,E,F,L,H,I,J
2006	2006	2006	2006	2006	2006	2006	2006	2006	:	year	Advantica report - Appendix A,B,C,E,F,L,H,I,J
12	16	14	13	16	16	15	14	14	:	hour	Advantica report - Appendix A,B,C,E,F,L,H,I,J
39	3	50	28	2	30	20	15	0	:	minute	Advantica report - Appendix A,B,C,E,F,L,H,I,J
44.01	44.01	44.01	44.01	44.01	44.01	44.01	44.01	44.01	:	mol. weight (g/mole)	Property as in MDA KitFox for CO2
186.25	186.25	186.25	186.25	186.25	186.25	186.25	186.25	186.25	:	normal boiling point (K)	Property as in MDA KitFox for CO2
154749	154749	154749	154749	154749	154749	154749	154749	154749	:	latent heat of evaporation (J/kg) at 20C	Property as in MDA KitFox for CO2
839.3	839.3	839.3	839.3	839.3	839.3	839.3	839.3	839.3	:	specific heat - vapor (J/kg-K) at 20C	Property as in MDA KitFox for CO2
4118.8	4118.8	4118.8	4118.8	4118.8	4118.8	4118.8	4118.8	4118.8	:	specific heat - liquid (J/kg-K) at 20C	Property as in MDA KitFox for CO2
773.3	773.3	773.3	773.3	773.3	773.3	773.3	773.3	773.3	:	density of liquid (kg/m**3) at 20C	Property as in MDA KitFox for CO2
-1	-1	-1	-1	-1	-1	-1	-1	-1	:	coefficient A for vapor pressure equation	?? Suggest use DIPPR formula (vapour/solid vapour pressure)
0	0	0	0	0	0	0	0	0	:	coefficient B for vapor pressure equation	?? Suggest use DIPPR formula (vapour/solid vapour pressure)
103.40	155.50	133.50	157.68	156.72	82.03	157.76	148.72	154.16	:	exit gauge pressure (bar)	mean (steady tests) or initial (transient tests) at vessel outlet
278.15	280.99	284.171	282.27	282.6252	290.59	420.27	422.52	342.32	:	source temperature (K)	mean (steady tests) or initial (transient tests) at vessel outlet
1.19E-02	1.19E-02	1.19E-02	2.56E-02	6.46E-03	1.19E-02	1.19E-02	1.19E-02	1.19E-02	:	source diameter (m)	
1.1	1.1	1.1	1.1	1.1	1.1	1.1	1.1	1.1	:	source elevation (m)	
HJ	HJ	HJ	HJ	HJ	HJ	HJ	HJ	HJ	:	source type (IR,HJ,AS,EP)	Horizontal jet (HJ)
L	L	L	L	L	L	G	G	G	:	source phase (L,C,G)	Liquid (L) or gas (G)
-99.9	-99.9	-99.9	-99.9	-99.9	-99.9	-99.9	-99.9	-99.9	:	source containment diameter (m)	
8.2	11.41	9.987826	41.17	3.5	7.12	4.07	3.8	6.05	:	spill/evaporation rate (kg/s)	8, 8R, 9 are time-varying releases (averaged rate taken over first 20s)
59	59	60	40	120	58	120	132	179	:	spill duration (s)	8, 8R, 9 are time-varying releases
-99.9	-99.9	-99.9	-99.9	-99.9	-99.9	-99.9	-99.9	-99.9	:	total released (kg)	
1.00E+06	1.00E+06	1.00E+06	1.00E+06	1.00E+06	1.00E+06	1.00E+06	1.00E+06	1.00E+06	:	initial concentration (ppm)	
0.9994	0.9582	0.9725	0.9854	0.9384	0.9602	0.95799	0.9571	0.9589	:	ambient pressure (bar)	Advantica report - Appendix A,B,C,E,F,L,H,I,J (except Test 8 - Leng)
74.4	96	95.8	96.7	100	94	100	100	99.9	:	relative humidity (%)	Advantica report - Appendix A,B,C,E,F,L,H,I,J
287.35	280.65	283.75	278.95	279.25	284.75	284.34	284.25	281.35	:	ambient temperature #1-lower (K)	Advantica report - Appendix A,B,C,E,F,L,H,I,J (except Test 8 - Leng)
0	0	0	0	0	0	0	0	0	:	measurement height for temperature #1 (m)	
-99.9	-99.9	-99.9	-99.9	-99.9	-99.9	-99.9	-99.9	-99.9	:	ambient temperature #2-upper (K)	
-99.9	-99.9	-99.9	-99.9	-99.9	-99.9	-99.9	-99.9	-99.9	:	measurement height for temperature #2 (m)	
285.35	278.65	281.75	276.95	277.25	282.75	282.34	282.25	279.35	:	soil temperature (K)	Following BP advice, assumed to be 2 degrees lower than ambient
1	1	1	1	1	1	1	1	1	:	soil moisture (1:dry,2:moist,3:water)	
4	3.44	3.37	5.13	2.2	5.99	4.71	0.76	4.04	:	wind speed (m/s)	Windspeed at 40m distance; average value before start release
1.65	1.65	1.65	1.65	1.65	1.65	1.65	1.65	1.65	:	measurement height for wind speed (m)	
-99.9	-99.9	-99.9	-99.9	-99.9	-99.9	-99.9	-99.9	-99.9	:	domain-avg wind speed (m/s)	
-99.9	-99.9	-99.9	-99.9	-99.9	-99.9	-99.9	-99.9	-99.9	:	domain-avg sigma-u (m/s)	
-99.9	-99.9	-99.9	-99.9	-99.9	-99.9	-99.9	-99.9	-99.9	:	domain-avg sigma-theta (deg)	
-99.9	-99.9	-99.9	-99.9	-99.9	-99.9	-99.9	-99.9	-99.9	:	measurement ht for domain-avg wind data (m)	
?	?	?	?	?	?	?	?	?	:	averaging time for wind and temperature data (s)	to check
0.1	0.1	0.1	0.1	0.1	0.1	0.1	0.1	0.1	:	roughness length z0 (m)	presumed
-99.9	-99.9	-99.9	-99.9	-99.9	-99.9	-99.9	-99.9	-99.9	:	friction velocity u-star (m/s)	
-99.9	-99.9	-99.9	-99.9	-99.9	-99.9	-99.9	-99.9	-99.9	:	bowen ratio estimate	
-99.9	-99.9	-99.9	-99.9	-99.9	-99.9	-99.9	-99.9	-99.9	:	inverse Monin-Obukhov length (1/m)	
?	?	?	?	?	?	?	?	?	:	cloud cover (%)	??? To check
4	4	4	4	4	4	4	4	4	:	Pasquill-Gifford stability class (A=1;D=4;F=6)	Assumed D
?	?	?	?	?	?	?	?	?	:	latitude (deg)	??? To apply SpadeAdam location
?	?	?	?	?	?	?	?	?	:	longitude (deg)	??? To apply SpadeAdam location
1	1	1	1	1	1	1	1	1	:	averaging time for peak concentration (s)	
11	11	11	11	11	11	11	11	11	:	averaging time for averaged concentration (s)	
-99.9	-99.9	-99.9	-99.9	-99.9	-99.9	-99.9	-99.9	-99.9	:	concentration of interest for modeling (ppm)	
1	1	1	1	1	1	1	1	1	:	suggested receptor height for modeling (m)	
4	4	4	4	4	4	4	4	4	:	number of distances downwind	
5	5	5	5	5	5	5	5	5	:	distance downwind (m)	
10	10	10	10	10	10	10	10	10	:	distance downwind (m)	
15	15	15	15	15	15	15	15	15	:	distance downwind (m)	
20	20	20	20	20	20	20	20	20	:	distance downwind (m)	
40	40	40	40	40	40	40	40	40	:	distance downwind (m)	
60	60	60	60	60	60	60	60	60	:	distance downwind (m)	
80	80	80	80	80	80	80	80	80	:	distance downwind (m)	
22.22	27.98	50.05779	-99.9	21.99	21.88	9.185435	8.813	15.58	:	max. conc. (mol %) based on tpeak	All sensors; Original MDA uses ppm instead of mol%
7.10	13.69	16.054	-99.9	8.5271	9.19	4.061425	4.0978	7.16	:	max. conc. (mol %) based on tpeak	All sensors
3.10	9.02	9.598	-99.9	4.7239	5.53	2.987029	2.7901	5.12	:	max. conc. (mol %) based on tpeak	All sensors
5.32	6.79	6.4985	14.244	4.5924	4.02	2.950585	2.391	3.68	:	max. conc. (mol %) based on tpeak	All Sensors
-99.9	6.12	7.143774	15.496	5.3699	4.82	2.563892	4.3929	4.99	:	max. conc. (mol %) based on tpeak	All sensors
-99.9	-99.9	5.0102	8.8944	-99.9	-99.9	-99.9	-99.9	-99.9	:	max. conc. (mol %) based on tpeak	All sensors
-99.9	-99.9	2.774052	6.3711	-99.9	-99.9	-99.9	-99.9	-99.9	:	max. conc. (mol %) based on tpeak	All sensors
21.14	27.46918	37.1426	-99.9	20.77245	21.146655	8.37158	7.705936	15.03	:	max. conc. (mol %) based on tavg	Excluding non-trusted sensors
6.23	12.93045	15.167	-99.9	7.978891	8.3783636	3.492025	3.287882	6.38	:	max. conc. (mol %) based on tavg	Excluding non-trusted sensors
2.27	8.2248	8.8559	-99.9	4.200045	4.1569909	2.119683	2.215382	4.29	:	max. conc. (mol %) based on tavg	Excluding non-trusted sensors
4.53	5.685891	5.905018	13.86173	3.083936	3.0273545	1.99604	1.712187	2.90	:	max. conc. (mol %) based on tavg	Excluding non-trusted sensors
-99.9	3.582927	3.220491	8.615255	2.2071	0.9010455	0.914108	1.860149	1.81	:	max. conc. (mol %) based on tavg	Excluding non-trusted sensors
-99.9	-99.9	3.119291	5.410327	-99.9	-99.9	-99.9	-99.9	-99.9	:	max. conc. (mol %) based on tavg	Excluding non-trusted sensors
-99.9	-99.9	1.58873	4.241636	-99.9	-99.9	-99.9	-99.9	-99.9	:	max. conc. (mol %) based on tavg	Excluding non-trusted sensors
-99.9	-99.9	-99.9	-99.9	-99.9	-99.9	-99.9	-99.9	-99.9	:	sigma-y (m) based on time-summed concentration	
-99.9	-99.9	-99.9	-99.9	-99.9	-99.9	-99.9	-99.9	-99.9	:	sigma-y (m) based on time-summed concentration	
-99.9	-99.9	-99.9	-99.9	-99.9	-99.9	-99.9	-99.9	-99.9	:	sigma-y (m) based on time-summed concentration	
-99.9	-99.9	-99.9	-99.9	-99.9	-99.9	-99.9	-99.9	-99.9	:	sigma-y (m) based on time-summed concentration	
-99.9	-99.9	-99.9	-99.9	-99.9	-99.9	-99.9	-99.9	-99.9	:	sigma-y (m) based on time-summed concentration	
-99.9	-99.9	-99.9	-99.9	-99.9	-99.9	-99.9	-99.9	-99.9	:	sigma-y (m) based on time-summed concentration	
-99.9	-99.9	-99.9	-99.9	-99.9	-99.9	-99.9	-99.9	-99.9	:	sigma-y (m) based on time-summed concentration	

Table 31. MDA data for BP DF1 CO2 experiments (input and measured data)

MDA INPUT VARIABLE								MEANING INPUT VARIABLE	REFERENCE / ADDITIONAL NOTE
Shell C02 pressurised field releases, SpadeAdam								Name of field experiments	
Carbon Dioxide								Chemical released	
CO2								: 3-char. abbreviation of chemical	
8								: number of trials included in MDA	
?								: time zone designation	??? To apply GMT time
CO2SH3	C02SH5	CO2SH11	CO2SH1	CO2SH2	CO2SH4	CO2SH14	CO2SH16	: trial ID	tests: liquid [steady 3,5,11 - transient 1,2,4], transient vapour [14,16]
17	14	10	9	14	30	24	26	: day	GL report - Table 1
9	10	11	9	9	9	11	11	: month	GL report - Table 1
2010	2010	2010	2010	2010	2010	2010	2010	: year	GL report - Table 1
18	14	14	16	18	12	19	16	: hour	GL report - Table 1
21	53	49	33	17	40	33	21	: minute	GL report - Table 1
44.01	44.01	44.01	44.01	44.01	44.01	44.01	44.01	: mol. weight (g/mole)	Property as in MDA KitFox for CO2
186.25	186.25	186.25	186.25	186.25	186.25	186.25	186.25	: normal boiling point (K)	Property as in MDA KitFox for CO2
154749	154749	154749	154749	154749	154749	154749	154749	: latent heat of evaporation (J/kg) at 20C	Property as in MDA KitFox for CO2
839.3	839.3	839.3	839.3	839.3	839.3	839.3	839.3	: specific heat - vapor (J/kg-K) at 20C	Property as in MDA KitFox for CO2
4118.8	4118.8	4118.8	4118.8	4118.8	4118.8	4118.8	4118.8	: specific heat - liquid (J/kg-K) at 20C	Property as in MDA KitFox for CO2
773.3	773.3	773.3	773.3	773.3	773.3	773.3	773.3	: density of liquid (kg/m**3) at 20C	Property as in MDA KitFox for CO2
-1	-1	-1	-1	-1	-1	-1	-1	: coefficient A for vapor pressure equation	?? Suggest use DIPPR formula (vapour/solid vapour pressure)
0	0	0	0	0	0	0	0	: coefficient B for vapor pressure equation	?? Suggest use DIPPR formula (vapour/solid vapour pressure)
144.80	126.40	80.30	143.00	118.00	148.20	151.60	150.60	: exit gauge pressure (bar)	datasheets - mean P08 (3,5,11), initial P08 (1,2,4), initial P03(14,16)
281.35	286.85	271.75	296.15	291.15	293.25	344.15	309.85	: source temperature (K)	datasheets - mean T09 (3,5,11), initial T09 (1,2,4), initial T03 (14,16)
0.0127	0.0254	0.0127	0.0127	0.0254	0.0063	0.0127	0.0127	: source diameter (m)	GL report - Section 3.1
1	1	1	1	1	1	1	1	: source elevation (m)	GL report - Section 3.1 (1m height with 5% accuracy)
HJ	HJ	HJ	HJ	HJ	HJ	HJ	HJ	: source type (IR,HJ,AS,EP)	Horizontal jet (HJ)
L	L	L	L	L	L	G	G	: source phase (L,C,G)	Liquid (L) or gas (G)
-99.9	-99.9	-99.9	-99.9	-99.9	-99.9	-99.9	-99.9	: source containment diameter (m)	
12.4	44.7	8.9	10.55	38.0	3.17	7.37	10.5	: spill/evaporation rate (kg/s)	1, 2, 4, 14, 16 are time-varying releases (initial rate taken)
120	40	120	90	145	>700	315	370	: spill duration (s)	1, 2, 4, 14, 16 are time-varying releases (initial rate taken)
-99.9	-99.9	-99.9	-99.9	-99.9	-99.9	-99.9	-99.9	: total released (kg)	
1.00E+06	1.00E+06	1.00E+06	1.00E+06	1.00E+06	1.00E+06	1.00E+06	1.00E+06	: initial concentration (ppm)	
1.017	0.905	0.995	1.006	1.005	0.9755	1.005	0.997	: ambient pressure (bar)	GL report - App. B.3,B.5,B.7;B.1,B.2,B.4;B.8,B.9
66	91	78	83	77	77	88	88	: relative humidity (%)	GL report - App. B.3,B.5,B.7;B.1,B.2,B.4;B.8,B.9
284.35	282.15	276.75	287.85	283.45	286.95	273.15	270.25	: ambient temperature #1-lower (K)	GL report - App. B.3,B.5,B.7;B.1,B.2,B.4;B.8,B.9
0	0	0	0	0	0	0	0	: measurement height for temperature #1 (m)	
-99.9	-99.9	-99.9	-99.9	-99.9	-99.9	-99.9	-99.9	: ambient temperature #2-upper (K)	
-99.9	-99.9	-99.9	-99.9	-99.9	-99.9	-99.9	-99.9	: measurement height for temperature #2 (m)	
282.35	280.15	274.75	285.85	281.45	284.95	271.15	268.25	: soil temperature (K)	Following BP advice, assumed to be 2 degrees lower than ambient
1	1	1	1	1	1	1	1	: soil moisture (1:dry,2:moist,3:water)	
4.05	1.3	2.76	3.93	5.43	1.98	1.34	1.48	: wind speed (m/s)	datasheets - mean value A1 prior to release
10	10	10	10	10	10	10	10	: measurement height for wind speed (m)	GL report - Section 4.1
-99.9	-99.9	-99.9	-99.9	-99.9	-99.9	-99.9	-99.9	: domain-avg wind speed (m/s)	
-99.9	-99.9	-99.9	-99.9	-99.9	-99.9	-99.9	-99.9	: domain-avg sigma-u (m/s)	
-99.9	-99.9	-99.9	-99.9	-99.9	-99.9	-99.9	-99.9	: domain-avg sigma-theta (deg)	
-99.9	-99.9	-99.9	-99.9	-99.9	-99.9	-99.9	-99.9	: measurement ht for domain-avg wind data (m)	
?	?	?	?	?	?	?	?	: averaging time for wind and temperature data (s)	to check
0.1	0.1	0.1	0.1	0.1	0.1	0.1	0.1	: roughness length z0 (m)	presumed
-99.9	-99.9	-99.9	-99.9	-99.9	-99.9	-99.9	-99.9	: friction velocity u-star (m/s)	
-99.9	-99.9	-99.9	-99.9	-99.9	-99.9	-99.9	-99.9	: bowen ratio estimate	
-99.9	-99.9	-99.9	-99.9	-99.9	-99.9	-99.9	-99.9	: inverse Monin-Obukhov length (1/m)	
?	?	?	?	?	?	?	?	: cloud cover (%)	??? To check
4	4	4	4	4	4	4	4	: Pasquill-Gifford stability class (A=1;D=4;F=6)	Assumed D
?	?	?	?	?	?	?	?	: latitude (deg)	??? To apply SpadeAdam location
?	?	?	?	?	?	?	?	: longitude (deg)	??? To apply SpadeAdam location
1	1	1	1	1	1	1	1	: averaging time for peak concentration (s)	no averaging time given by GL report; presumed value
-99.9	-99.9	-99.9	-99.9	-99.9	-99.9	-99.9	-99.9	: averaging time for averaged concentration (s)	
-99.9	-99.9	-99.9	-99.9	-99.9	-99.9	-99.9	-99.9	: concentration of interest for modeling (ppm)	
1	1	1	1	1	1	1	1	: suggested receptor height for modeling (m)	
4	4	4	4	4	4	4	4	: number of distances downwind	
5	5	5	5	5	5	5	5	: distance downwind (m)	
10	10	10	10	10	10	10	10	: distance downwind (m)	
15	15	15	15	15	15	15	15	: distance downwind (m)	
20	20	20	20	20	20	20	20	: distance downwind (m)	
40	40	40	40	40	40	40	40	: distance downwind (m)	
60	60	60	60	60	60	60	60	: distance downwind (m)	
80	80	80	80	80	80	80	80	: distance downwind (m)	
33.74	39.00	16.00	23.87	43.11	12.18	18.26	20.73	: max. conc. (mol %) based on tpeak	datasheets - All O2 sensors; original MDA uses ppm instead of mol%
13.98	20.11	8.31	9.68	19.75	4.86	6.94	8.45	: max. conc. (mol %) based on tpeak	datasheets - max. of all O2 sensors at given distance downstream
8.79	18.36	7.87	5.45	12.39	2.98	6.34	8.17	: max. conc. (mol %) based on tpeak	datasheets - max. of all O2 sensors at given distance downstream
6.41	12.35	5.04	4.77	10.59	2.57	3.28	4.91	: max. conc. (mol %) based on tpeak	datasheets - max. of all O2 sensors at given distance downstream
3.98	5.83	3.02	2.82	5.75	1.39	1.88	2.86	: max. conc. (mol %) based on tpeak	datasheets - max. of all O2 sensors at given distance downstream
2.34	3.06	1.68	1.54	2.74	1.04	1.16	1.61	: max. conc. (mol %) based on tpeak	datasheets - max. of all O2 sensors at given distance downstream
1.92	2.69	3.73	1.42	2.67	0.61	0.91	4.30	: max. conc. (mol %) based on tpeak	datasheets - max. of all O2 sensors at given distance downstream
-99.9	-99.9	-99.9	-99.9	-99.9	-99.9	-99.9	-99.9	: max. conc. (mol %) based on tavg	
-99.9	-99.9	-99.9	-99.9	-99.9	-99.9	-99.9	-99.9	: max. conc. (mol %) based on tavg	
-99.9	-99.9	-99.9	-99.9	-99.9	-99.9	-99.9	-99.9	: max. conc. (mol %) based on tavg	
-99.9	-99.9	-99.9	-99.9	-99.9	-99.9	-99.9	-99.9	: max. conc. (mol %) based on tavg	
-99.9	-99.9	-99.9	-99.9	-99.9	-99.9	-99.9	-99.9	: max. conc. (mol %) based on tavg	
-99.9	-99.9	-99.9	-99.9	-99.9	-99.9	-99.9	-99.9	: max. conc. (mol %) based on tavg	
-99.9	-99.9	-99.9	-99.9	-99.9	-99.9	-99.9	-99.9	: max. conc. (mol %) based on tavg	
-99.9	-99.9	-99.9	-99.9	-99.9	-99.9	-99.9	-99.9	: sigma-y (m) based on time-summed concentration	
-99.9	-99.9	-99.9	-99.9	-99.9	-99.9	-99.9	-99.9	: sigma-y (m) based on time-summed concentration	
-99.9	-99.9	-99.9	-99.9	-99.9	-99.9	-99.9	-99.9	: sigma-y (m) based on time-summed concentration	
-99.9	-99.9	-99.9	-99.9	-99.9	-99.9	-99.9	-99.9	: sigma-y (m) based on time-summed concentration	
-99.9	-99.9	-99.9	-99.9	-99.9	-99.9	-99.9	-99.9	: sigma-y (m) based on time-summed concentration	
-99.9	-99.9	-99.9	-99.9	-99.9	-99.9	-99.9	-99.9	: sigma-y (m) based on time-summed concentration	
-99.9	-99.9	-99.9	-99.9	-99.9	-99.9	-99.9	-99.9	: sigma-y (m) based on time-summed concentration	

Table 32. MDA data for Shell CO_2 experiments (input and measured data)

A.4 Finite-duration dispersion (Kit Fox experiments)

The input data for the Kit Fox experiments are given below as taken from the MDA database from Hanna and Chang (1999)[23].

Series	Kit Fox - URA continuous
Substance	CO_2
Release height (m)	0
Release direction	Vertical
Ref. height for windspeed (m)	2
Ref. height for air temperature (m)	2.1
Surface roughness length (m)	0.01
Dispersing surface	Land
Solar flux (W/m2)	500
Averaging time (s)	20

URA continuous experiment	KF0604	KF0805	KF0702	KF0808	KF0605	KF0703	KF0705	KF0606	KF0811	KF0709	KF0609	KF0712
Release duration (s)	120	150	140	120	120	180	180	180	240	180	300	255
Release rate (kg/s)	1.758	1.513	1.913	1.622	1.881	1.651	1.733	2.072	1.498	1.722	1.47	1.544
Release temperature (K)	305.22	305.23	307.57	303.25	303.77	306.46	305.81	302.45	300.53	303.62	302.29	302.2
Release velocity (m/s)	0.496	0.420	0.531	0.451	0.523	0.459	0.481	0.579	0.416	0.478	0.408	0.432
Stability class	D	D	E	E	E	E	E	E	E	F	F	F
Wind speed at ref. height (m/s)	4.09	3.36	4.03	3.36	3.18	2.98	2.82	2.31	2.25	2.24	1.8	1.75
Ambient temperature (K)	309.84	309.84	311.42	309.84	309.11	311.02	310.68	308.53	307.36	308.48	307.12	307.11
Ambient pressure (Pa)	90442	90412	90433	90433	90443	90433	90433	90453	90473	90443	90463	90453
Relative humidity (fraction)	0.14	0.15	0.1	0.15	0.14	0.1	0.1	0.14	0.16	0.12	0.14	0.12
Dispersing surface temp. (K)	307.08	308.2	309.17	307.29	306.35	308.52	307.96	305.96	305.11	305.94	304.98	305.04
Release density of CO2 (kg/m3)	1.580	1.605	1.605	1.605	1.605	1.605	1.605	1.595	1.605	1.605	1.605	1.593

Series	Kit Fox - ERP continuous
Substance	CO_2
Release height (m)	0
Release direction	Vertical
Ref. height for windspeed (m)	2
Ref. height for air temperature (m)	2.1
Surface roughness length (m)	0.12
Dispersing surface	Land
Solar flux (W/m2)	500
Averaging time (s)	20

ERP continuous experiment	KF0503	KF0504	KF0206	KF0305	KF0508	KF0404
Release duration (s)	120	120	360	300	180	450
Release rate (kg/s)	3.915	3.701	3.887	3.986	3.769	3.89
Release temperature (K)	298.71	297.26	306.37	298.71	296.76	295.76
Release velocity (m/s)	1.08	1.02	1.08	1.10	1.05	1.08
Stability class	D	E	F	F	F	F
Wind speed at ref. height (m/s)	2.63	2.21	1.84	1.45	1.22	0.82
Ambient temperature (K)	306.6	306.28	306.03	305.64	304.55	303.17
Ambient pressure (Pa)	90544	90554	90402	90453	90574	90483
Relative humidity (fraction)	0.15	0.16	0.16	0.05	0.16	0.06
Dispersing surface temp. (K)	303.27	303.01	303.97	303.06	301.77	301.24
Release density of CO_2 (kg/m3)	1.616	1.618	1.605	1.615	1.605	1.605

Series	Kit Fox - URA puff
Substance	CO_2
Release height (m)	0
Release direction	Vertical
Release duration (s)	20
Ref. height for windspeed (m)	2
Ref. height for air temperature (m)	2.1
Surface roughness length (m)	0.01
Dispersing surface	Land
Solar flux (W/m2)	500
Averaging time (s)	20

URA puff experiment	KF0801	KF0601	KF0803	KF0802	KF0804	KF0602	KF0603	KF0806	KF0807	KF0809	KF0706	KF0810
Release rate (kg/s)	1.109	1.282	1.618	1.619	1.651	1.654	1.712	1.589	1.756	1.572	1.498	1.576
Release temperature (K)	309.76	308.39	308.42	309.13	307.84	307.74	307.02	305.18	304.67	303.3	305.47	303.34
Release velocity (m/s)	0.308	0.365	0.449	0.450	0.459	0.459	0.476	0.441	0.488	0.437	0.423	0.438
Stability class	D	D	D	D	D	D	D	D	E	E	E	E
Wind speed at ref. height (m/s)	4.62	4.42	4.31	4.29	4.20	4.03	3.85	3.36	3.24	3.09	2.66	2.47
Ambient temperature (K)	311.67	310.19	311.47	311.59	311.09	310.05	309.97	310.26	310.05	309.43	309.92	308.68
Ambient pressure (Pa)	90422	90442	90412	90422	90412	90443	90443	90422	90422	90443	90433	90453
Relative humidity (fraction)	0.15	0.14	0.15	0.15	0.15	0.14	0.15	0.15	0.15	0.15	0.11	0.15
Dispersing surface temp. (K)	309.75	307.65	309.27	309.49	308.62	307.46	307.27	307.68	307.55	306.92	307.08	306.25
Release density of CO_2 (kg/m3)	1.605	1.566	1.605	1.605	1.605	1.605	1.605	1.605	1.605	1.605	1.579	1.605

URA puff experiment	KF0812	KF0704	KF0708	KF0710	KF0607	KF0711	KF0608	KF0713	KF0714
Release rate (kg/s)	1.46	1.675	1.638	1.697	1.785	1.631	1.635	1.389	1.41
Release temperature (K)	300.3	306.21	305.02	303.32	302.44	303.31	302.42	301.97	302.1
Release velocity (m/s)	0.406	0.465	0.455	0.471	0.496	0.453	0.457	0.386	0.392
Stability class	E	F	F	F	F	F	F	F	F
Wind speed at ref. height (m/s)	2.21	2.77	2.61	2.01	1.94	1.93	1.89	1.58	1.40
Ambient temperature (K)	307.2	310.94	308.97	308.1	307.94	307.73	307.64	306.52	306.06
Ambient pressure (Pa)	90473	90433	90443	90443	90453	90443	90463	90453	90463
Relative humidity (fraction)	0.17	0.1	0.11	0.12	0.14	0.12	0.14	0.13	0.13

Dispersing surface temp. (K)	304.75	308.3	306.23	305.69	305.64	305.38	305.45	304.65	304.18
Release density of CO2 (kg/m3)	1.605	1.605	1.605	1.605	1.605	1.605	1.595	1.605	1.605

Series	Kit Fox - ERP puff
Substance	CO2
Release height (m)	0
Release direction	Vertical
Ref. height for windspeed (m)	2
Ref. height for air temperature (m)	2.1
Surface roughness length (m)	0.12
Dispersing surface	Land
Solar flux (W/m2)	500
Averaging time (s)	20

ERP puff experiment	KF0201	KF0301	KF0302	KF0502	KF0501	KF0303	KF0505	KF0506	KF0304	KF0507	KF0403	KF0306	KF0307
Release duration	25	20	20	20	20	20	20	20	20	20	20	20	20
Release rate (kg/s)	4.277	4.085	4.3	4.027	3.996	3.802	3.755	3.742	3.75	3.976	3.896	3.758	3.647
Release temperature (K)	306.41	305.27	304.34	303.17	307.6	303.35	297.42	297.97	302.33	297.82	300.3	298.67	298.4
Release velocity (m/s)	1.21	1.13	1.19	1.12	1.11	1.06	1.04	1.04	1.05	1.10	1.08	1.04	1.01
Stability class	7	7	7	7	7	7	8	8	8	9	9	9	9
Wind speed at ref. height (m/s)	2.88	3.07	2.74	2.7	2.64	2.19	2.24	1.67	1.66	1.43	1.24	1.22	1.14
Ambient temperature (K)	308.81	308.21	307.87	306.8	307.15	307.16	306.15	305.38	306.36	304.9	303.93	304.56	304.17
Ambient pressure (Pa)	90382	90443	90443	90534	90524	90443	90554	90574	90442	90574	90483	90463	90463
Relative humidity (fraction)	0.14	0.04	0.05	0.15	0.15	0.05	0.16	0.16	0.05	0.16	0.06	0.05	0.05
Dispersing surface temp. (K)	307.51	305.77	305.18	303.45	304.2	304.37	302.82	302.27	303.56	301.95	301.88	302.38	302.06
Release density of CO2 (kg/m3)	1.576	1.605	1.605	1.605	1.605	1.605	1.605	1.605	1.592	1.606	1.605	1.611	

A.5 PHMSA Validation Cases

LNG Experiments

The main assumptions for the LNG releases are outlined below:

- LNG is modelled as pure methane. This is in line with our recommendation for multi-component releases in Phast 6.7, since methane is the main component for all LNG releases. The LNG Model Validation Database also states this is generally an acceptable approach to model LNG vapour from evaporating pools.

- For these experiments, the methane was released from an elevated height with a very low momentum. This results in close to 100% rainout almost immediately.

- Coyote and Burro the spills were into a water basin, and we specify the “shallow open water” pool surface type. This has a minimum pool depth of 1 mm, and allows for ice formation underneath the pool. Given its offshore location, and in the absence of evidence to the contrary, we have run Maplin Sands using “deep open water” which does not allow ice formation. For Burro and Coyote the subsequent dispersion was over land, whereas the substrate is water for Maplin Sands.

- “Short” averaging time releases use t_{av} = 18.75s (equivalent to instantaneous maximum concentration when accounting for wind meander). “Long” averaging time releases use the specified value of t_{av} and use a time-centred rolling average calculation over that period to calculate concentrations. This corresponds to “Method 2” in the V12 database guide.

- For Coyote, custom processing within Phast and post-processing of exported results has been performed in order to remove the post-ignition data from the calculated time series..

- Phast normally uses a post-processing correction to unaveraged results (i.e. generated using t_{av}=18.75 s) to account for different averaging times. This is done for performance reasons when users are interested in multiple averaging times. Here however for maximum accuracy we run all calculations at the desired averaging time. This applies to all experiments, not just LNG.

- We have assumed low release velocity (0.1 m/s) and the maximum permissible droplet size (1 cm) in all cases. Results are insensitive to changes in these inputs over realistic ranges.

The Phast default parameters should be sufficient for all other settings. A comprehensive set of input data for the LNG experiments is provided in Table 33.

Description	Units	MSN27	MSN34	MSN35	BU03	BU07	BU08	BU09	CO03	CO05	CO06
RELEASE DATA											
Release type		Continuous	Continuous	Continuous	Continuous	Continuous	Continuous	Continuous	Continuous	Continuous	Continuous
Released material name		Methane	Methane	Methane	Methane	Methane	Methane	Methane	Methane	Methane	Methane
Duration	s	160	95	135	167	174	107	167	65	98	82
Mass released	kg	3714	2044	3658	1E+05	17289	12453	10730	6532	12676	10139
Flowrate	kg/s	23.21	21.51	27.09	87.98	99.46	116.9	136	100.7	129	123
Temperature of release component	K	111.65	111.65	111.65	110.85	110.85	110.85	110.85	110.75	110.75	110.75
Liquid mass fraction of release component	kg/kg	1	1	1	1	1	1	1	1	1	1
Droplet diameter (SMD)	m	0.01	0.01	0.01	0.01	0.01	0.01	0.01	0.01	0.01	0.01
Release velocity	m/s	0.1	0.1	0.1	0.1	0.1	0.1	0.1	0.1	0.1	0.1
Release height	m	0.5	0.7	0.5	1.5	1.5	1.5	1.5	1.5	1.5	1.5
Release angle [from horizontal]	degrees	0	0	0	0	0	0	0	0	0	0
AMBIENT DATA											
Pasquill stability class	-	C/D	D	D	C	D	E	D	C	C	D
Wind speed at reference height	m/s	5.5	8.6	9.8	5.58	8.75	1.94	5.94	6.77	10.47	5.04
Reference height for windspeed	m	10	10	10	3	3	3	3	3	3	3
Temperature at reference height	K	288.1	288.4	289.3	307.75	306.96	306.02	308.52	311.45	301.49	297.26
Pressure at reference height	N/m2	101325	101325	101325	94840	94028	94130	94029	93624	93928	94232
Reference height for temperature /pressure	m	1.9	1.9	1.9	1.0	1.0	1.0	1.0	1.0	1.0	1.0
Atmospheric humidity (fraction)	-	0.53	0.9	0.77	0.052	0.074	0.045	0.144	0.113	0.221	0.228
SUBSTRATE DATA											
Surface roughness length	m	0.0003	0.0003	0.0003	0.0002	0.0002	0.0002	0.0002	0.0002	0.0002	0.0002
Dispersing surface type		Water	Water	Water	Land	Land	Land	Land	Land	Land	Land
Temperature of dispersing surface	K	288.8	289	289.8	307.75	306.96	306.02	308.52	311.45	301.49	297.26
POOL DATA											
Pool surface type		Deep Open Water	Deep Open Water	Deep Open Water	Shallow Open Water	Shallow Open Water	Shallow Open Water	Shallow Open Water	Shallow Open Water	Shallow Open Water	Shallow Open Water
Temperature of pool surface	K	288.8	289	289.3	307.75	306.96	306.02	308.52	311.45	301.49	297.26
Bund diameter (<=0: no bund)	m	0	0	0	58	58	58	58	58	58	58
Bund height	m	0	0	0	0	0	0	0	0	0	0

Table 33: UDM Input Data for all PHMSA LNG experiments

Thorney Island Continuous Experiments

The geometry of the release was complicated: a vertical pipe releasing gas into a 2m diameter plate 0.5m above the surface to ensure low vertical momentum. The arrangement is shown in Figure 26, with the images taken from McQuaid & Roebuck (McQuaid & Roebuck, 1985)[29].

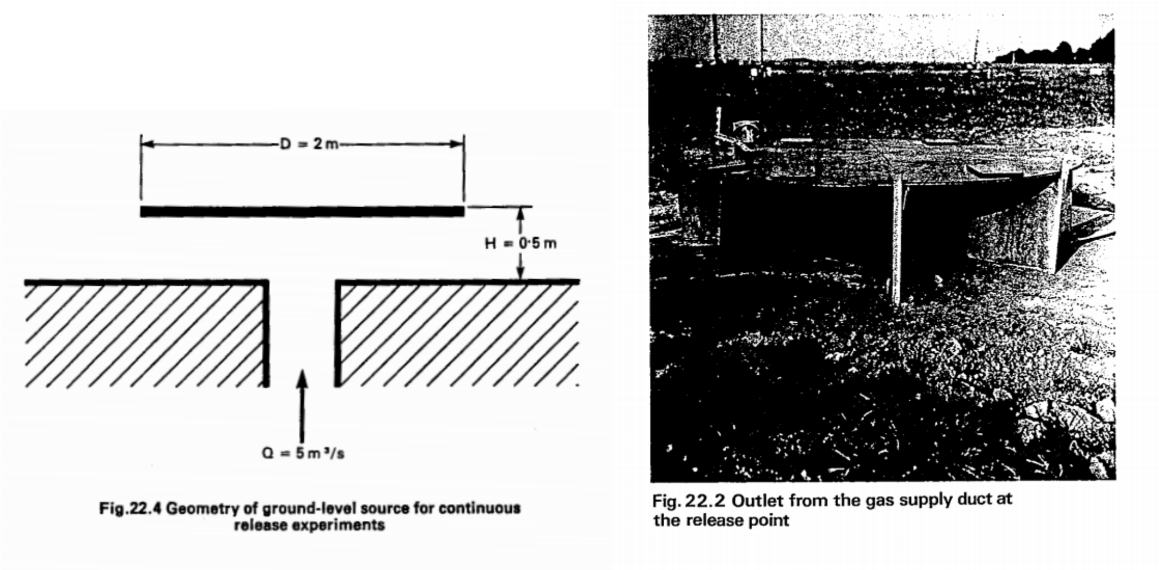

Figure 26: Thorney Island Source for continuous release experiments.

It is not obvious how such a cylindrical source should be modelled in Phast. This is in-effect is a low momentum ‘cylindrical wall’ gas source, released in all directions before being dispersed downwind. Phast requires the provision of a flow rate and a velocity, from which a (planar) release area will be calculated. We have chosen a very low momentum horizontal jet, with horizontal velocity u equal to the calculated source exit velocity assuming a pipe of diameter $D_{source} = 2\,m$ and plate height $h = 0.5\,m$

$$\boldsymbol{u = \frac{Q}{A\rho_v} = \frac{Q}{\pi\rho_v}}$$

Here Q is the release rate (kg/s), A is the source area (= $\pi D_{source} h$) and ρv the vapour density of the Freon-12 / N2 mixture. This gives an equivalent release source with the correct velocity and flow rate, although the full mass flux is initially directed in a single direction. The height associated with the release is selected to be 0.25 m, half the height of the diverting plate.

While the overall flow rate and exit velocity are accurately represented in Phast, the directionality at the source is not: net horizontal momentum for the actual release is zero, and this could affect near-field concentrations

For TI45, the actual stability class is E-F, whereas in Phast one must choose either E or F. We have chosen F, this does not affect results significantly down to the 1% or so concentration level.

All measurements are based on an averaging time of 30s. The input data used for the Thorney Island experiments are presented in Table 34.

Description	Units	TI45	TI47
RELEASE DATA			
Release type		Continuous	Continuous
Released material name		Freon (32%) N2 (68%)	Freon (32%) N2 (68%)
Duration	s	455	465
Mass released	kg	4855	4752
Flowrate	kg/s	10.67	10.22
Temperature of release component	K	286.25	287.45
Liquid mass fraction of release component	kg/kg	0	0
Release velocity	m/s	1.383	1.325
Release height	m	0.25	0.25
Release angle [from horizontal]	degrees	0	0
AMBIENT DATA			
Pasquill stability class	-	F	F
Wind speed at reference height	m/s	2.3	1.5
Reference height for windspeed	m	10	10
Temperature at reference height	K	286.25	287.45
Pressure at reference height	N/m2	101325	101325
Reference height for temperature and pressure	m	2.0	2.0
Atmospheric humidity (fraction)	-	1.0	0.974
SUBSTRATE DATA			
Surface roughness length	m	0.01	0.01
Dispersing surface type		Land	Land
Temperature of dispersing surface	K	285.95	287.65

Table 34: UDM input data for Thorney Island (continuous) experiments

Wind Tunnel Experiments

These wind-tunnel experiments involved isothermal releases. They corresponded to CO_2 (CHRC-A) and SF_6 (BA-Hamburg, BA-TNO) vapour area sources at ground level. Only the unobstructed experiments have been modelled.

All the experiments have been modelled at field scale rather than at the experimental scale. The UDM default atmospheric wind-speed profile (a function of vertical height, stability class and surface roughness) is appropriate for outdoor conditions but may not be appropriate for the wind tunnel. The wind profile exponent is calculated for a fixed geometric mean height for the boundary layer of 32.6m. Instead one should ideally use a best power-law fit to the experimentally observed wind-speed profile, but currently Phast does not support the direct input of a wind exponent. Therefore we have used the scaled data in our simulations. The UDM passive dispersion coefficients σ_y, σ_z (as function of downwind distance, stability class, averaging time, etc.) are based on typical outdoor ambient turbulence and may again not be valid for wind tunnel conditions (although this may be less of an issue for neutral conditions).

Thus overall one needs to be very careful applying the standard UDM model to wind tunnel conditions, particularly with reference to establishing the ambient conditions (wind speed, turbulence) inside the wind-tunnel. Since modification of these ambient conditions is not currently possible by the Phast user, we have therefore selected to model the full-scale comparison only.

In each case, the release source is at ground level over a relatively wide field-scale area with low gas velocity. Such releases can be specified in Phast as a ‘pool source (radius)’ on the ‘user-defined source’ window representing the release. The user needs to specify the flow rate, temperature and radius corresponding to the given source area, with the release velocity calculated from these values.

The input data used for the wind tunnel experiments are presented in Table 35. The largest changes in the input data from the previous V11 database are related to the BA-Hamburg experiments, and largely related to uncertainties regarding the obstructed experiments. The changes that impact the unobstructed cases are:

- Clarification of the release flow rate and the source/ambient temperatures associated with the experiments.
- A recommendation for modellers to select the appropriate surface roughness which gives closest agreement with the vertical velocity and turbulence intensity profiles published by Marotzke and presented in the V12 database guide (Stewart, Coldrick, Gant, & Ivings, 2016).

The Marotzke velocity profile has been fitted to the UDM power law formulation to give a best fit roughness of 0.0039 m, which has been used for both BA-Hamburg experiments. This is within the stated range of 0.0055m ± 0.0045m for the equivalent field scale surface roughness.

Description	Units	CHRC A	Hamburg DA0120	Hamburg DAT223	TNO TUV01	TNO FLS
RELEASE DATA						
Release type		Continuous	Continuous	Continuous	Continuous	Continuous
Released material name		CO2	SF6	SF6	SF6	SF6
Duration	s	1470	2881	1024	883	883
Mass released	kg	-	-	-	-	-
Flowrate	kg/s	291.1	60	300	13.43	56.2
Temperature of release component	K	296	283.5	283.5	293	293
Liquid mass fraction of release component	kg/kg	0	0	0	0	0
Release velocity	m/s	0.02	0.094	0.471	0.0399	0.167
Release height	m	0.0 (Pool Source)	0.0 (Pool Source)	0.0 (Pool Source)	0.0 (Pool Source)	0.0 (Pool Source)
Release angle [from horizontal]	degrees	-	-	-	-	-
AMBIENT DATA						
Pasquill stability class	-	D	D	D	D	D
Wind speed at reference height	m/s	4.9	6.92	9.47	5.12	6.88
Reference height for windspeed	m	10	1.178	2.24	0.65	1.17
Temperature at reference height	K	296	287.2	287.2	293	293
Pressure at reference height	N/m2	97880	101325	101325	101325	101325
Reference height for temperature and pressure	m	0.0	0.0	0.0	0.0	0.0
Atmospheric humidity (fraction)	-	0.7	0.7	0.7	0.7	0.7
SUBSTRATE DATA						
Surface roughness length	m	0.108	0.0039	0.0039	0.0039	0.0039
Dispersing surface type		Land	Land	Land	Land	Land
Temperature of dispersing surface	K	296	287.2	287.2	293	293

Table 35: UDM input data for wind tunnel experiments

Appendix B. Definition of cloud width

The cloud width for a continuous release is calculated according to the availability and definition of the experimental cloud width:

1. No experimental cloud width data

In the cases where no experimental data is available the UDM effective cloud half width is plotted. This is defined as follows (see UDM theory manual for further details)

$$W_{eff} = \frac{1}{c(x,0,z)} \int_0^\infty c(x,y,z)dy = \int_0^\infty F_h(y)dy = \Gamma(1+\frac{1}{m})R_y(x) \quad (11)$$

2. SMEDIS data

The cloud width b (m) for SMEDIS[11]output is defined by

$$b^2 = \frac{\int_0^\infty y^2 c(x,y,z)dy}{\int_0^\infty c(x,y,z)dy} = \frac{\int_0^\infty y^2 F_h(y)dy}{\int_0^\infty F_h(y)dy} = \frac{\Gamma(\frac{3}{m})}{\Gamma(\frac{1}{m})} R_y(x)^2 \quad (12)$$

and therefore

$$b = \sqrt{\frac{\Gamma(\frac{3}{m})}{\Gamma(\frac{1}{m})}} \; R_y(x) \quad (13)$$

3. Hanna's Data

Hanna's[10] cloud width is defined as the lateral distance at which the cloud concentration has fallen to a factor $e^{-0.5}$ times the centreline concentration:

$$\frac{c(x,b,z)}{c(x,0,z)} = e^{-0.5} \quad (14)$$

From this definition the following relationship may be defined:

$$c(x,b,z) = c_o(x)\, F_h(b) = c_o(x) \exp\left[-\left(\frac{b}{R_y(x)} \right)^m \right] \quad (15)$$

hence from the given definition

$$\exp\left[-\left(\frac{b}{a_2(x)} \right)^m \right] = \exp(-0.5) \quad ; \quad b = \frac{R_y(x)}{2^{1/m}} = 2^{\frac{1}{2}-\frac{1}{m}} \sigma_y \quad (16)$$

4. PHMSA data

For the Burro and Coyote experiments, the UDM cloud width has been calculated in line with the LNG guideline by Coldrick et al[3]. Thus the width is calculated using the Pasquill definition of cloud width, $b_{PASQUILL}$. See the UDM theory manual for the UDM concentration profile, which expresses the concentration c(x,y,z) as a function of downwind distance x, crosswind distance y and vertical height z. By insertion of this profile into the formula for the cloud width, the UDM cloud width has been evaluated (m = vertical cross-wind concentration profile exponent, R_y = UDM cloud crosswind radius, Γ = Gamma function):

$$b_{PASQUILL} = \sqrt{\frac{\int_0^\infty y^2 c(x,y,z)dy}{\int_0^\infty c(x,y,z)dy} - \left\{\frac{\int_0^\infty y\, c(x,y,z)dy}{\int_0^\infty c(x,y,z)dy}\right\}^2} = R_y(x)\sqrt{\left\{\frac{\Gamma(\frac{3}{m})}{\Gamma(\frac{1}{m})} - \frac{\Gamma(\frac{2}{m})}{\Gamma(\frac{1}{m})}\right\}} \qquad (17)$$

Comparison of cloud widths

Figure 27 plots each of the four above definitions for cloud width (as a proportion to RADY), as a function of the exponent m in the crosswind conentration profile. According to the UDM theory manual, m is a function of the density ratio r = $(\rho_{cld} - \rho_a)/\rho_a$ with m=2 for r=0 and m→ 50 for values 5 larger than 5. Thus for a heavy gas release, m will typically vary from m=50 (top-hat profile) in the near-field to m=2 (Gaussian profile) in the far-field.

- As m → 50 (typically in the near-field), the Hanna width becomes close to the effective cloud width, while the SMEDIS and PHMSA definitions become smaller.
- As m → 2 (downwind distance x → ∞) the definitions by Hanna, SMEDIS and PHMSA become identical. Thus for experimental datapoints sufficiently downwind, all the latter three defintions lead to identical result.

Time-varying release

All the above formulas are applicable to continuous releases. For the datasets currently in the experimental database effects of time-varying dispersion are only applicable to the Kit Fox experiments (finite-duration releases; MDA Hanna's definition of cloud width b; along-wind diffusion effects relevant) for to the experimennts involving pools (Burro, Coyote, Maplin Sands; PHMSA definition of cloud width b; along-wind diffusion effects not relevant).

Hanna's equation (14) can also be applied for time-varying releases, where for validation purposes (to evaluate MG, VG) the maximum value of the cloud width b over all times is adopted.

The SMEDIS and PHMSA integral definitions of cloud width given by Equations (12) and (17) could be applied in general for time-varying releases, but this would require an evaluation of the integrals and again a maximum value of y over all times could be adopted. However if one would ignore effects of along-wind diffusion and observer mass correction, one can again use the analytical expressions (13) and (17) in terms or R_y and m to evaluate the cloud width b, where again for validation purposes (to evaluate MG, VG) the maximum value of the cloud width b over all times is adopted.

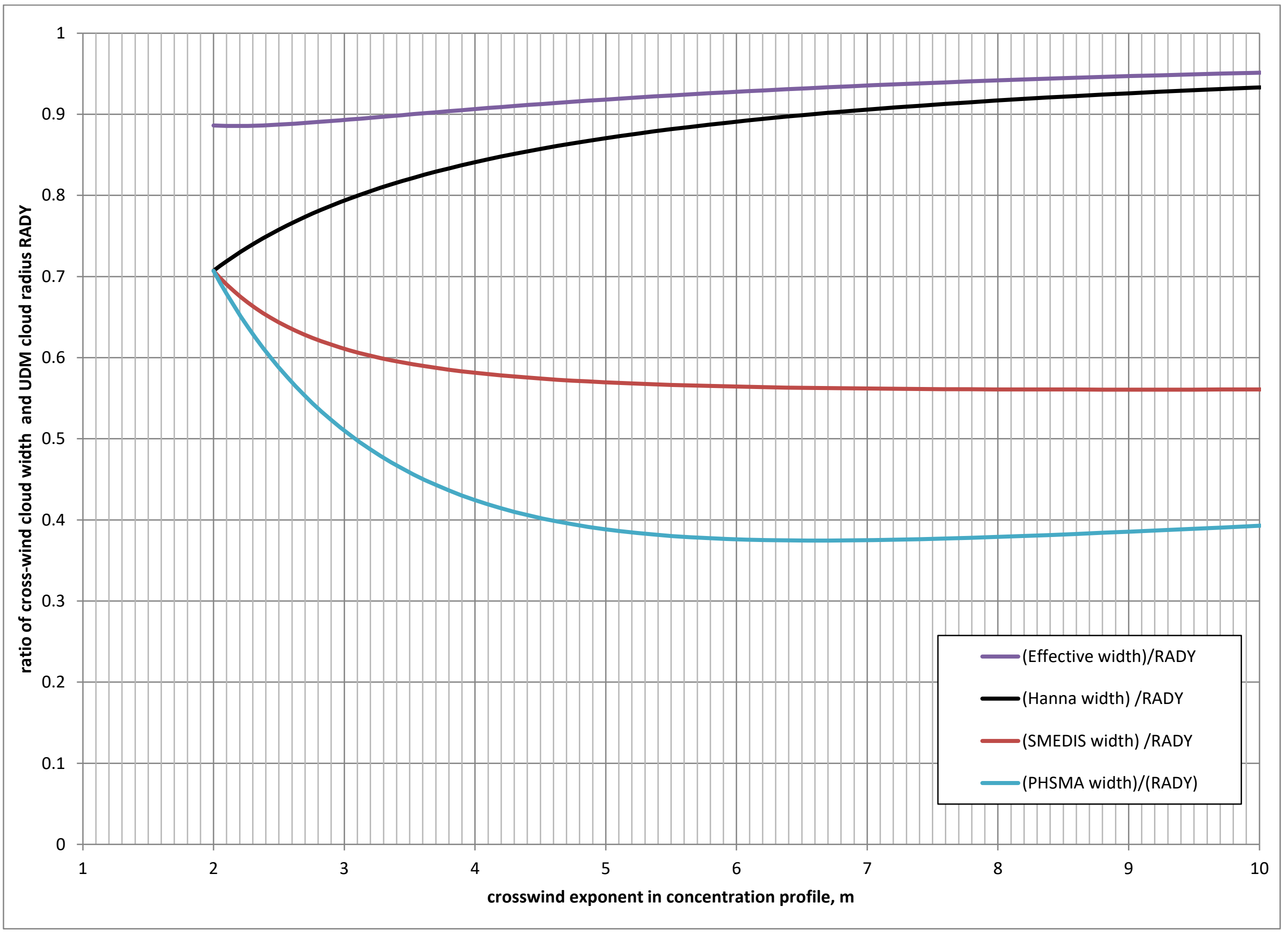

Figure 27. Comparison of cloud widths

Appendix C. Chronological comparison of the performance of the UDM

The tables below present a statistical comparison of the UDM predictions with the measured experimental data for different releases of the UDM, from Version 5.2 to the present release.

Phast 6.0 considerably improved predictions over earlier versions. Since 6.0, the performance of the UDM has been relatively stable. Changes for Phast 6.7 results reflect the first PHMSA validation process (using the v11 database) and show differences for LNG and related experiments. The most significant changes occurred for v8.0 with the introduction of “observer” based dispersion modelling and AWD. Most recently, the Goldfish simulations for v8.4 have been updated to use purely McFarlane experimental data.

Another trend apparent from the table is the gradual extension of the experimental database to include additional datasets. The Coyote and Maplin Sands LPG experiments were added for v6.7; Thorney Island continuous were added for v6.7; BP and Shell CO_2 were added for v8.0. This trend is likely to continue. From v8.4, all cases are available from DNV as Phast study files.

From Phast 8.4, the cases comprising the PHMSA validation set have been introduced in their entirety. The PHMSA v12 validation database has introduced a more detailed data set than previously including expanded point-wise concentrations (including Maplin Sands and Thorney Island which were previously arc-wise only), refined sensor co-ordinates and removal of post-ignition data for the Coyote experiments. Furthermore the arc-wise calculation for PHMSA is based on a sub-set of the observed and predicted concentrations at the sensor locations on an arc (as opposed to arc-wise predictions being the centre-line concentration at the arc). Making direct comparison between the current and previous mean and variance values for the PHMSA cases is difficult given these changes to the data set and the calculation method. As such from Phast 8.4 the PHMSA set as calculated by the PHMSA methodology will be presented. Previous values which were calculated using a sub-set of the current PHMSA data (e.g Maplin Sands, Burro, Coyote) will not be carried forward for comparison.

		Concentration		Half Width	
Series	**Phast /Safeti version**	**Mean**	**Variance**	**Mean**	**Variance**
Prairie Grass[19]	6.0	0.91	1.67	0.80	1.19
	6.42	0.91	1.67	0.88	1.19
	6.7	0.93	1.79	0.88	1.19
	8.0	0.94	1.67	0.89	1.19
	8.4	0.98	1.69	0.88	1.22
	8.6	0.95	1.69	0.90	1.21
	8.9	0.95	1.69	0.90	1.21
Desert Tortoise[20]	6.0	1.00	1.21	1.00	1.06
	6.42	1.01	1.20	1.06	1.07
	6.7	0.98	1.20	1.06	1.07
	8.0	1.01	1.21	1.03	1.06
	8.4	1.01	1.21	1.04	1.05

[19] Hanna values only. PG8 and 17 width from SMEDIS omitted

[20] SMEDIS values only (DT1 and 2), Hanna omitted

	8.6	1.00	1.18	1.06	1.03
	8.9	1.00	1.18	1.07	1.02
Goldfish	6.0	1.81	1.61	0.48	1.78
	6.42	1.81	1.62	0.48	1.78
	6.7	1.84	1.65	0.48	1.78
	8.0	1.86	1.66	0.49	1.71
	8.4	1.69	1.51	0.48	1.77
	8.6	0.87	1.22	0.77	1.13
	8.9	0.87	1.22	0.77	1.13
BP CO2	8.0	1.34	1.19	-	-
	8.4	1.33	1.19	-	-
	8.6	1.34	1.19	-	-
	8.9	1.34	1.19	-	-
Shell CO2	8.0	1.16	1.09	-	-
	8.4	1.16	1.09	-	-
	8.6	1.14	1.08	-	-
	8.9	1.16	1.09	-	-
COSHER	8.9	0.98	1.11	-	-
Maplin Sands LPG	6.7	2.03	2.19	-	-
	8.0	2.15	2.28	-	-
	8.4	1.86	1.84	-	-
	8.6	1.86	1.83	-	-
	8.9	1.87	1.85	-	-
EEC	6.1	1.36	1.15	1.60	1.29
	6.42	1.36	1.15	1.60	1.29
	6.7	1.36	1.15	1.59	1.29
	8.0	1.36	1.16	1.59	1.29
	8.4	1.36	1.15	1.60	1.29
	8.6	1.37	1.16	1.60	1.29

	8.9	1.37	1.16	1.60	1.29
FLADIS	6.1	0.53	3.65	1.48	1.23
	6.42	0.53	3.68	1.48	1.23
	6.7	0.55	3.60	1.47	1.21
	8.0	0.56	3.57	1.46	1.21
	8.4	0.83	11.48	1.48	1.22
	8.621	0.78	1.69	1.39	1.17
	8.9	0.78	1.69	1.39	1.17
Thorney Island	6.42	1.31	1.61	-	-
(instantaneous)	6.7	1.31	1.57	-	-
	8.0	0.88	1.34	-	-
	8.4	0.87	1.35	-	-
	8.6	0.87	1.35	-	-
	8.9	0.87	1.35	-	-
KitFox URA	8.0	0.94	1.09	0.99	1.05
(Continuous)	8.4	0.93	1.10	1.03	1.05
	8.6	0.93	1.10	1.03	0.93
	8.9	0.93	1.10	1.03	1.05
KitFox URA	8.0	0.49	2.07	0.72	1.19
(Puff)	8.4	0.54	2.08	0.77	1.15
	8.6	0.54	2.08	0.77	1.15
	8.9	0.54	2.08	0.77	1.15
Jack Rabbit 2	8.6	0.98	1.87	0.32	3.89
	8.9	0.98	1.87	0.32	3.89

Table 36. Chronological performance for MG/VG values

		Pointwise	
Series	**Version**	**MG**	**VG**

[21] Changes reflect corrections to the validation data used for this experiment set

Maplin Sands	8.4	12.95	>1000
	8.6	8.38	>1000
	8.9	8.37	>1000
Burro (long)	8.4	0.88	2.31
	8.6	0.89	2.27
	8.9	0.89	2.37
Burro (short)	8.4	1.19	1.95
	8.6	1.18	1.97
	8.9	1.18	1.97
Coyote (long)	8.4	0.47	5.16
	8.6	0.43	5.57
	8.9	0.43	5.57
Coyote (short)	8.4	0.47	5.16
	8.6	0.78	2.52
	8.9	0.78	2.52
Thorney Island (cont)	8.4	1.98	4.16
	8.6	1.32	3.01
	8.9	1.32	3.01
Wind tunnel	8.4	1.93	2.36
	8.6	1.98	2.38
	8.9	1.99	2.40

Table 37: Chronological list (starting at v8.4) for the PHMSA validation set

NOMENCLATURE

A	-	Area (m^2)
b	-	SMEDIS cloud width (m)
c ()	-	Concentration (mol%)
c_o()	-	Centre-line concentration (mol%)
H	-	User specified height (m)
z_{cld}	-	Centreline height (m)
W_{eff}	-	Effective cloud half width (UDM) (m)
x	-	Downwind distance (m)
y	-	Crosswind distance (m)
z	-	Vertical height (m)

About DNV

We are the independent expert in risk management and quality assurance. Driven by our purpose, to safeguard life, property and the environment, we empower our customers and their stakeholders with facts and reliable insights so that critical decisions can be made with confidence. As a trusted voice for many of the world's most successful organizations, we use our knowledge to advance safety and performance, set industry benchmarks, and inspire and invent solutions to tackle global transformations.

Digital Solutions

DNV is a world-leading provider of digital solutions and software applications with focus on the energy, maritime and healthcare markets. Our solutions are used worldwide to manage risk and performance for wind turbines, electric grids, pipelines, processing plants, offshore structures, ships, and more. Supported by our domain knowledge and Veracity assurance platform, we enable companies to digitize and manage business critical activities in a sustainable, cost-efficient, safe and secure way.

DNV | digital@dnv.com | dnv.com/digital

REFERENCES

[1] Daish, N.C., Britter, R.E., Linden, P.F., Jagger. S.F., and Carissimo, B., “SMEDIS: Scientific Model Evaluation techniques applied to dense gas dispersion models in complex situations”, International Conference and Workshop on Modelling the Consequences of Accidental Releases of Hazardous Materials, CCPS, San Francisco, California, September 28 – October 1 (1999)

[2] Witlox, H.W.M., and Harper, M., “Validation of Phast dispersion model UDM against experiments in LNG Model Validation Database”, DNV, April 2011

[3] Coldrick, S., Lea, C.J. and Ivings, M.J., “Validation database for evaluating vapour dispersion models for Safety Analysis of LNG facilities”, Guide to the LNG model validation database, Health and Safety Laboratory, Revision May 2010 (2010)

[4] Ivings, M.J., Jagger, S.F., Lea, C.J., and Webber, D.M., “Evaluating vapour dispersion models for safety analysis of LNG facilities research project”, Health and Safety Laboratory, April 2007 (2007)

[5] Britter, R.E., “Recent Research on the dispersion of hazardous materials” European Commission Report EUR 18198 EN

[6] Lowesmith, B. (2013). COSHER: Large Scale Experiments to Study the Rupture of a High Pressure CO2 Pipeline: Detailed Results of Test 1. In Hewett Conclusive Report NS051-SS-REP-000-00024 (2021). UK Government Department of Business, Energy and Industrial Strategy.

[7] M. Ahmad et al., “COSHER joint industry project: Large scale pipeline rupture tests to study CO2 release and dispersion,” International Journal of Greenhouse Gas Control 37, 340 (2015).

[8] Witlox, H.W.M. Harper, M., Oke,A. and Stene, J., “Validation of discharge and atmospheric dispersion for unpressurised and pressurised carbon dioxide releases”, Special CCS Safety issue of Journal of Process Safety and Environmental Protection 92 , pp. 3-16 (2014)
http://www.sciencedirect.com/science/article/pii/S0957582013000505

[9] Witlox, H.W.M., Holt, A., and Harper, M., “Validation of the Unified Dispersion Model Against Kit Fox Field Data”, Contract 44003900 for Exxon Mobil, DNV, London (2005)

[10] Hanna, S.R., D.G.Strimaitis, and J.C.Chang, “Hazard response modelling uncertainty (A quantitative method)”, Sigma Research Corp. report, Westford, MA for the API (1991)

[11] Jagger, S., Private Communication on SMEDIS input data for UDM (1998)

[12] McFarlane, K., Prothero, A., Puttock, J.S., Roberts, P.T. and Witlox, H.W.M, “Development and validation of atmospheric dispersion models for ideal gases and hydrogen fluoride” Report TNER.90.015 (non-confidential), Thornton Research Centre, Shell Research, Chester, England (1990)

[13] Woodward, J.L. Memorandum 775. “Model Validation for PHAST and SAFETI.” 3/10/92

[14] McFarlane, K., Prothero, A., Puttock, J.S., Roberts, P.T., and Witlox, H.W.M., “Development and validation of atmospheric dispersion models for ideal gases and hydrogen fluoride”, Part I: Technical Reference Manual, Shell Report TNER.90.015, Thornton Research Centre (1990)

[15] Nielsen, M. and Ott, S., “FLADIS field experiments”, Final report Risø-R-898(EN), Risø National Laboratory, Roskilde, Denmark, July 1996 (1996)

[16] Witlox, H.W.M., and Fernandez, M., “Atmospheric expansion modelling – literature review, model refinement and validation”, Report no. 984B0034 (2015)

[17] Schatzmann, M., Snyder, W.H. and Lawson,R.E. “Experiments with heavy gas jets in laminar and turbulent cross-flows,” Atmospheric Environment. Part A. General Topics, vol. 27, p. 1105–1116, 5 1993.

[18] Donat, J. “Wind tunnel experiments on the propagation of heavy gas jets (PhD Thesis),” Meteorological Institute, University of Hamburg, Centre for Marine and Climate Research, Hamburg, 1996

[19] C. Vidali, M. Marro, L. Gostiaux, H. Correia, S. Jallais, D. Houssin, E. Vyazmina and P. Salizzoni, “Atmospheric dispersion of heavy gas and passive scalar emission from elevated source” 2019

[20] P. Quillatre, “Relevance of the current modelling methods for the prediction of LNG vapour dispersion and development to be carried on,” Hazards 27, 2017

[21] Evans, J.A., and Graham, I., “Experiments to study flow and dispersion for releases of dense phase carbon dioxide”, Confidential report by Advantica for BP (2007)

[22] Allason, D. and Armstrong, k., “Liquid and supercritical carbon dioxide release and dispersion experiments on behalf of Shell International Exploration and Production BV”, GL Noble Denton Report 10793, Spadeadam Test Site, Gisland, Cumbria, UK (2011)

[23] Hanna, S.R and Chang, J.C., “New MDA database version of Kit Fox”, Provided as part of official CD together with overall Kit Fox report by Hanna, Chang and Briggs, “Dense gas dispersion model modifications and evaluations using the Kit Fox Field Observations”. Report P011F by Hanna Consultants, 3911 Carolyn Ave, Fairfax, VA22031, prepared for the American Petroleum Institute, 1220 L Street, NW, Washington, DC (1999)

[24] Mazzola T., Hanna S., Chang J., Bradley S., Meris R., Simpson S., Miner S., Gant S., Weil J., Harper M., Nikmo J., Kukkonen J., Lacome J.-M., Nibart M., Bjornham O., Khajehnajafi S., Habib K., Armand P., Bauer T., Fabbri L., Spicer T., Ek N. “Results of comparisons of the predictions of 17 dense gas dispersion models with observations from the Jack Rabbit II chlorine field experiment” Atmospheric Environment 244 (2021) 117887

[25] J. R. Stewart, S. Coldrick, S. E. Gant and M. J. Ivings, “Validation database for evaluating vapour dispersion models for safety analysis of LNG facilities, Guide to the LNG model validation database Version 12” Health & Safety Laboratory, 2016.

[26] M. J. Ivings, S. E. Gant, S. F. Jagger, C. J. Lea, J. R. Stewart and D. M. Webber, "Evaluating vapour dispersion models for safety analysis of LNG facilities," Health & Safety Laboratory, 2016
[27] Witlox, H.W.M., "Data review and Phast analysis (discharge and atmospheric dispersion) for BP DF1 CO_2 experiments", Contract 96000056 for DNV (CO2PIPETRANS Phase 2 JIP WP1), DNV, London, UK (2012)
[28] Witlox, H.W.M., "Data review and Phast analysis (discharge and atmospheric dispersion) for Shell CO_2 experiments", Contract 984C0004 for DNV (CO2PIPETRANS Phase 2 JIP WP1), DNV, London, UK (2012)
[29] J. McQuaid and B. Roebuck, "Large Scale Field Trials on Dense Vapour Dispersion. Final Report to Sponsors on the Heavy Gas Dispersion Reials at Thorney Island 1982-1984," Health & Safety Executive, 1985.